Addis Ababa University

Addis Ababa Institute of Technology

African Railway Center of Excellence

Master of Science in Railway Engineering (Rolling Stock)

Fatigue Life Prediction of a Railway Bogie Frame due to Wheel Out-of-Roundness. A Case Study of Ethio-Djbouti Railway.

A Thesis Submitted to the School of Graduate Studies of Addis Ababa University in Partial Fulfillment of the Requirements for the Degree of Masters of Science in Railway Engineering (Rolling Stock).

Submitted by: **HAKIZIMANA JEAN DE DIEU**

GSR/5408/14

Advisor: Dr. Haileleoul Sahle HABTE

August, 2023

Addis Ababa, Ethiopia

Approval

The undersigned have examined this thesis entitled **"Fatigue Life Prediction of a Railway Bogie Frame due to Wheel Out-of-Roundness. A Case Study of Ethio-Djibouti Railway"** presented by HAKIZIMANA Jean De Dieu, a candidate for the degree of Master of Science in Railway Engineering (Rolling Stock) and hereby certify that it is worthy of acceptance as approved by the examining board.

Dr. Haileleoul Sahle Habte		August 15, 2023
Advisor	Signature	Date
Dr. Ing. Demiss Alemu		25/8/2023
Internal Examiner	Signature	Date
Mr. Behailu Mamo		15/08/23
External Examiner	Signature	Date
Mr. Zewdie Moges		Aug-15-2023
ARCE Chairperson	Signature	Date

Director of Postgraduate Program
Addis Ababa University
Addis Ababa Institute of Technology

Declaration

I, HAKIZIMANA Jean de Dieu hereby declare that this thesis entitled as **"Fatigue Life Prediction of a Railway Bogie Frame due to Wheel Out-of-Roundness. A Case Study of Ethio-Djibouti Railway."** is my original work except the referenced works and it has never been submitted in any learning institution or elsewhere.

Signature: .....

Date: 15../.08/ ..2023

HAKIZIMANA Jean de Dieu

Dedication

I dedicate this work to God Almighty Father for giving me life and energy to accomplish the work, dedicated also to my parents and friends.

Acknowledgement

First overall, I give thanks and glory to God Almighty Father for the great gift of good health and life that help me to accomplish this work.

Secondary, I would like to give grateful appreciation to my supervisor Dr Haileleoul Sahle HABTE for his guidance and valuable advice throughout the whole research work. His motivation and availability to review the work with valuable advice at each step was very helpful to accomplish the work on time.

Thirdly, much appreciation to the African Railway Center of Excellence, Addis Ababa Institute of Technology as well as Addis Ababa University for sponsoring my studies as well as thesis work. I have learned a lot in the program which will help me in my future career to be valuable to the family, country and continent.

Furthermore, I raise my gratitude to the colleagues Mr Edison, Mazuri, Rodger, Alphonse, Victor, Jonex, Mohammed, all Ethiopian colleagues and various families and friends I meet in Addis Ababa for your valuable support, guidance and love which helped me to enjoy the life while doing my studies and research in foreign country distancing from my home.

Last but not least, I extend my appreciation and thanks to my home family and friends the way they have showing love and caring on me by making follow up to my studies and life.

Abstract

Railway transportation is one of the most common effective, safe and efficient mode of transportation used in many countries around the world. However, the failure of a bogie frame as a vital component that supports almost overall weight of the vehicle, can significantly affect the operation system. Mostly, it fails due to fatigue phenomenon brought on by various impact. The purpose of this research is to predict the fatigue life of a bogie frame due to wheel out-of-roundness (OOR). This research was focused on a freight bogie at Ethio-Djibouti railway (EDR), mostly faced with fatigue failure due to high load compare to a passenger vehicle. Wheel OOR cases have been integrated into a multibody system model with SIMPACK where dynamic loads that act on a frame have been extracted and applied to the finite element model with ANSYS to get stress and strain distributions used to predict lifecycles. Through the simulation scenarios with three cases of out-of-roundness with maximum radius deviation of 1 mm, 2 mm and 5 mm, the results show that the wheel OOR with high amplitude induce high non-monotonic impact forces that account for high stresses and reduce the life of a bogie frame. The results from this study show that the lifecycles are $8.2e^7$, $7.2e^6$ and $4.4e^5$ cycles for the case of out-of-roundness with 1 mm, 2 mm and 5 mm radius deviation, respectively. It shows that the bogie frame can operate below recommended fatigue lifecycles which is $2e^6$ cycles at the case of OOR with 5 mm and the study recommend to operate at wheel OOR with radius deviation below 2 mm. This study has significant to the maintenance department to enhance the countermeasures for minimizing the effects of OOR on bogie frame's life.

Keywords: A bogie frame, fatigue life, wheel out-of-roundness, finite element method, multibody system.

Table of contents

Approval i
Declaration ii
Dedication iii
Acknowledgement iv
Abstract v
Table of contents vi
List of figures viii
List of tables x
Acronyms and abbreviations xi
Chapter 1. Introduction 1
1.1. Background 1
1.2. Statement of the problem 2
1.3. Research questions 3
1.4. Objectives 3
1.4.1. Main objective 3
1.4.2. Specific objectives 3
1.5. Significance of this study 3
1.6. Scope of the research 4
1.7. Limitation of the study 4
1.8. Organization of the work 4
Chapter 2. Literature review 5
2.1. Introduction 5
2.2. Out-of-roundness theory 5

2.3. Measurement of out-of-roundness 6

2.4. Analysis of out-of-roundness forms 8

2.5. Related previous works to the topic 10

Chapter 3. Methodology 20

3.1. Introduction 20

3.2. Data collection 21

3.3. Vehicle dynamic system 24

3.4. Modelling 32

3.4.1. Wheel out-of-roundness 32

3.4.2. Modelling of multibody system in SIMPACK 33

3.4.3. CAD and FEM modelling 40

Chapter 4. Results and discussion 43

4.2. Impact load due to wheel out-of-roundness variation 43

4.3. Finite element analysis 54

4.4. Fatigue life estimation 58

Chapter 5. Conclusion, Recommendation and Future work 62

5.1. Conclusion 62

5.2. Recommendation 62

5.3. Future work 63

References 64

Appendix 69

Appendix A. Technical parameters used 69

Appendix B. Out-of-roundness data used (from maintenance department at EDR) 73

List of figures

Figure 2. 1. Impact of out-of-roundness on operation [20]..... 6
Figure 2. 2. Measurement of out-of-roundness with V- block method [20]..... 7
Figure 2. 3. Limitation of angular spacing in measurement of out-of-roundness [20]..... 7
Figure 2. 4. Analysis of out-of-roundness form [20]..... 8
Figure 2. 5. Local form deviation of roundness feature [21]..... 9
Figure 2. 6. Errors in wheel roundness [22]..... 9
Figure 3. 1. Methodology flowchart 20
Figure 3. 2. Physical view of CW4 freight wagon used at Ethio-Djibouti line (Source: Ethio-Djibouti railway line project office) 21
Figure 3. 3. Technical dimensions of CW4 freight wagon used at Ethio-Djibouti (Source: Ethio-Djibouti railway line project office) 22
Figure 3. 4. Typical example of wheel defect field measured record from Indode maintenance depot at EDR on CW4 wagon..... 23
Figure 3. 5. Vehicle connection system [50] 25
Figure 3. 6. Typical railway vehicle dynamic model [51]..... 30
Figure 3. 7. OOR excitations with: (a) 1 mm, (b) 2 mm and (c) 5 mm max radius deviation..... 32
Figure 3. 8. Model tree for railway vehicle in SIMPACK..... 34
Figure 3. 9. Rigid body properties 35
Figure 3. 10. Integration of OOR excitation to the vehicle system 36
Figure 3. 11. Multibody vehicle model in SIMPACK..... 37
Figure 3. 12. Preloading condition for model validation purpose 38
Figure 3. 13. Results tree in post-processor of SIMPACK..... 39
Figure 3. 14.Extraction of dynamic force time history..... 40
Figure 3. 15. 3D CAD model of front bogie frame in SOLIDWORKS 41
Figure 3. 16. FEM model in ANYS Workbench 42
Figure 4. 1. Vertical force at 1 mm: (a) right side, (b) enlargement of (a), (c) left side and (d) enlargement of (c). 44
Figure 4. 2. Lateral force at 1 mm: (a) right side, (b) enlargement of (a), (c) left side and (d) enlargement of (c). 45

Figure 4. 3. Longitudinal force at 1 mm: (a) right side, (b) enlargement of (a), (c) left side and (d) enlargement of (c). 46
Figure 4. 4. Vertical force at 2 mm: (a) right side, (b) enlargement of (a), (c) left side and (d) enlargement of (c). 47
Figure 4. 5. Lateral force at 2 mm: (a) right side, (b) enlargement of (a), (c) left side and (d) enlargement of (c). 48
Figure 4. 6. Longitudinal force at 2 mm: (a) right side, (b) enlargement of (a), (c) left side and (d) enlargement of (c). 49
Figure 4. 7. Vertical force at 5 mm: (a) right side, (b) enlargement of (a), (c) left side and (d) enlargement of (c). 51
Figure 4. 8. Lateral l force at 5 mm: (a) right side, (b) enlargement of (a), (c) left side and (d) enlargement of (c). 52
Figure 4. 9. Longitudinal force at 5 mm: (a) right side, (b) enlargement of (a), (c) left side and (d) enlargement of (c). 53
Figure 4. 10. Fixed support and load conditions 54
Figure 4. 11. Mesh independence analysis 55
Figure 4. 12. Stress distribution under OOR with: (a) 1 mm, (b) 2 mm and (c) 5 mm 56
Figure 4. 13. Strain distribution under OOR with: (a) 1 mm, (b) 2 mm and (c) 5 mm 57
Figure 4. 14. Total deformation distribution 58
Figure 4. 15. Simulation lifecycles under OOR with: (a) 1 mm, (b) 2 mm and (c) 5 mm 59

List of tables

Table 2. 1. Summary of literature review 15

Table 3. 1. Chemical properties for Q450NQR1 Weathering steel used for bogie frame at EDR [54] 42

Table 3. 2. Mechanical properties for Q450NQR1 Weathering steel used for bogie frame at EDR [54] 42

Table 4. 1. Summary of maximum dynamic forces induced on a bogie frame 53

Table 4. 2. Comparison between simulated and calculated life 61

Acronyms and abbreviations

OOR: Out-of-Roundness

FEM: Finite Element Method

CAD: Computer Aided Design

MBS: Multibody System

FE: finite element

EDR: Ethio-Djibouti Railway

AALRT: Addis Ababa Light Rail Transit

Chapter 1. Introduction

1.1. Background

Railway transportation is one of the safest and most efficient modes of transportation in many countries. It can be needed for transportation of both passengers and freight, especially over longer distances. The railway system remains the most cost-effective mode of freight transportation that should be used to move freight (goods) from city to city within the same country or from one country to another. A railroad vehicle is composed of a lot of components that are interconnected to perform the desired activities in an efficient and effective manner. The most important component of a train that supports practically all of the vehicle's weight is a railway bogie frame, and its reliability can directly affect the safe operation of the system. Additionally, its vibration can impact the stability and safety of the vehicle [1]. Various studies have been conducted to analyze the performance and various failure modes of a bogie, including both experimental and field tests and simulations. The failure of a railway bogie frame as a critical component of a vehicle should cause fatal incidents such as derailment, high vibration, instability, etc. Dynamic characteristics from rail joints, track curves, and rail and wheel imperfections, which might influence high vehicle vibration, can affect the fatigue life of the frame. Railway wheel OOR is one of the wheel irregularities that is considered to be an excitation to the track-vehicle system and can increase system vibration and reduce the lifespan of both track and vehicle components [2]. Wheel OOR generally can occur to almost all kinds of railway trains including high speed trains [3-6], locomotives[7-11], metro train [12-16], mono-rail trains [17, 18] etc.

Previous research and studies on the impact of wheel OOR on various railway vehicles and track components have been conducted, as some reviewed from various published papers such as in [2, 19] has been performed. However, there is a limited study among the current researches which develop clear understanding on the influence of wheel OOR to the lifecycle of a bogie frame as the crucial component of the vehicle. Wheel out-of-roundness is frequently process around the circumferential of the wheel, but the wheel OOR can occur gradually under various radius deviations. Once there are limited researches that can explain well the effect of wheel OOR to the life of a bogie frame, this can reduce attention to the maintenance team in preventive measure. Therefore, by clear understanding on how wheel out-of-roundness is developed and its influence

to the life of railway bogie frame as a part which carry almost the total weight of a vehicle train, will strengthen the countermeasures to mitigate or reduce the impacts of wheel out-of-roundness with purpose to increase the lifecycle of a railway bogie. This research aims to analyse how wheel out-of-roundness can affect a railway bogie frame's fatigue life. In order to analyze the effect of wheel out-of-roundness to the fatigue life of a railway bogie frame, the study was carried out on a high loaded freight bogie frame case of Ethio-Djibouti, where out-of-roundness collected was integrated into multibody system and finite element tools for further analysis about their impact on bogie frame's life.

1.2. Statement of the problem

The fatigue failure of a railway bogie frame as a critical component underneath a vehicle's structure is a serious problem that can affect the operation of the railway system and result in fatal accidents. Ethio-Djibouti railway provide transportation services to both people and goods or freights. The freight service operate on high duty with around 11.2 millions tonnes annually that expect to be rised to 24.9 tonnes by 2025. This high freight load in combination with various operating conditions such as curves, coefficient of friction, speed variation, rail corrugation, track irregularities, wheel imperfections and other defects may induce high dynamic load that can affect the life of a bogie frame. The wheel out-of-roundness is among serious problem that can affect the performance of a railway system as the wheel is immediately connect train and track. Currently Ethio-Djibouti line dealing with wheel defects by performing scheduled re-profiling maintenance based on existing operation limits especially with flange thickness greater or equal to 26 mm and tread circumference wear less than 3 mm as shown on appendix figure A.1. But, due to variation in operating conditions the wheel on one side can be affected by serious out-of-roundness with high tread wear amplitude exceeding the existing operation limits as shown on figure 3.5 as typical example from EDR Indode rolling stock maintenance depot, before scheduled re-profiling activity, this induced out-roundness may influence the failure of important component especially the bogie frame. The analysis of the effect of that unexpected induced out-of-roundness on the system has to be considered for safety purpose.

Several studies and researches have been conducted on the fatigue life of a railway bogie frame by taking into account various traits and techniques [23-31]. But to the best of my knowledge, no in-

depth previous studies had examined the impact of wheel out-of-roundness to the fatigue life of a bogie frame as important part of a vehicle subjected to the high load. Therefore, based on collected OOR data this research provide a better way to analyze the effect of out-of-roundness to the life of bogie frame and how control measures can be enhanced with aim of improving performance, increase safety, and decrease maintenance costs for railway operations.

1.3. Research questions

- How does wheel OOR affect dynamic load of vehicle system?
- How does wheel OOR affect the stress and deformation distributions on a bogie frame?
- How does wheel OOR affect the fatigue life of a railway bogie frame?

1.4. Objectives

1.4.1. Main objective

The main objective of this research is to analyse and predict of a railway bogie frame's fatigue life due to wheel out-of-roundness. Ethiopia-Djibouti line case study

1.4.2. Specific objectives

- To show how the integration of wheel out-of-roundness to the multibody vehicle system can influence high impact load.
- To analyse the influence of wheel OOR variation on a bogie frame's stress and deformation distributions.
- To analyze the influence of wheel out-of-roundness on the fatigue lifecycles of a bogie frame.

1.5. Significance of this study

Well performance of a bogie frame and its attachments has a significant impact on the effectiveness of the operation as well as the cost of maintenance. The research significance from this study is classified into two parts that are input to the maintenance team and input to the research community as explained as the following: This study is focused on analysis and prediction of the fatigue life of freight bogie frame on the Ethio-Djibouti line under consideration of wheel out-of-roundness, therefore, the study is benefit to the Ethio-Djibouti maintenance team to see how wheel out-of-

roundness can affect the life of a bogie frame and the recommended measures to mitigate the effect. Furthermore, there have been a few published studies in this area; thus, this study has benefit for future researchers from both an academic and an industry standpoint.

1.6. Scope of the research

The scope of this research is the prediction of the fatigue lifecycle of a railway bogie frame due to the impact of wheel out-of-roundness on the Ethio-Djibouti railway line. Furthermore, the study focus on the simulation of the model using the finite element method (FEM) integrated with the multibody system (MBS). Based on previous approaches for various studies related to multibody modelling for a complex trainset system where it is difficult to analyse whole system due to computational purpose, therefore in this study the effect between adjacent wagons was not considered means that a representative single freight vehicle model composed by one carbody, rear and front bogies has been modelled in SIMPACK software and the required input parameters for this system has been integrate to generate the induced dynamic loads on a bogie frame. The study has based on analysis of the lifecycles of a highly affected bogie frame based on the dynamic loads from multibody SIMPACK software.

1.7. Limitation of the study

Due to the unavailability of some manufacturer data from EDR office, the type of material for studied bogie frame at EDR is Q450NQR1 steel but its actual properties was not found in the office therefore, the study considered the properties for the same type material referenced in paper [56] as shown in tables 3.1 and 3.2.

1.8. Organization of the work

This thesis is organized into five chapters, where chapter one talk about introduction by demonstrate about background, problem statement, objectives, significance, scope and limitation of the work. Chapter two details about Literature review from previous works about wheel OOR and fatigue life of a bogie frame. Chapter three is about materials and method used to accomplish this work. Chapter four is about results and discussion from SIMPACK, FEM (ANSYS) and nCode results for lifecycles. All requires results in terms of graphs, tables and figures have been demonstrated in this chapter four. Finally chapter five is about conclusion, recommendation and future work about this work.

Chapter 2. Literature review

2.1. Introduction

This section of the study contains the reviews from different literatures of research works that have been conducted previously that relate to the fatigue life of a railway bogie frame. In this section, there are identifications of various gaps and some recommended solutions provided by different researchers in the field of the study. This section also contains reviews of research related to wheel out-of-roundness and its impact on various vehicle and track components. Each of these above-mentioned points shall be reviewed and presented in a chronological manner, which helps to identify the overall research gap to be studied in this work in order to achieve the objectives. Several previous studies on the prediction of the fatigue life of a railway bogie frame under consideration of different factors have been conducted and reported in this chapter.

2.2. Out-of-roundness theory

Out-of-roundness refer to the irregularity in circumferential of round component. Sometimes the measurement of diameter cannot be relied up on to the measurement of out-of-roundness, to understand this can be demonstrated based on the example on figures 2.1 (a) and (b) where (a) shows a 3-lobed workpiece of 25 mm diameter, anyone can think that it can fit into the hole of same diameter of 25 mm, but in real situation this is not true because of the effect of out-of-roundness. Instead this piece can fit into the hole of at least 28.9 mm of diameter as shown in figure 1(b).

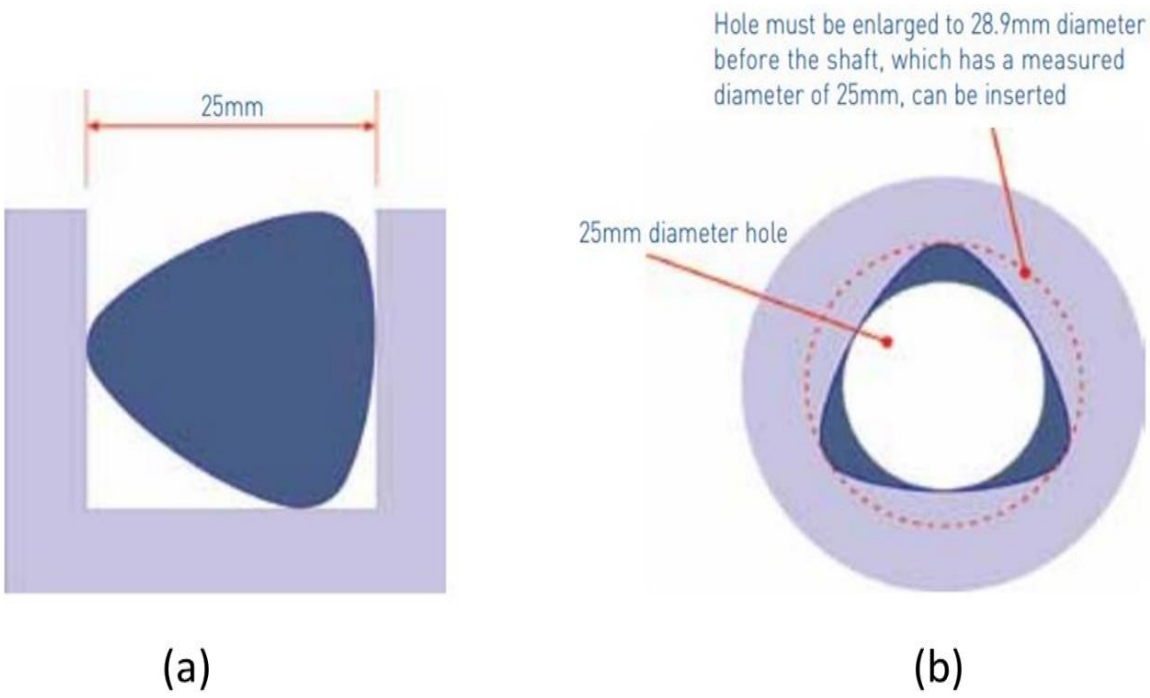

Figure 2. 1. Impact of out-of-roundness on operation [20]

2.3. Measurement of out-of-roundness

The use of diameter in measurement of out-of-roundness has severe effect because always must be assessed independent of size. Out-of-roundness can be measured with effective method such as the simplest one of V-block method illustrated on figure 2.2. This method is based on rotating the part into a vee-shaped block and be in contact with dial gauge or similar indicator. The part must be rotated carefully by avoiding to disturb the block and gauge stand. Any presence of irregularities due to out-of-roundness will cause the part to move up and down as it attaches on both sides of vee block and those irregularities will move the plunger of the dial gauge; while if the part is smoothly round with negligible defects, the dial gauge pointer will not be displaced or moved. The displacement of the dial gauge pointer will be significant when the plunger of gauge and arms of vee block are in contact with peaks or valleys of the circular part.

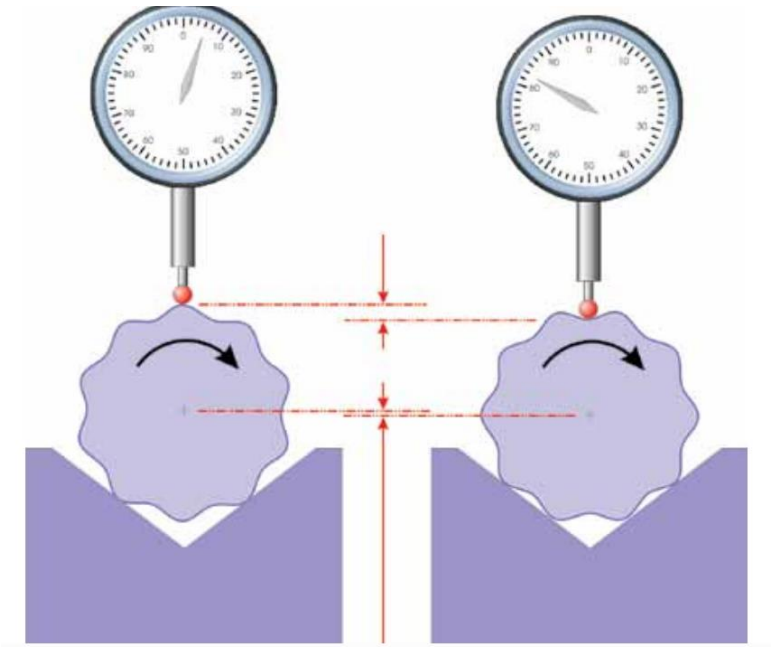

Figure 2. 2. Measurement of out-of-roundness with V- block method [20]

Even though the 3-point method of V block is used, but it has limitation of that results can be varied depends up on the angle of vee block and the spacing of irregularities as illustrated on figure 2.3.

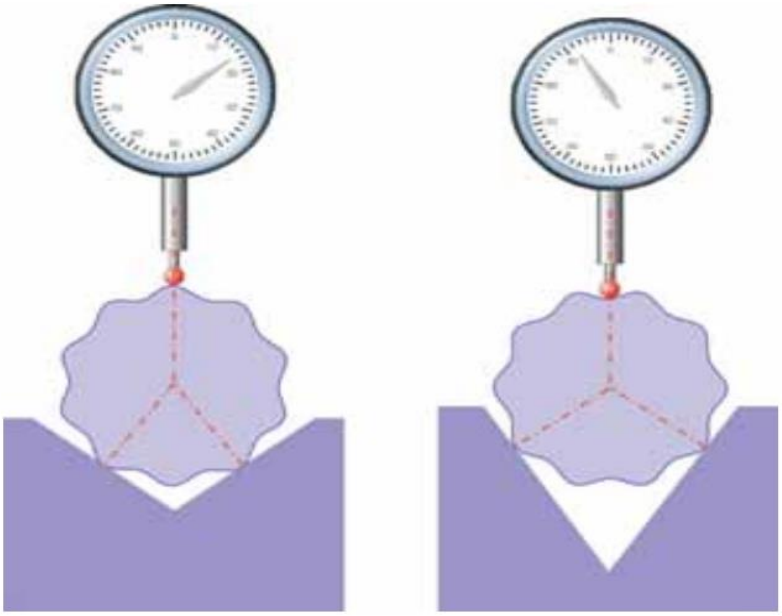

Figure 2. 3. Limitation of angular spacing in measurement of out-of-roundness [20]

2.4. Analysis of out-of-roundness forms

Out-of-roundness can be expressed in terms of the maximum deviations of peaks and valleys as illustrated on figure 2.4. Where RON, P, V and RONt stand for roundness, peak, valley and roundness total, respectively. And figure 2.5 shows local form deviation of roundness feature.

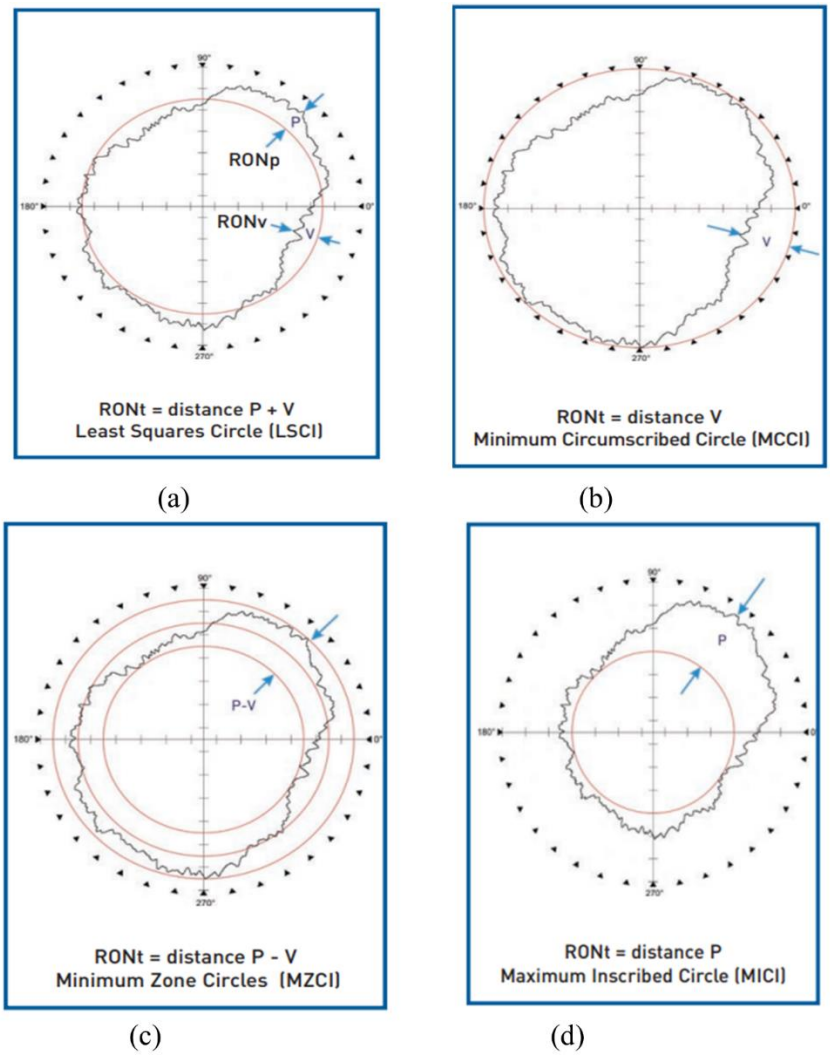

Figure 2. 4. Analysis of out-of-roundness form [20]

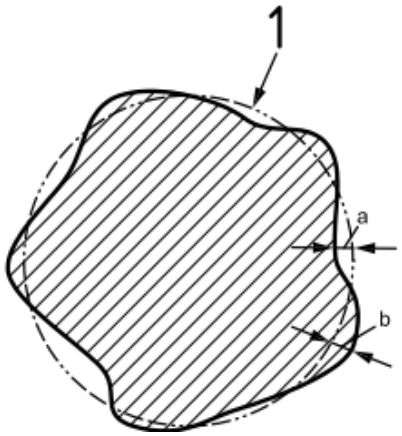

Figure 2. 5. Local form deviation of roundness feature [21]

Key:

1: represents reference circle

a: represents negative local deviation and

b: represents positive local deviation

The figure 2.6 shows errors in wheel roundness. Where Ro stand for nominal radius while Δr stand for deviation in rolling radius; φ stand for wheel rotation angle that is between horizontal axis and the initial contact radius of out-of-roundness railway wheel at instant time.

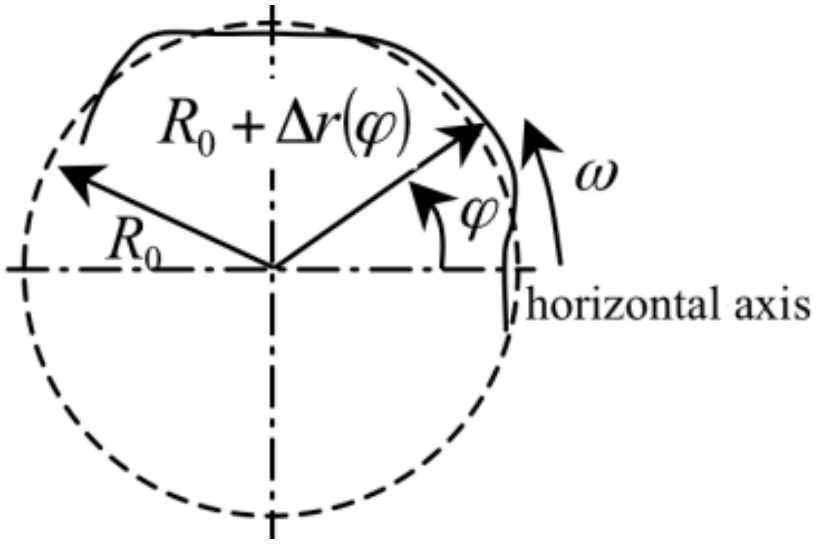

Figure 2. 6. Errors in wheel roundness [22]

For periodic wheel out-of-roundness such as wheel polygonization, the increment in rolling radius Δr, can be expressed in terms of wheel rotation angle φ as follows [22]:

$$\Delta r = a\sin\left(\theta \times \varphi\right) \qquad (2.1)$$

Where θ is out-of-roundness order which is generally range from 1 to 20 orders in railway system. α is out-of-roundness amplitude generally for the case of periodic out-of-roundness is equal to the half of difference between maximum and minimum value of nearly sinusoidal curve.

2.5. Related previous works to the topic

Zehsaz et al.,2011 [23] studied the consequences of increasing the speed of trains on the stress distribution on a bogie frame. Finite element analysis was used to model a biaxial bogie frame for this study. Comparable stresses used in the frame's strength calculation were von Mises stresses. The train's speed used in Zehsaz's study has been adjusted from 20 m/s to 40 m/s while carrying various weights, and the analysis process was displayed. His findings demonstrated that the bogie bowl consistently produced the most stress. The maximum stresses were determined to be 83.159 MPa and 107.86 MPa at 20 m/s and 40 m/s, respectively. This indicates that the maximum stress at 40 m/s is approximately 26% higher than that at 20 m/s. This indicates how increasing the train speed causes more stress to be placed on various areas of the bogie frame. The gap in his study is that he considered only vertical displacement, while longitudinal and lateral vibrations should also affect the bogie frame. He recommended also considering the effect of acceleration or deceleration on the train as important dynamic parameters for further studies.

Seo et al.,2017 [24] a full-scale test for evaluation of the bogie frame's life was performed. In the study, the EN 13798 standard was considered in determining the static loads, which were divided into nine cases for exceptional loads and four cases for service loads. The primary suspension's springs were constrained by boundary conditions. Under extreme loads, the bogie frame's maximum stresses should not exceed the material's yield strength. The examined electric railcar bogie frame conducted a fatigue test using EN 13749, with lateral load, twist, and vertical load as the loading conditions. Furthermore, during the fatigue test, the loads were composed of both static (the quasi-static load) and dynamic (the fatigue test was conducted in three steps. Step 1 was carried out with an initial load of up to 6×10^6 cycles. For step 2, the quasi-static load and dynamic load were increased by 1.2 times, and then fatigue damage was determined. In the third step, the

load was increased by 1.4 times. By comparing the first and third stages, the damage in the third stage was multiplied by 6.6. In this research, the results showed that very small cracks are acceptable in Step 3 but should not appear after the fatigue test in Steps 1 or 2. The damage due to fatigue in the track test was 0.02; in contrast, it was 0.07, 0.2, and 0.46 for steps 1, 2, and 3 of the fatigue test, respectively. Therefore, it is clear that as load magnitude increased, fatigue damage also increased. Among the three steps under EN 13749, it was determined from this study that the load magnitude of the second and third steps is specified more conservatively than that of in-service running conditions as the fatigue damage is very high.

Li et al.,2014 [25] researchers studied fatigue evaluation approaches that can be used to predict the fatigue life of a bogie frame. The two crucial techniques, cumulative damage and the endurance limit, were examined in the study. The cumulative damage strategy can be utilized for materials without a defined endurance limit or when some repetitive stresses exceed the endurance limit in areas where all dynamic stress cycles are less than the material's fatigue limit. In this evaluation, the finite element method and line test method were used, and the results were compared. The study's findings revealed that the simulation with the finite element method may have more concern points than expected, whereas the concern points in the line test are less than those with the finite element method. In this study, Goodman diagrams were used to examine 46 test points, and the findings indicated that when taking the same safety factor into account, the Haigh-Goodman and Smith-Goodman diagrams are identical.

Xiu et al., 2020 [26] studied about the methods for assessing the fatigue life of railroad bogie frames. They discovered that standard prescribed loads, measured loads, or simulated load spectra are frequently used to evaluate the fatigue life of railway car bogie frames. Design loads, which may be static or cyclic, are included in the list of standard prescribed loads. The dynamic load approach increases the accuracy of bogie frame fatigue life estimates because the static design load method produces conservative results. According to the study, many analyses of actual or simulated load spectra used to estimate the fatigue life of bogie frames consider track irregularity. The most direct and accurate method is to use the measured load spectrum, but because it is expensive, takes a long time to test, and is not suitable during the design stage, only a small number of bogie frames may be selected for field testing. The study concluded that the simulation methods that consider impact, including braking forces, should be better.

Wang et al., 2021 [27] a study was done on the subject of predicting fatigue damage of a metro bogie frame with loads measured. The actual fatigue damage from service measured loads of a comparable existing bogie frame that functioned under the same conditions was compared to the expected fatigue damage of a bogie frame during the investigation. The objective of the study was determination the damage of a bogie frame A with measured loads of frame B. The simulations scenarios had conducted in order to assess the load-strain transfer relationship at each position on frame A by applying thirteen different types of measured loads to the finite element model of frame A. The associated stress responses were recorded in the simulation program. The study's findings demonstrated that the predicted fatigue damage closely matched the actual fatigue damage. The study's gap is that the service line's rail corrugation was not taken into account.

Guo et al., 2019 [28] conducted the study on effect of internal excitation from gear meshing to the life assessment of a powered bogie frame. Many standards, according to the research, only consider external excitation from wheel and rail interactions, whereas there are some internal excitations to consider, such as gear meshing impacts from traction units on powered bogie. In this study, the integration of mesh stiffness and error from gear and tooth backlash into a torsional vibration model was considered. A flexible coupled vehicle multibody dynamic system with FEM was also simulated in order to analyze the dynamic responses and compute the fatigue damage and life of the bogie frame using gear meshing excitation. The results show that stress history rose by around 17% when gear meshing excitation was considered, demonstrating the importance of considering internal excitation like gear meshing when estimating the service lifetime of a bogie frame. The shortcoming of this study was that more research is required to support the evaluation of fatigue life based on a flexible model that accounts for both internal excitations of gear meshing and motor ripple torque.

Lagoda et al., 2022 [29] had reviewed on calculation of fatigue life for metal structures based on smith Watson Topper parameters and its modification. In the research the various technique based on strain criterion, stress criterion and energy criterion had been discussed. The study showed that modified Smith Watson Topper that take into account both stress and strain criteria is the best method that can be used in estimation of fatigue life for metal components.

O.A.Nour,2017 [30] carried out research on developing a new material in order to enhance the life of existing bogie frame case of Addis Ababa Light Rail Transit. In this study ANSYS and FEMFAT tool was used in order to analyze the difference in strength between a new material which is AISI 4140 alloy steel normally characterized by high strength, abrasion and impact resistance, toughness, and torsional strength and existing material which is steel UNI 10025 S355J2G3C. The results from the study showed that the new selected material prove high strength than existing material, because it experienced low equivalent stress, high safety factor and high endurance limit. The gap from this study is the lack of showing the fatigue lifecycle for proposed material and it did not consider the dynamic behavior of impact loads.

Daher,2017 [31] carried out study on fatigue strength analysis of a composite bogie frame case of Addis Ababa Light Rail Transit AALRT. In this study a 3D bogie frame model was modelled by using SOLIDWORKS software and the model had been imported into ANSYS Workbench 2016 in order to analyze the effect of applied loads on the bogie frame. The fatigue life was analyzed by comparing two different material bogie frames where conventional AALRT frame was made in steel while the proposed frame was made in composite material of carbon/epoxy. The results showed that the maximum deformation and equivalent stress for carbon/epoxy were 2.1101e-6 mm and 209.55MPa respectively while for structure steel were 0.74025 mm and 225.39 MPa respectively. The study showed that the bogie frame made of carbon/epoxy composite material had a good strength performance in comparison to structure steel because in the stress life method mostly used technique in fatigue life assessment the stress is inversely proportion to the life and this composite can be considered as the best effective way to reduce the weight of railway vehicle. In this study only static loading condition without considering dynamic parameters like changing speed were used.

Moreover, in this section, some of the previous research on wheel OOR and its effects in a railway system has been reviewed. Some of the previous research showed that the wheel out-of-roundness influence high dynamic loads between wheel and rail [32-38], it can cause unwanted noise problem either inside or outside of the train [2, 4, 39, 40], it can affect also the stress behavior of wheelset axle [41, 42]. Wheel OOR can affect railway infrastructure like rail fatigue, degradation of rail joints, and sleepers [43]; OOR can also have an impact on vehicle components and affecting

passenger comfort [43]. Polygonalized wheels can influence the high vibrations between the vehicle and track system [13] and high-order polygon wheel wear has become a significant challenge in ensuring safe operation [44]. However, even if these researches try to mention some effects of OOR to the operation and comfort of passengers, but among them there is no one that showed how the variation of OOR can affect the lifecycles of a bogie frame which is directly connected with the wheels and support almost overall weight of the vehicle.

Sun et al., 2022 [45] carried out research on wheel out-of-roundness field measurements on one Chinese metro bogie that failed with the cross beam's bending. The model through multibody system was created for this study in order to analyze the stress distribution in the body. The findings show that wheel OOR under different wheel phase shifts contributes to the high bogie vibration and change characteristics of the stress. However, this research didn't show how the variation of OOR can affect the lifecycles of the bogie frame.

Tao et al.,2020 [46] According to a review of studies on wheel OOR in the form of polygonization, wheel polygonization is a common non-uniform wear type that is likely to occur on railroad wheels. In addition to that, wheel polygonization can have a severe impact on the ride comfort, vehicle, and track system by increasing noise, vibration, etc. In this study, the three important formation mechanisms of polygonization have been explained: initial defects of wheels, natural vibration of the vehicle track system, and thermoelastic instability. Simulation methods and various countermeasures for mitigating the polygonization effect have also been presented.

G. Tao et al.,2021[47] studied about the interaction of wheel and rail under wheel OOR and how it is transmitted between wheelsets. The vehicle and track rigid-flexible dynamic coupled model has been created by integrating SIMPACK and ANSYS software, and the model has been validated through field vibration measurement results for the vehicle and track. The findings demonstrated that a defective or polygonised wheelset's dynamic interaction with the rail might be transferred to the other wheelset of the same bogie. This study suggests that to prevent the effect of wheel OOR transmission, the wheelsets appeared on the same bogie must be re-profiled at the same time if the radial run-out for one wheelset exceeds the required limit. In this study, the effects of vibration transmission developed between wheelset and track weren't taken into consideration in the model for OOR development.

Song et al., 2013 [22] studied about the influence of different types of wheel defects to the vehicle-track coupling system. The numerical simulations under different variation of parameters such as train speed, out-of-roundness amplitude and order have been performed to analyse their dynamic responses to the system. The simulation results showed that the vertical dynamic loads have significant dependence to the wheel out-of-roundness features. The authors recommended that for purpose improvement safety and stability of the railway system as well as the reduction of maintenance costs, it is very crucial to provide the safety operational range of out-of-roundness values and improve the diagnostics and monitoring system as well as maintaining the defective wheels before failure. The limitation on this study was that it focused only on wheel polygonization cases without considering even the general out-of-roundness cases. Also in this study the effect of impact forces due to wheel defects to the life of vehicle components was not analyzed.

Table 2. 1. Summary of literature review

No	Reference	Objectives	Study parameter and focus	Findings	Gap
1.	Zehsaz et al. [23]	Analysis the effect of increasing train speed on stress distribution	Stress distribution on biaxle bogie frame with finite element analysis	The findings from this research showed that stress distribution on the bogie frame increases as the speed of the vehicle increases for example the stress increased about 26% at 40 m/s higher than at 20 m/s, which may affect the life of the bogie frame.	In this study the dynamic parameters such as vibration which can be induced between wheel-rail interactions due to out-of-roundness had not considered.
2.	Seo et al.,2017 [24]	The study was about fatigue test and	Fatigue damage due to Lab test and track	The result from this study showed that the fatigue damage increases	In this study the fatigue due to load changing was

		evaluation	test for SM490A Korea bogie frame	as the magnitude of load increase and the fatigue life depends on stresses and strains history	considered but not considering the effect due wheel excitation.
3	Li et al.,2014 [25]	The study aimed at fatigue assessment approaches	Cumulative damage and endurance limit with FEM and line test methods	The study showed that during cumulative damage approach, Haibach modified S-N curve which combine stress and strain effect is highly recommended	In this study, they considered the maximum stress component in fatigue life evaluation without considering distribution history which can be influenced by wheel imperfections and other irregularities.
4	Xiu et al., 2020 [26]	Reviewed on fatigue life estimation methods	Measured and simulated spectrum loads were compared	The findings in this study showed that, the measured load spectrum method is more accurate, but significantly more expensive, than the simulated methods.	In the study, the consideration of braking effects which can influence wheel OOR was ignored.
5	Wang et al., 2021 [27]	Fatigue damage prediction based on measured loads	Fatigue damage for Metro bogie frame at similar operating conditions	The loads measured can be used in the prediction of fatigue damage for the same type of bogie frame under similar conditions.	In the study, rail corrugation and other wheel-rail imperfections were not taken into account

6	Guo et al., 2019 [28]	Impact of gear meshing excitation on fatigue life estimation	Stress distribution and fatigue damage on powered high speed bogie frame	The findings from the study showed that, the internal excitation like gear meshing increases stress distribution and affect fatigue damage of bogie frame	In this study only internal excitation was considered but external wheel-rail excitation such as wheel OOR was not taken into account.
7	Sun et al., 2022 [45]	Dynamic stress analysis due to wheel out-of-roundness.	Vibration and stresses distribution on one metro line Chinese failed metro bogie due to bending of cross beam	The findings from the study showed that wheel out-of-roundness influence vibration of bogie frame.	The study didn't show how the variation of wheel OOR can affect the fatigue life cycle of a bogie frame.
8	G. Tao et al.,2021 [47]	Dynamic interaction of wheel-rail due to wheel OOR	Vibration on Metro train wheels in china with SIMPACK rigid-flexible model	Wheel OOR can affect how much the wheelset vibrates when it bends, which can increase wheelset vibration and wheel/rail dynamic interaction.	Effects of vibration transmission developed between wheelset and track didn't taken into consideration in the model for OOR development.
9	Song et al., 2013 [22]	Analysis the effect of wheel periodic non-roundness to the dynamic response of vehicle system.	Numerical simulation to the high speed railway vehicle by variation of speed and OOR amplitude and order	The results showed that the vertical dynamic loads have significant dependence to the wheel defects features.	The effect of impact forces due to wheel defects to the life of vehicle components was not analyzed.

10	Lagoda et al., 2022 [29].	Review on faigue life calculation methods for metal structures	Smith Watson Topper parameter and its modification under stress-strain criterion.	The study showed that the modified Smith Watson Topper that take into account both stress and strain criteria is the globally updated technique that can be the best method for life calculations of metal structures.	No detailed comparison for life assessment works using this technique shown and its limitation.
11	O.A.Nour [30]	developing a new material in order to improve the fatigue life of existing bogie frame case of AALRT	Comparing the structural strength of AISI 4140 alloy steel with existing Steel UNI 10025 S355J2G3C. In this study ANSYS and FEMFAT had used	The results from the study showed that the new selected material prove high strength than existing material, because it experienced low equivalent stress, high safety factor and high endurance limit.	The gap from this study is the lack of estimating the fatigue lifecycle for proposed new material and it did not consider the dynamic behavior of impact loads.
12	Daher [31]	Study on fatigue strength analysis of a composite bogie frame case of AALRT.	Comparing material properties of existing steel at AALRT to the new proposed one of composite carbon/epoxy	The results showed that the carbon/epoxy had a good fatigue performance in comparison to structure steel.	Only static loading condition without considering dynamic parameters like changing speed were used.

As a bogie frame is a critical part of a train and supports almost the weight of a vehicle, and the major factors such as high impact load, high vibration, cyclic load, hunting instability [48] that can be influenced by wheel out-of-roundness affect the life of a bogie frame, Therefore, it is of great importance to analyse the life of a bogie frame under consideration of wheel out-of-roundness. To the best of my knowledge, no previous work had been conducted to quantify the effect of wheel out-of-roundness variation to the fatigue lifecycles of a railway bogie frame. Therefore, this research aims to predict the bogie frame's fatigue lifecycles due to the wheel OOR.

Chapter 3. Methodology

3.1. Introduction

This section explains the methodological process and approaches that has been used in this study to accomplish the objectives. In this study, all the data used has be collected from literature and the Ethio-Djibouti line. Three different cases of OOR have been considered to analyse their impact on the system. The wheel OOR cases have been integrated as wheel irregularity into the vehicle multibody system model in SIMPACK, where dynamic loads for each case have been extracted and applied to the FEM bogie frame model to analyze the effect of the wheel OOR on the fatigue life of the bogie frame.

The method used is summarized in the chart as shown in figure 3.1.

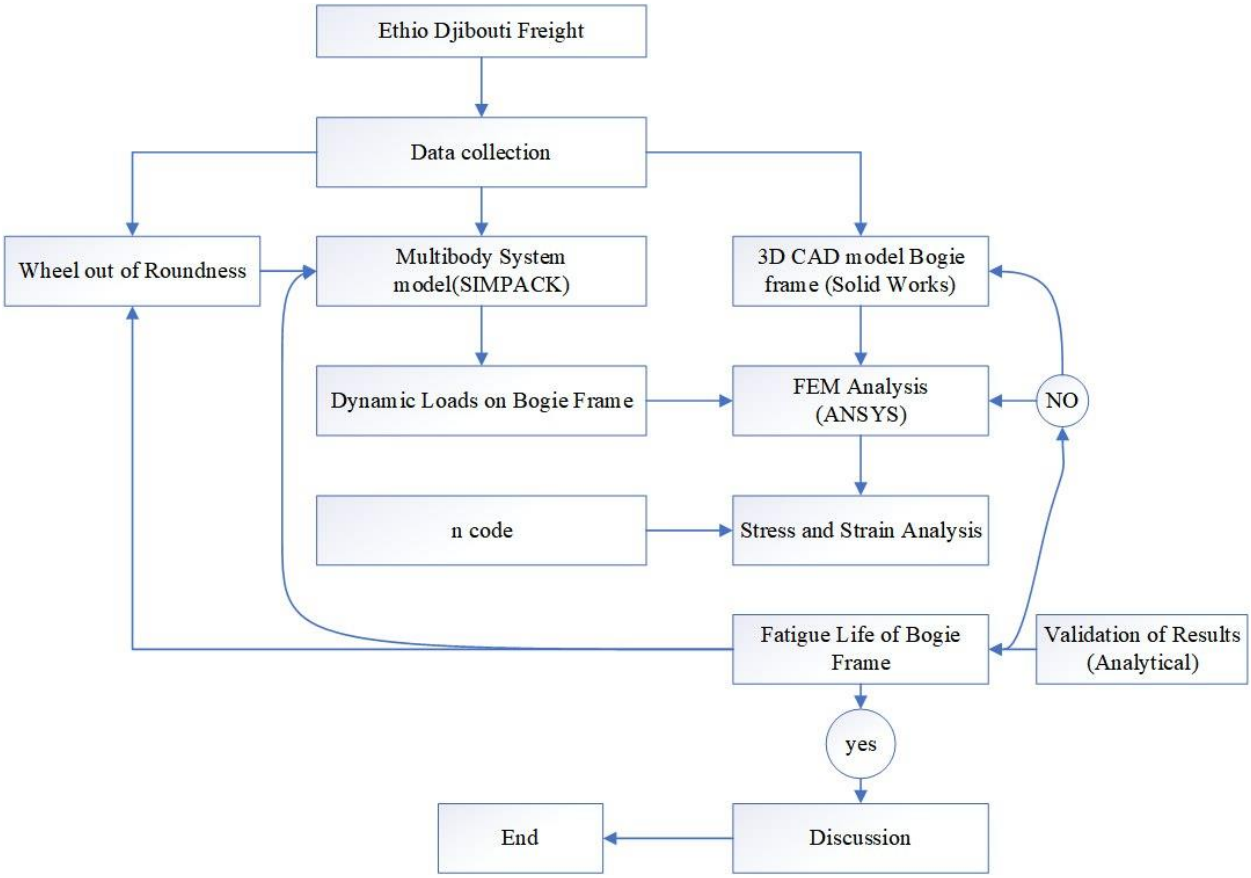

Figure 3. 1. Methodology flowchart

3.2. Data collection

Data used to accomplish this research has been collected from the Ethio-Djibouti Railway Line as a case study and related literature review. The related literature includes previously published articles, journals, conferences, books, and international standards protocols for railroads like EN and UIC. The dimensions for the wheel, rail, bogie, Carbody as well as all vehicle parameters required for multibody system design, such as weight, suspensions, and so on, has been collected.

In this study the most common used container freight wagon shown on figure 3.2 of model CW4 wagon used at Ethio-Djibouti railway line, applicable for running on standard gauge of 1435mm together with its bogie of model ZW35 bogie shown on figure 3.4 have been considered and their technical parameters have been described as appeared in appendix A . This CW4 wagon has been selected as a case to study because it is among the most affected wagon used at EDR that mostly being maintained due to high wheel defects problem which can have tread wear of up to 5 mm or higher as shown on figure 3.5 as one example of field measured wheel record during maintenance activitiy at EDR.

Figure 3. 2. Physical view of CW4 freight wagon used at Ethio-Djibouti line (Source: Ethio-Djibouti railway line project office)

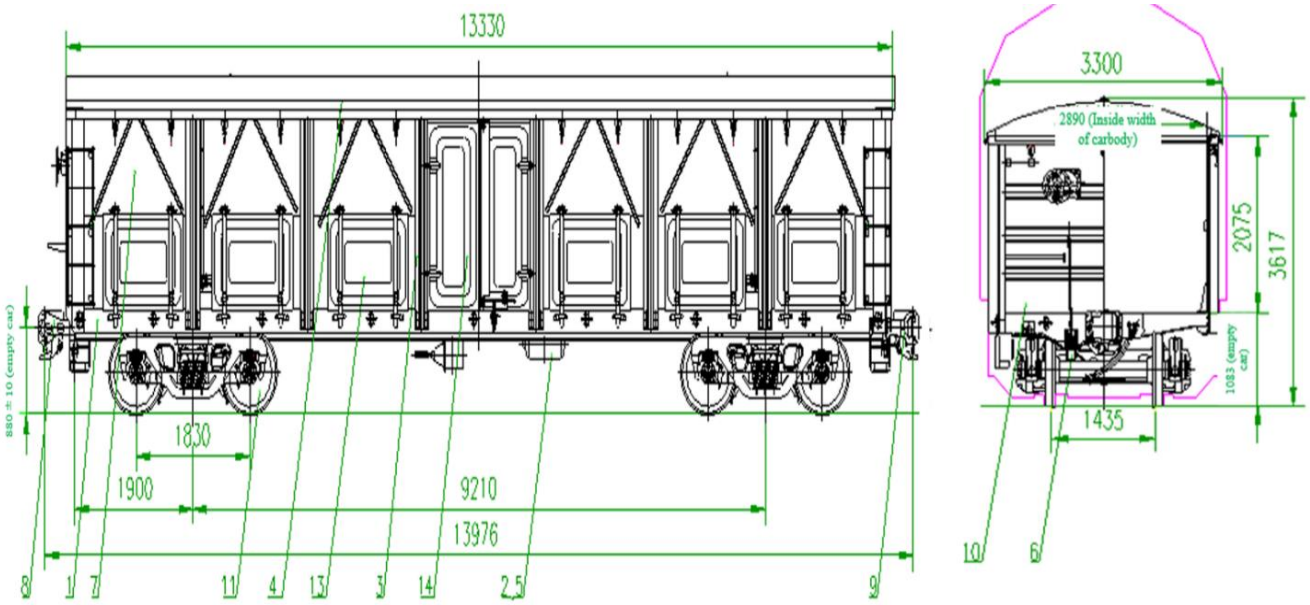

Figure 3. 3. Technical dimensions of CW4 freight wagon used at Ethio-Djibouti (Source: Ethio-Djibouti railway line project office)

Notation:

1. Underframe assembly 2. Underframe accessories 3. Side wall assembly 4. Side wall assembly 5. Air brake device 6. Hand brake device 7. Marking 8. Coupler and draft gear (Position 1) 9. Coupler and draft gear (Position 2) 10. End wall assembly 11. WZ35 bogie (Position 2) 12. WZ35 bogie (Position 1) 13. Lower side door 14. Side door

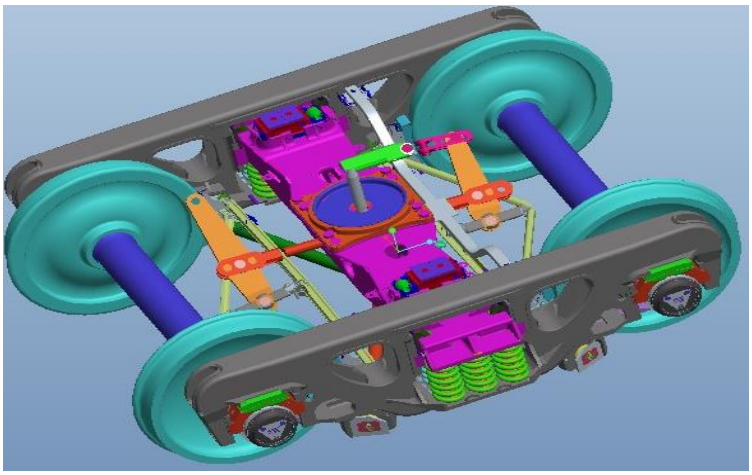

Figure 3. 4. ZW35 bogie used at Ethio-Djibouti (Source: Ethio-Djibouti railway line project office)

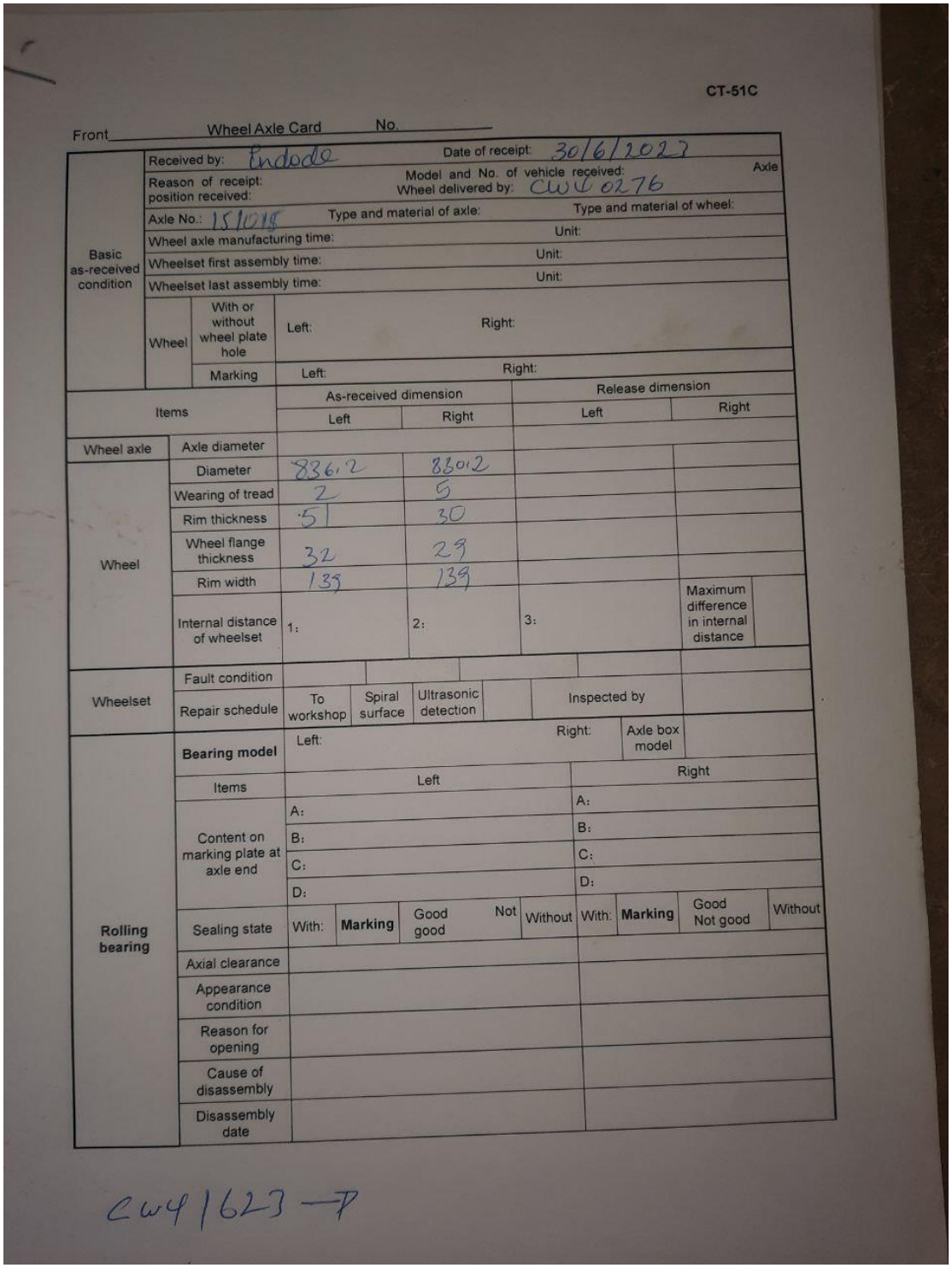

CT-51C

Front Wheel Axle Card No.

Basic as-received condition	Received by: Indode		Date of receipt: 30/6/2023			Axle
	Reason of receipt: position received:		Model and No. of vehicle received: Wheel delivered by: CW4 0276			
	Axle No.: 151014		Type and material of axle:		Type and material of wheel:	
	Wheel axle manufacturing time:			Unit:		
	Wheelset first assembly time:			Unit:		
	Wheelset last assembly time:			Unit:		
	Wheel	With or without wheel plate hole	Left:	Right:		
		Marking	Left:	Right:		

Items		As-received dimension		Release dimension	
		Left	Right	Left	Right
Wheel axle	Axle diameter				
Wheel	Diameter	836.2	836.2		
	Wearing of tread	2	5		
	Rim thickness	31	30		
	Wheel flange thickness	32	29		
	Rim width	139	139		
	Internal distance of wheelset	1:	2:	3:	Maximum difference in internal distance
Wheelset	Fault condition				
	Repair schedule	To workshop / Spiral surface / Ultrasonic detection		Inspected by	

Rolling bearing	Bearing model	Left:				Right:			Axle box model
	Items	Left				Right			
	Content on marking plate at axle end	A:				A:			
		B:				B:			
		C:				C:			
		D:				D:			
	Sealing state	With:	Marking	Good / Not good	Without	With:	Marking	Good / Not good	Without
	Axial clearance								
	Appearance condition								
	Reason for opening								
	Cause of disassembly								
	Disassembly date								

CW4/623-P

Figure 3. 4. Typical example of wheel defect field measured record from Indode maintenance depot at EDR on CW4 wagon.

3.3. Vehicle dynamic system

The vehicle dynamic of a railway system can be described by using the equation generally expressed in a matrix form as shown from equation 3.1 [49].

$$[M_v]\ddot{D}_v + [C_v]\dot{D}_v + [K_v]D_v = [F_{vt}] \quad (3.1)$$

Where $[M_v]$, $[C_v]$, [Kv], and $[F_{vt}]$ are mass, damping, stiffness, and external force matrices, respectively; while $\ddot{D}_v$,$\dot{D}_v$ and D_v are vectors for acceleration, velocity, and displacement of the vehicle subsystem, respectively. Furthermore, the subscripts v and t stand for the vehicle and track of the subsystem, respectively.

The whole trainset dynamic system is mostly described by the interaction between longitudinal, vertical and lateral dynamics. The trainset dynamic can be described by traction and braking system, rolling resistance, air resistance curving resistance, the effect of grades and pneumatic braking. The longitudinal dynamics define the motions of the vehicles in the direction of the track, it includes the motion of whole train and any relative motions that can be induced between the vehicles of rolling stock due to the looseness of connections between them. In the railway context, the relative motion between vehicles is called slack action because they are primarily allowed by the free slack in wagon connections. The longitudinal behavior of trains is depending on train control inputs from locomotive, topography of a track, curvature of the track, train brake inputs, characteristics of rolling stock and bogie as well as the characteristics of wagon connections. The wagons connection in longitudinal dynamics can be described by a system of differential equations. These differential equations can be developed by considering the generalized three mass connected vehicles as shown on figure 3.6 where leading is noted as m_1, in-train is m_2 and tail vehicle is m_3. All the vehicles are subjected to retardation and grade forces while traction and dynamic brake forces are added to powered vehicles.

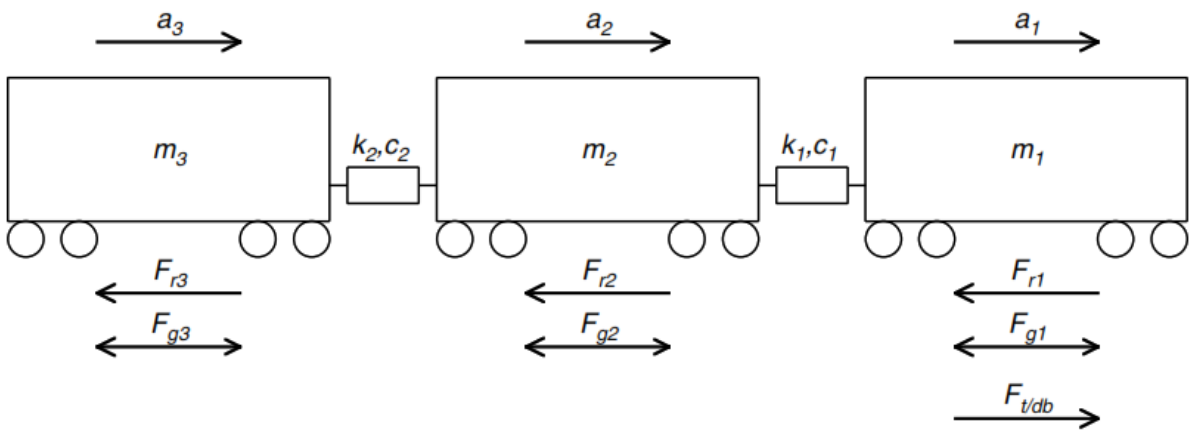

Figure 3. 5. Vehicle connection system [50]

Key: a is vehicle acceleration in m/sec^2; k is spring constant in N/m; c is damping constant in Nsec/m; m is vehicle mass in kg; v is vehicle velocity in m/sec; x is vehicle displacement in m; F_g is gravity force components due to track grade in N; F_r is the sum of retardation forces in N; and $F_{t/db}$ is traction and dynamic brake forces from a locomotive unit in N.

From the figure 3.6 it is noted that the grade force can be oriented in either direction. The total retardation forces F_r, is composed by summation of rolling resistance, curving resistance or curve drag, air resistance and braking (excluding dynamic braking which is more conveniently grouped with locomotive traction in the $F_{t/db}$ term). Rolling and air resistances can be usually grouped as a term known as propulsion resistance F_{pr}, so the equation for Fr can be written as

$$F_r = F_{pr} + F_{cr} + F_b \qquad (3.2)$$

Where F_{pr} is the propulsion resistance; F_{cr} is the curving resistance; and F_b is the braking resistance due to pneumatic braking. The three differential equations for three connected vehicles can be developed.

For linear wagon connection models the differential equations can be written as follows:

$$m_1a_1 + c_1(v_1 - v_2) + k_1(x_1 - x_2) = F_{t/db} - F_{r1} - F_{g1} \qquad (3.3)$$

$$m_2a_2 + c_1(v_2 - v_1) + c_2(v_2 - v_3) + k_1(x_2 - x_1) + k_2(x_2 - x_3) = -F_{r2} - F_{g2} \qquad (3.4)$$

$$m_3a_3 + c_2(v_3 - v_2) + k_2(x_3 - x_2) = -F_{r3} - F_{g3} \qquad (3.5)$$

Note that a positive value for gravity force F_g is taken as an upward grade. i.e., a retarding force.

Those equations (3.3), (3.4) and (3.5) can be proved by the help of free body diagram for each car from figure 3.6 as shown below:

For m_1

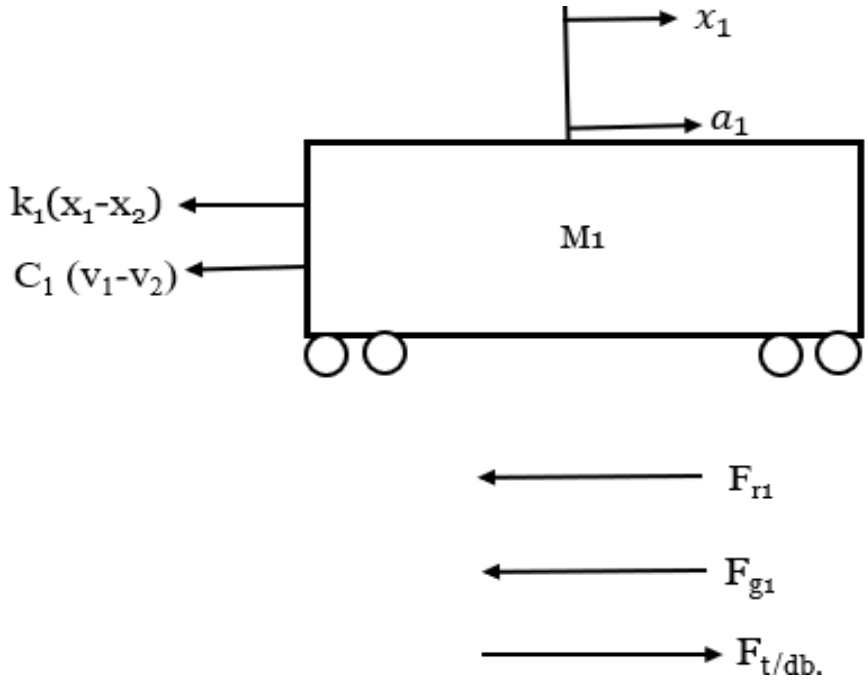

From Newton's second law of motion.

$$\Sigma F = ma, \text{ so, } \quad \Sigma F = m_1 a_1$$

$$F_{\frac{t}{db}} - F_{r_1} - F_{g1} - k_1(x_1 - x_2) - c_1(v_1 - v_2) = m_1 a_1$$

$$F_{\frac{t}{db}} - F_{r_1} - F_{g_1} = m_1 a_1 + k_1(x_1 - x_2) + c_1(v_1 - v_2)$$

$$m_1 a_1 + k_1(x_1 - x_2) + c_1(v_1 - v_2) = F_{\frac{t}{db}} - F_{r_1} - F_{g_1}$$

For m_2

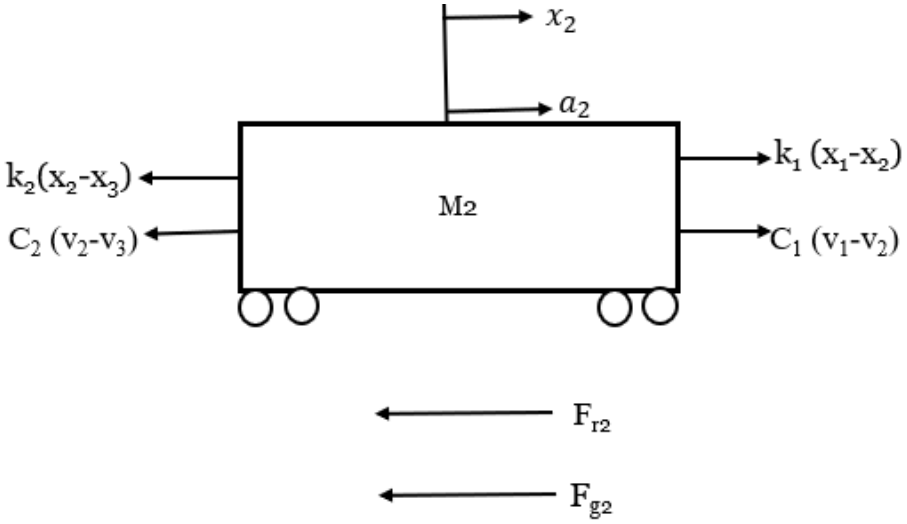

$$m_2a_2 = k_1(x_1 - x_2) + c_1(v_1 - v_2) - F_{r1} - F_{g_2} - k_2(x_2 - x_3) - c_2(v_2 - v_3)$$
$$m_2a_2 + k_2(x_2 - x_3) + c_2(v_2 - v_3) - k_1(x_1 - x_2) - c_1(v_1 - v_2) = -F_{r_2} - F_{g_2}$$
$$m_2a_2 + k_2(x_2 - x_3) + c_2(v_2 - v_3) + k_1(x_2 - x_1) + c_1(v_2 - v_1) = -F_{r_2} - F_{g2}$$

For m_3

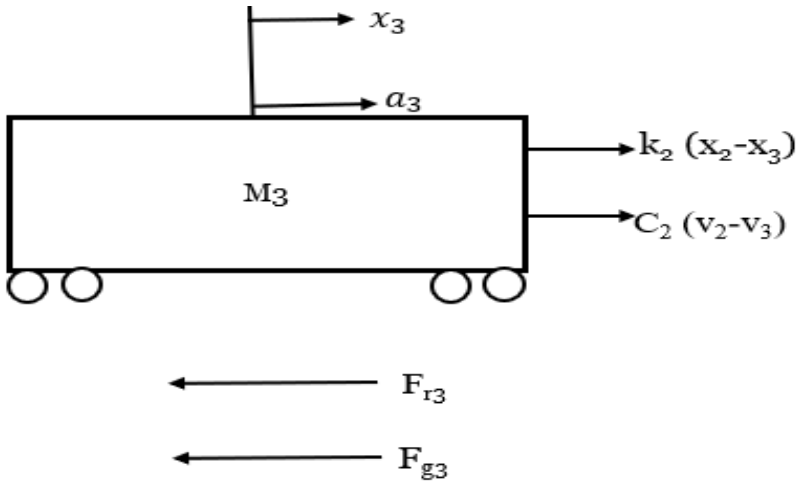

$$k_2(x_2 - x_3) + c_2(v_2 - v_3) - F_{r_3} - F_{g3} = m_3a_3$$
$$m_3a_3 + k_2(x_3 - x_2) + c_2(v_3 - v_2) = -F_{r_3} - F_{g_3}$$

By allowing the locomotives to be placed at any train position and make extension for notation of equation for a trainset of a given number of vehicles or wagons, a more general set of differential equations of motion can be written as follow:

i. For the front or leading vehicle we have:

$$m_1 a_1 + c_1(v_1 - v_2) + k_1(x_1 - x_2) = F_{t/db1} - F_{r1} - F_{g1} \quad (3.6)$$

ii. For the ith vehicle we have:

$$m_i a_i + c_{i-1}(v_i - v_{i-1}) + c_i(v_i - v_{i+1}) + k_{i-1}(x_i - x_{i-1}) + k_i(x_i - x_{i+1}) = F_{t/dbi} - F_{ri} - F_{gi} \quad (3.7)$$

iii. For the nth or the last vehicle in a trainset will be expressed as:

$$m_n a_n + c_{n-1}(v_n - v_{n-1}) + k_{n-1}(x_n - x_{n-1}) = F_{t/dbn} - F_{rn} - F_{gn} \quad (3.8)$$

Note: by integrating the $F_{t/db}$ in each equation of every vehicle, this indicates that these equations can be applied to any locomotive placement or system of distributed power. For the unpowered vehicles this term of $F_{t/db}$ will be taken as zero as no traction or dynamic braking forces due to power system.

For complex nonlinear connected system, the stiffness and damping constants are replaced with functions where the stiffness is usually expressed as a function of displacement and damping expressed as a function of velocity. Furthermore, more complex functions that incorporate a second independent variable (i.e. displacement and velocity for a stiffness function) can be used also. In this case the generalized non-linear differential equations can be expressed as follow:

i. For the front or leading vehicle:

$$m_1 a_1 + f_{wc}(v_1, v_2, x_1, x_2) = F_{t/db1} - F_{r1} - F_{g1} \quad (3.9)$$

ii. For the ith vehicle:

$$mia_i + f_{wc}(v_i, v_{i-1}, x_i, x_{i-1}) + f_{wc}(v_i, v_{i+1}, x_i, x_{i+1}) = F_{t/dbi} - F_{ri} - F_{gi} \quad (3.10)$$

iii. For the nth or the last vehicle in trainset will be expressed as :

$$m_n a_n + f_{wc}(v_n, v_{n-1}, x_n, x_{n-1}) = F_{t/dbn} - F_{rn} - F_{gn} \qquad (3.11)$$

Where f_{wc} is the non-linear function that describe the full wagon connection characteristics.

In general, the solution and simulation of the above dynamic set of equations is too complicated by the need to calculate the forcing inputs to the system, i.e. $F_{t/db}$, F_r and F_g. The traction-dynamic brake force term $F_{t/db}$, must be updated continually for driver control adjustments and any changes to the speed of locomotive. The resistance forces F_r, are depending on settings of braking, curvature, speed and rolling stock design. The components of gravity force F_g, are depending on track grade and the position of the vehicle on the track. The most challenges for modelling and simulation of train dynamic are due to the nonlinearities of air gap (coupler slack), draft gear spring characteristic, (polymer or steel) and stick-slip friction provided by a wedge system.

As discussed above on basic train vehicle dynamic system, the basic interconnected mass-damper-spring type model that representing the train vehicle masses and wagon connections provide a complicated system due to nonlinear spring, nonlinear gap and stick slip friction elements. This complexity may provide limitation in modelling and simulation with available software packages i.e. the whole system models are computationally expensive, therefore, some simplification to allow the reasonable run times for simulation studies has to been made.

Based on previous approaches for various studies related to multibody modelling for a complex trainset system where it is difficult to analyse whole system due to computational purpose, therefore in this study the effect between adjacent wagons was not considered means that a representative single freight vehicle model composed by one carbody, rear and front bogies has been modelled in SIMPACK software and the required input parameters for this system has been integrate to generate the induced dynamic loads on a bogie frame. The study has based on analysis of the lifecycles of a highly affected bogie frame based on the dynamic loads from multibody SIMPACK software.

The figure 3.9 shows typical representative railway vehicle dynamic model composed by 1 carbody, 2 bogie frames, 4 wheelsets, 2 sets of secondary suspension and 4 sets of primary suspension and it is clearly shown that can be used to represent a studied CW4 single wagon shown on figure 3.2 and 3.3.

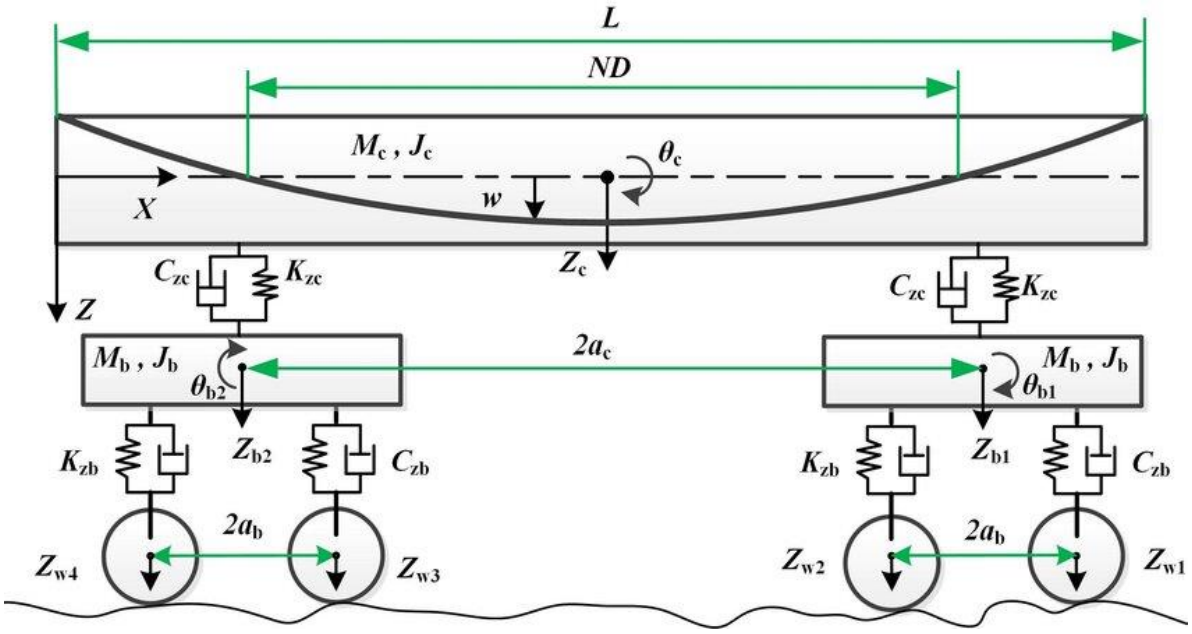

Figure 3. 6. Typical railway vehicle dynamic model [51]

In this simplified vehicle model, the 7 degrees of freedom (DOFs) which are elastic vibration caused by first order vertical bending (FVB) mode of carbody, carbody bouncing Z_c and pith θ_c, two bogie frames bounce and pitch Z_{b1}, Z_{b2}, θ_1 and θ_2 are the most dominate. The wheelsets are supposed to be closely on the rails so that no wheel jumping happens and the wheelsets vertical movement are exactly the same as track irregularities.

When the carbody is assumed to be free-free uniform cross-section Euler-Bernoulli beam (UCEB), the elastic carbody equation of the motion can be expressed as *[51]*:

$$EI\frac{\partial^4 w(x,t)}{\partial x^4} + \mu I\frac{\partial^5 w(x,t)}{\partial x^4 \partial t} + \rho A\frac{\partial^2 w(x,t)}{\partial t^2} = F_{zc1}\delta(x - x_1) + F_{zc2}\delta(x - x_2) \qquad (3.12)$$

Where $w(x,t)$ is the vertical displacement of the carbody, EI is the bending stiffness, ρA is the mass/length which is assumed to be constant over length L, μI is the structural damping coefficient, $\delta(x)$ is Dirac function, F_{zci} is external load which act at the point x_i on the secondary suspension location.

The expression for the displacement response $w(x,t)$ of carbody at any location x can be expressed as the superposition of carbody two rigid modes and first order vertical bending mode of a carbody as follow:

$$w(x,t) = Z_c(t) + (x - \frac{L}{2})\theta_c(t) + Y_1(x)q_1(t) \qquad (3.13)$$

Where $Y_1(x)$ stands for FVB modal shape while $q_1(t)$ stands for its principal coordinate.

The equation of the motion for vehicle model on figure 3.9 can be expressed in matrices form as

$$M\ddot{z} + C\dot{z} + Kz = Q \qquad (3.14)$$

Where Z is $[Z_c \quad \theta_c \quad q_1 \quad Z_{b1} \quad \theta_{b1} \quad Z_{b2} \quad \theta_{b2}]^T$; M is mass matrix that is diag(m_c, J_c, 1, m_b, J_b, m_b, J_b); K is stiffness matrix; C is damping matrix and Q is external excitation forces vector.

$$\boldsymbol{K} = \begin{bmatrix} 2k_{zc} & 0 & 2k_{zc}Y_1(x_1) & -k_{zc} & -k_{zc} & 0 & 0 \\ 0 & 2k_{zc}a_c^2 & 0 & -k_{zc}a_c & k_{zc}a_c & 0 & 0 \\ 2k_{zc}Y_1(x_1) & 0 & 2k_{zc}Y_1^2(x_1) + k_q & -k_{zc}Y_1(x_1) & -k_{zc}Y_1(x_1) & 0 & 0 \\ -k_{zc} & -k_{zc}a_c & -k_{zc}Y_1(x_1) & 2k_{zb} + k_{zc} & 0 & 0 & 0 \\ -k_{zc} & k_{zc}a_c & -k_{zc}Y_1(x_1) & 0 & 2k_{zb} + k_{zc} & 0 & 0 \\ 0 & 0 & 0 & 0 & 0 & 2k_{zb}a_b^2 & 0 \\ 0 & 0 & 0 & 0 & 0 & 0 & 2k_{zb}a_b^2 \end{bmatrix} \qquad (3.15)$$

$$\boldsymbol{C} = \begin{bmatrix} 2c_{zc} & 0 & 2c_{zc}Y_1(x_1) & -c_{zc} & -c_{zc} & 0 & 0 \\ 0 & 2c_{zc}a_c^2 & 0 & -c_{zc}a_c & c_{zc}a_c & 0 & 0 \\ 2c_{zc}Y_1(x_1) & 0 & 2c_{zc}Y_1^2(x_1) + c_q & -c_{zc}Y_1(x_1) & -c_{zc}Y_1(x_1) & 0 & 0 \\ -c_{zc} & -c_{zc}a_c & -c_{zc}Y_1(x_1) & 2c_{zb} + c_{zc} & 0 & 0 & 0 \\ -c_{zc} & c_{zc}a_c & -c_{zc}Y_1(x_1) & 0 & 2c_{zb} + c_{zc} & 0 & 0 \\ 0 & 0 & 0 & 0 & 0 & 2c_{zb}a_b^2 & 0 \\ 0 & 0 & 0 & 0 & 0 & 0 & 2c_{zb}a_b^2 \end{bmatrix} \qquad (3.16)$$

$$\boldsymbol{Q} = c_{zb}\begin{bmatrix} 0 \\ 0 \\ 0 \\ \dot{z}_{w1} + \dot{z}_{w2} \\ \dot{z}_{w3} + \dot{z}_{w4} \\ a_b(\dot{z}_{w1} - \dot{z}_{w2}) \\ a_b(\dot{z}_{w3} - \dot{z}_{w4}) \end{bmatrix} + k_{zb}\begin{bmatrix} 0 \\ 0 \\ 0 \\ z_{w1} + z_{w2} \\ z_{w3} + z_{w4} \\ a_b(z_{w1} - z_{w2}) \\ a_b(z_{w3} - z_{w4}) \end{bmatrix} \qquad (3.17)$$

3.4. Modelling

3.4.1. Wheel out-of-roundness

The wheel OOR excitations have to be expressed in terms of radius deviation against wheel rotation angle, where the expression for radius deviation can be shown on equation 3.12 [52].

$$\Delta r = R(x) - Ro \qquad (3.12)$$

Where Δr stand for deviation in radius from mean radius, R(x) is radial profile and Ro is mean or nominal wheel radius. The three cases of wheel OOR excitations with maximum radius deviation of 1 mm, 2 mm and 5 mm considered in this study based on the data from maintenance department as appeared in appendix B have been shown in the figures 3.10 (a), (b) and (c), respectively.

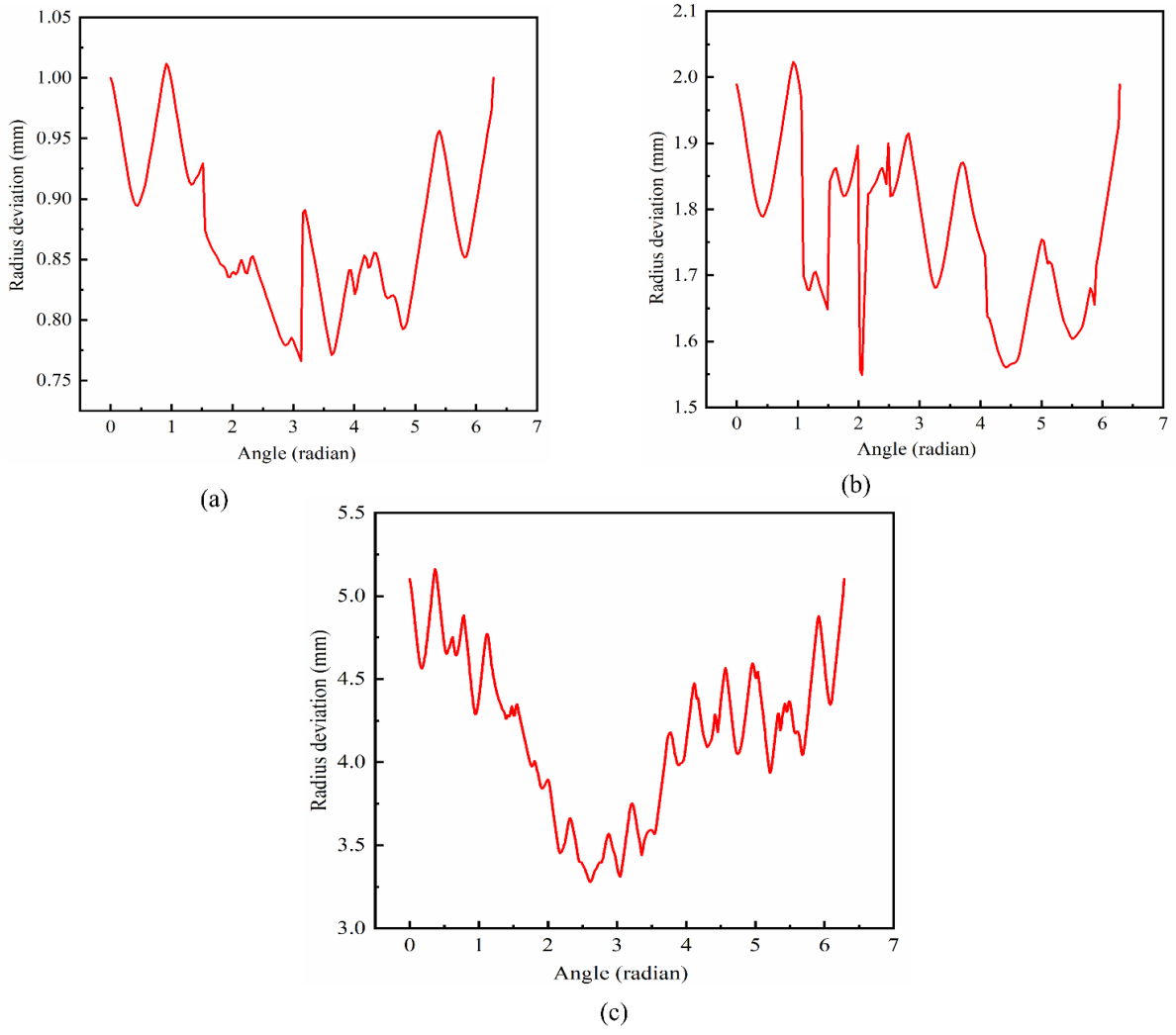

Figure 3. 7. OOR excitations with: (a) 1 mm, (b) 2 mm and (c) 5 mm max radius deviation

3.4.2. Modelling of multibody system in SIMPACK

The design and dynamic analysis of a railway vehicle nowadays can be performed through computational programs, where a railway vehicle can be modelled as a multibody mechanical system. The dynamic effect of a railway vehicle can be analyzed with the commercial software based on a representative railway vehicle model which reflects its essential mechanical properties. The multibody system approach in a railway is powerful and most widely used method when dynamic behaviors of running vehicle need to be analyzed in cost-effective manner. The outputs results from a representative railway vehicle model analysis with multibody system can be used to provide accurate predictions of dynamic behavior of a vehicle and its track interaction. The typical freight wagon in multibody system is composed by three main subsystems which are the wagon body, front and rear bogies. Carbody, bogie frame and wheelset are the most dominating body components as they represent the main vehicle mass [53]. When they used as a rigid bodies they are defined by their mass, moments of inertia and position of center of gravity. SIMPACK software has been used in this study to provide a representative multibody dynamic model of a freight wagon at EDR composed by one carbody, two bogies, four wheelsets, primary suspension as well as secondary suspension system as shown on figure 3.14. Also rail-wheel contact has been demonstrated so that can help to integrate the out-of-roundness of wheel to the system. Rail-wheel contact used has been demonstrated based on simplified version of non-linear equation of FASTSIM.

3.4.2.1. Process followed to design a freight wagon vehicle system in SIMPACK Preprocessor

The multibody freight vehicle model used in this study has been developed in one of the most well-known multibody software SIMPACK used in railway system. SIMPACK software has both pre and post-processor, where pre-processor is used for modelling a complete vehicle model and the results of interest are provided from post-processor. The multibody model used in this study is presented by one carbody, two bogies, four wheelsets where these bodies are interconnected by force elements such as spring and dampers which form primary and secondary suspension system, where primary suspension connect wheelset to the bogie frame and secondary suspension connect bogie to the carbody, and joints or similar constraints have been used. Entire system has been modelled through vehicle model, track model as well as wheel-rail contact based on specifications. Inertia characteristics such as mass, moments of inertia and position of the center of gravity of

these bodies have been integrated in SIMPACK during modelling. In ideal condition without any irregularity the front and rear bogies receive identical loading from a carbody through secondary suspension. But in this study where wheel out-of-roundness has to be analyzed the following assumptions have been considered:

- The wheel out-of-roundness excitation has been integrated on wheel for front bogie, therefore the highly affected bogie frame is for front bogie that has been considered in finite element analysis to estimate its lifecycles.

Figure 3.8 shows the tree model steps followed to design multibody freight model in SIMPACK.

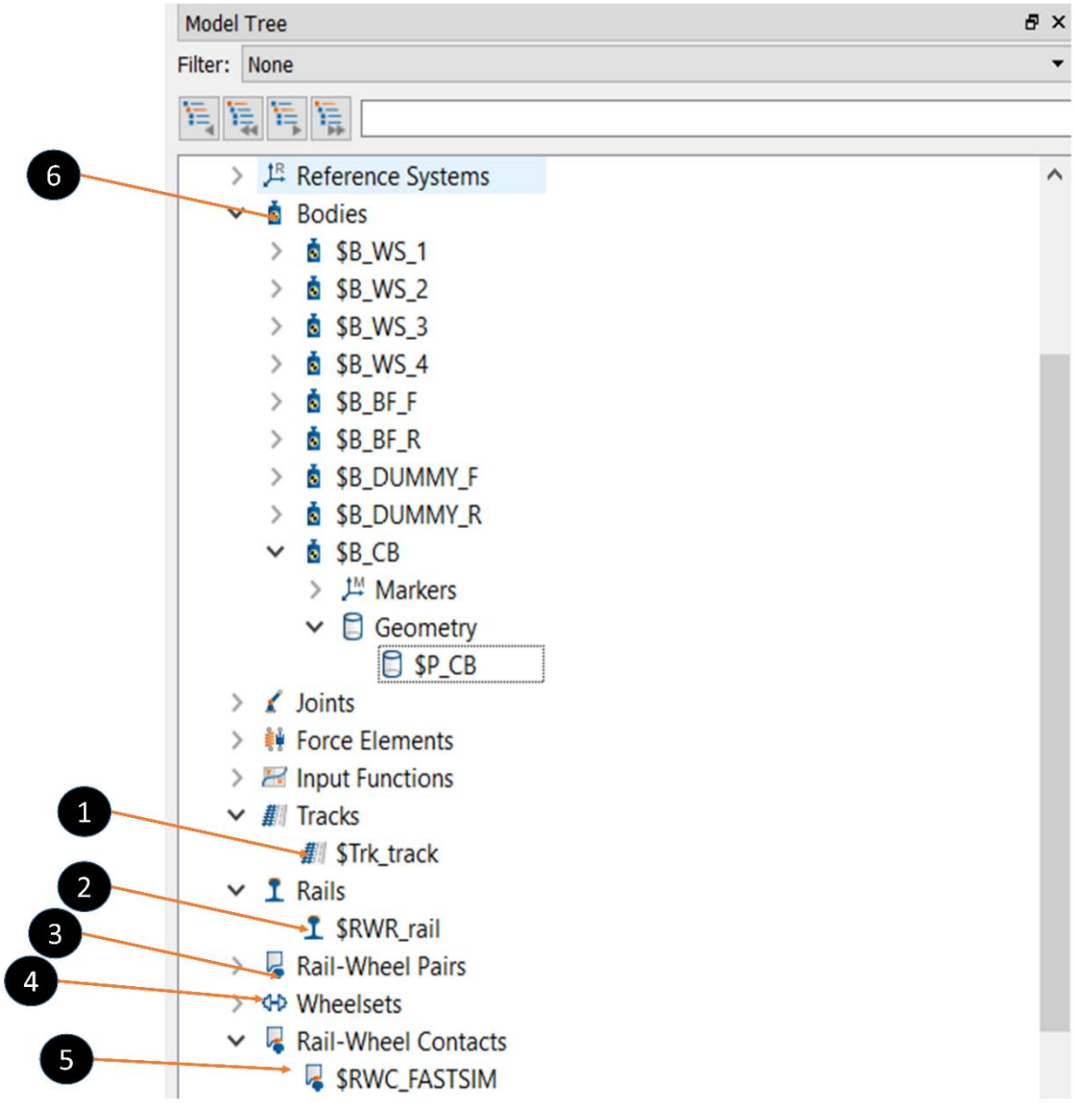

Figure 3. 8. Model tree for railway vehicle in SIMPACK

1 is based on creation rail track that hold the whole system. 2 is based on creation rails both right and left rails that used as guidance for the wheel. 3 is based on creation wheel and rail pairs. 4 is about creation of wheelsets which is simply a set of 2 wheels and 1 axle. 5 is creation of rail-wheel contacts. 6 is based on creation of vehicle model bodies such as carbody (CB), front bogie frame (BF_F), rear bogie frame (BF_R), all four wheelsets (WS) as shown on the figure 3.11. These bodies are considered as rigid body where their mass-inertia properties and the position of center of the gravity have been integrated as seen from figure 3.12 as an example for carbody (CB) properties.

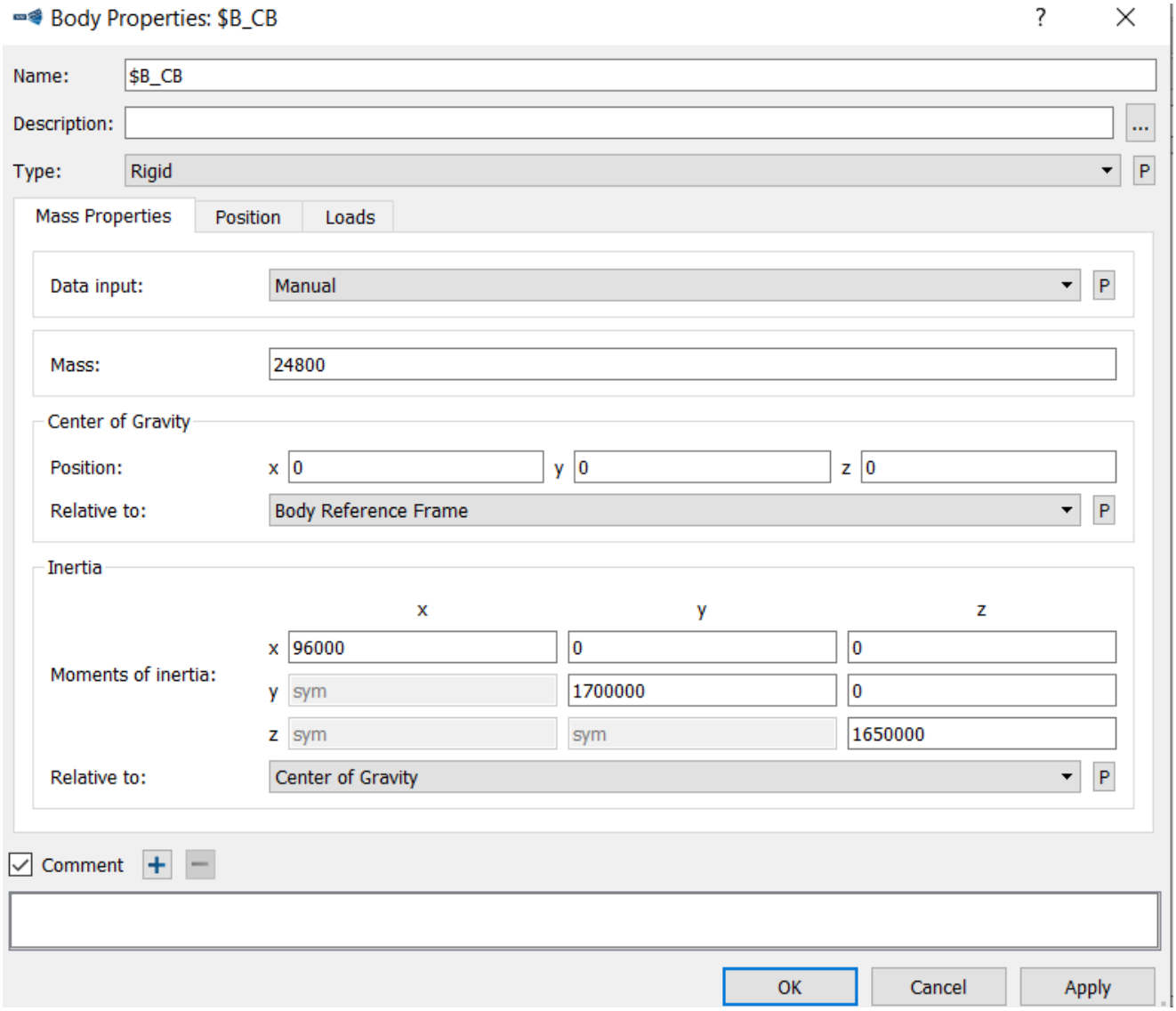

Figure 3. 9. Rigid body properties

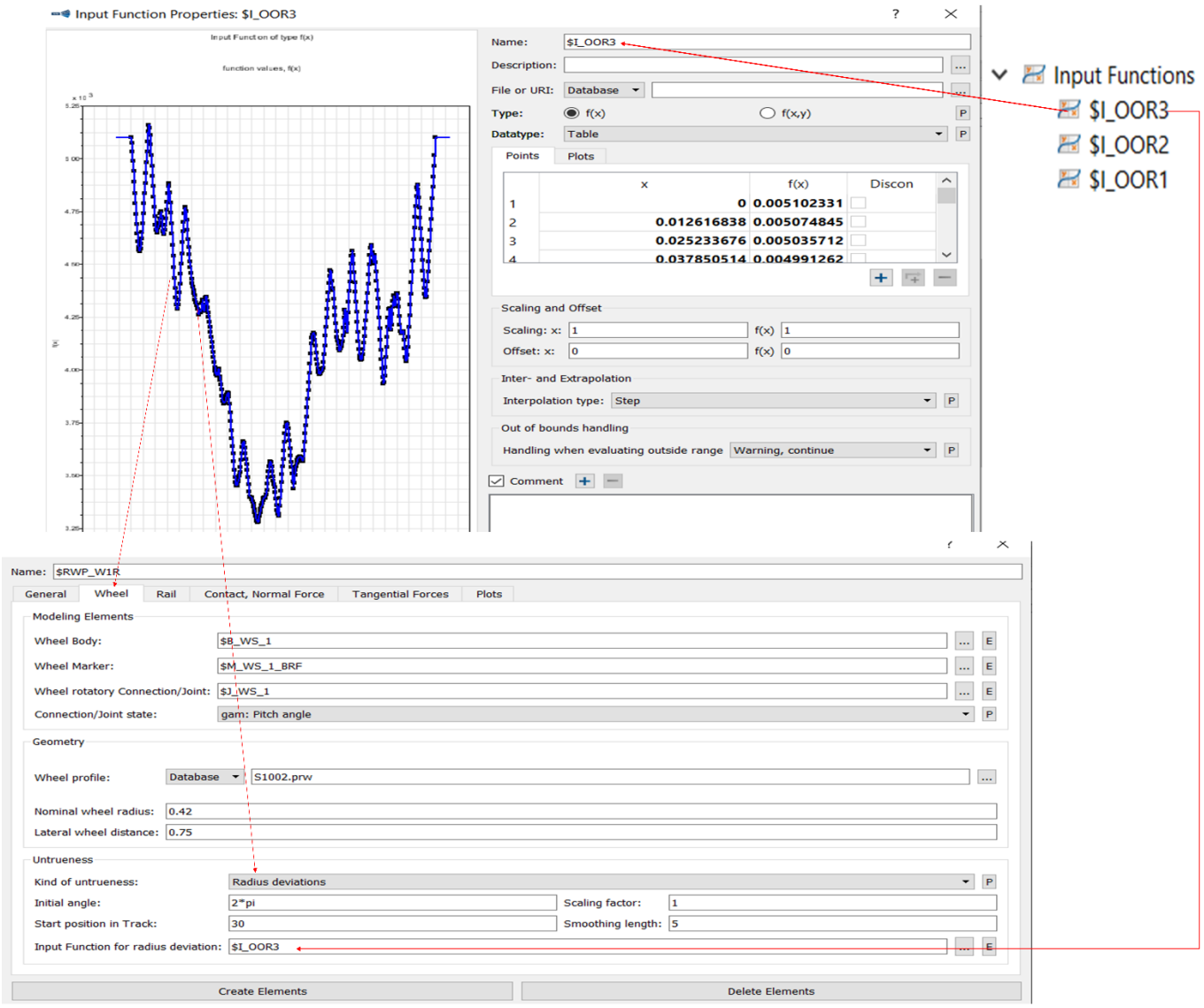

Figure 3. 10. Integration of OOR excitation to the vehicle system

The figure 3.13 shows the steps followed for the integration of wheel out-of-roundness data to the vehicle system in SIMPACK. Where it starts with creation of input functions for each OOR cases where OOR1 is for roundness with maximum radius deviation of 1 mm, OOR2 is for the case of 2 mm and OOR3 is for the case of 5 mm. By creation of input function the system shows you where to put coordinates, X stands for wheel rotation angles in radian while f(x) stands for radius deviations in m. After integration of the data, system generate required excitation itself and the

next step is to integrate the generated excitation to the wheel of interest through wheel-rail pairs of the model tree.

After integration of all specifications and related data to the system, we have a complete freight wagon multibody vehicle model as shown on figure 3.14

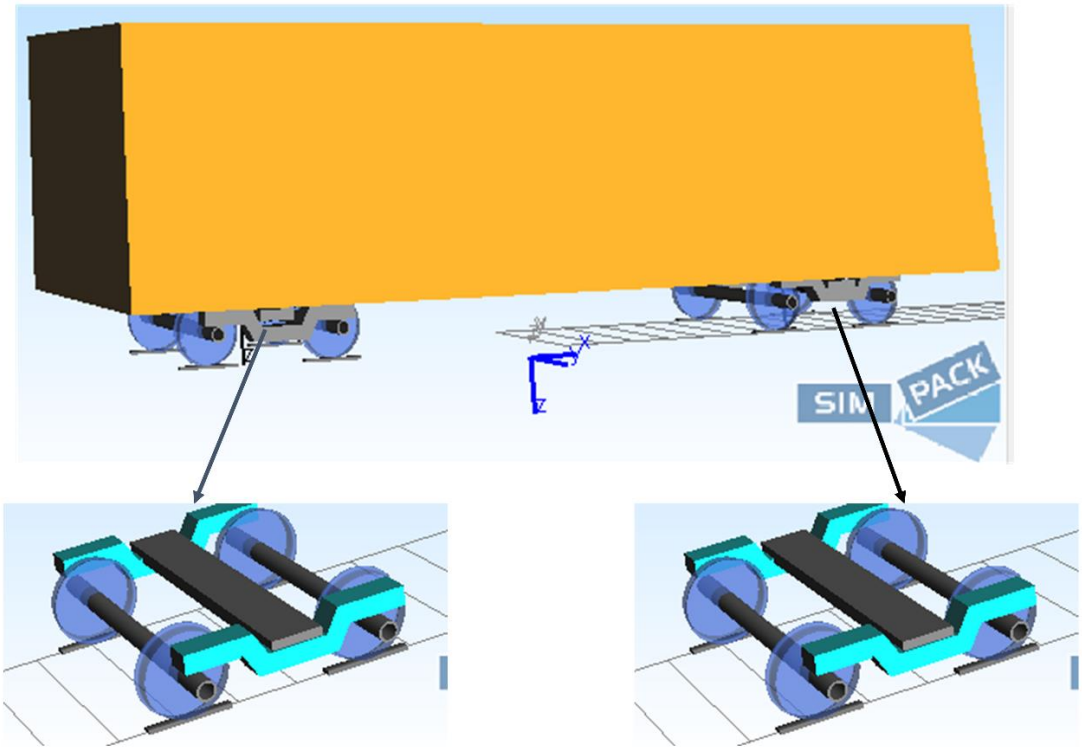

Figure 3. 11. Multibody vehicle model in SIMPACK

Validation of Multibody vehicle in SIMPACK

In multibody system software SIMPACK, the model is validated if the preload condition gives constant contact forces to all wheel contacts. In this study the freight wagon model has been validated based on preloading condition and the results showed that the model is validated as the contact forces to all wheelset is the same (50.766 KN) as shown on figure 3.15

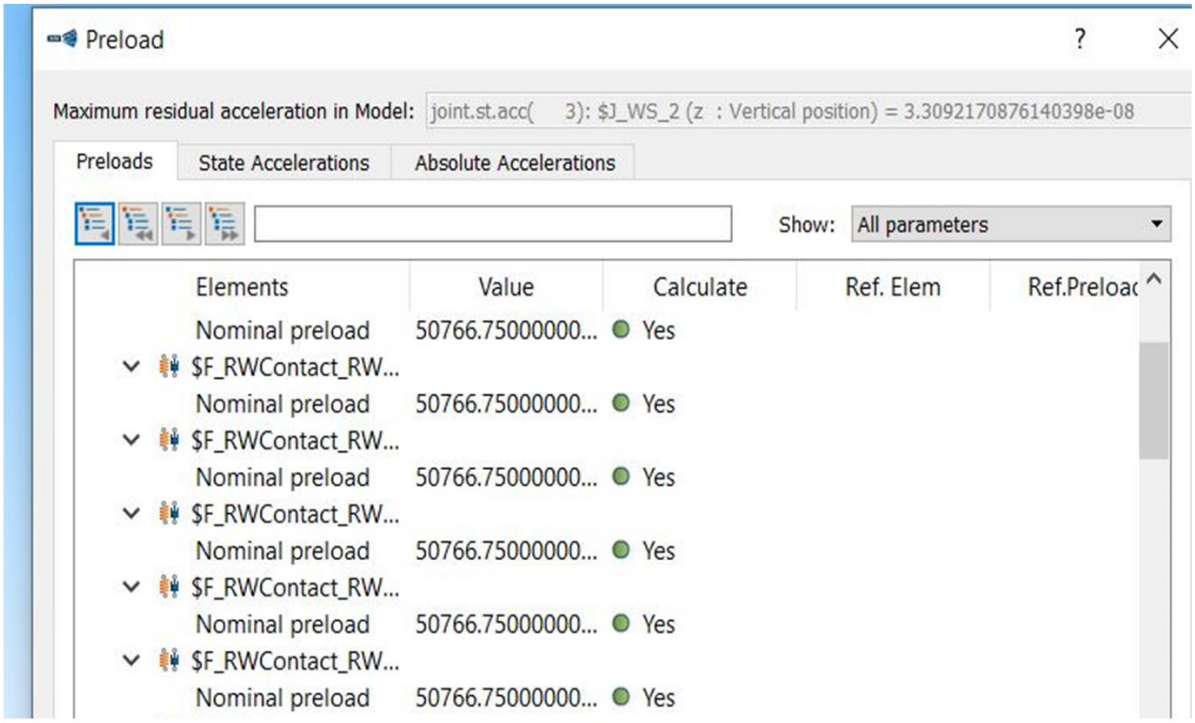

Figure 3. 12. Preloading condition for model validation purpose

3.4.2.2. Post-processor in SIMPACK

This post-processor is the part of SIMPACK software that is used to display various results of interests resulted from running the system from pre-processor under time integration through solver settings. Through the simulation of complete railway vehicle model in SIMPACK the various dynamic results on specific part of interests can be recorded. Therefore in this study the part of interest is the dynamic loads induced on a bogie frame due to wheel out-of-roundness. The assumption made to accomplish the aim of the study is based on integration of wheel out-of-roundness to the one wheel of front bogie, therefore the highly influenced bogie frame is recognized as a front bogie frame where both vertical, lateral and longitudinal impact dynamic loads induced on front bogie frame have been recorded and plotted and their maximum magnitude forces have been applied to the representative front bogie frame designed with its specification from Ethio-Djibouti Railway in finite element with ANYS Workbench. After that the stress, strain and deformation distributions on that FEM front bogie frame have been recorded on each OOR case and used in estimation of the fatigue lifecycles of a bogie frame under the influence of wheel OOR.

The figure 3.16 shows the results tree in SIMPACK post-processor. Notation 1 shows where you can extract the wheel-rail contact force outputs for each wheel of the model mainly used when you want to analyse dynamic behavior of a railway wheel-rail contact. Notation 2 shows where the display of dynamic forces on primary suspension system exits for front bogie while notation 3 shows primary suspension for rear bogie. Notation 4 shows where dynamic forces on secondary suspension which represent the dynamic forces induced on the bogie frame are displayed for front bogie frame on both right and left sides while notation 5 represent induced dynamic forces on the rear bogie frame for both right and left sides. (SS stand for secondary suspension, PS for primary suspension, F for front side, R for rear side). As mentioned in above discussion in this study the wheel OOR cases have been integrated on the wheel for front bogie, therefore the results showed that the highly influenced bogie frame is front bogie frame so in the fatigue life analysis the highly influenced front bogie frame has been selected and the dynamic forces results induced on it due to the impact from whole vehicle system have been extracted and their maximum magnitude used in FEM analysis.

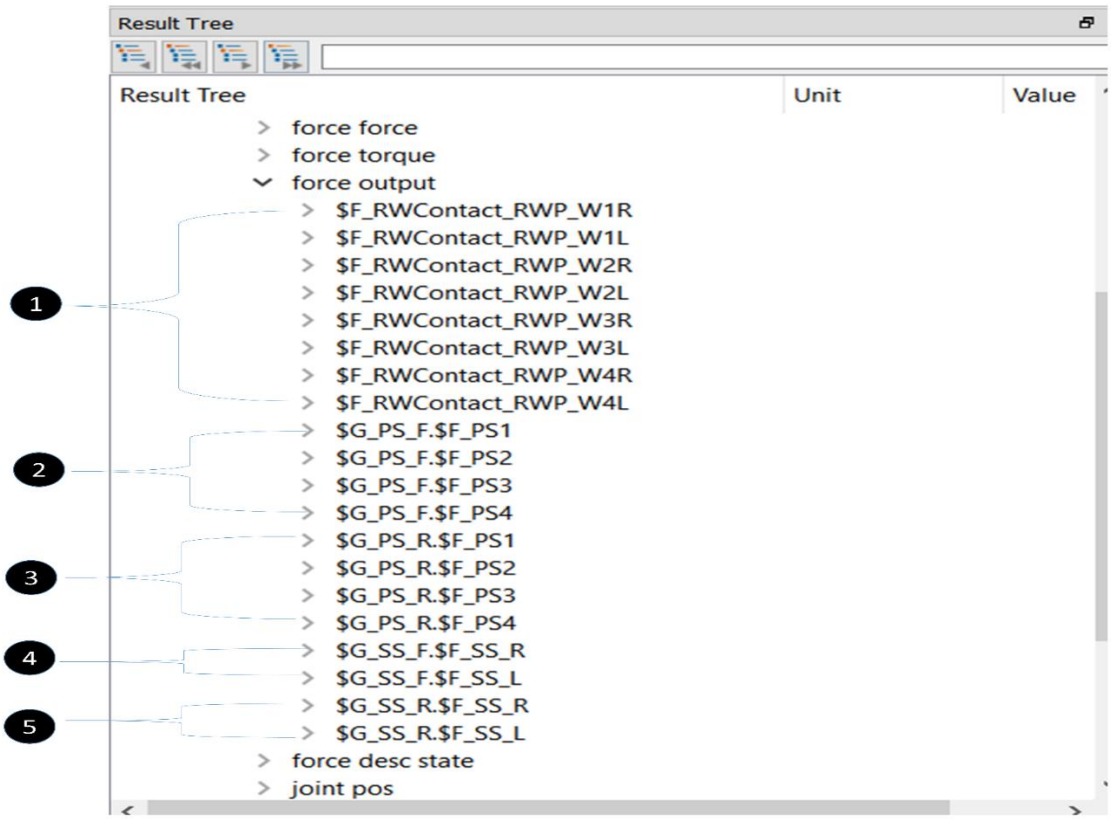

Figure 3. 13. Results tree in post-processor of SIMPACK

Figure 3.17 shows the technique used to extract the dynamic load time history induced on a highly influenced front bogie frame for for both vertical, lateral and longitudinal directions. These forces have been plotted for each OOR case and their maximum magnitude have been applied to the designed front bogie frame in FEM as shown in the next section of FEM modeling.

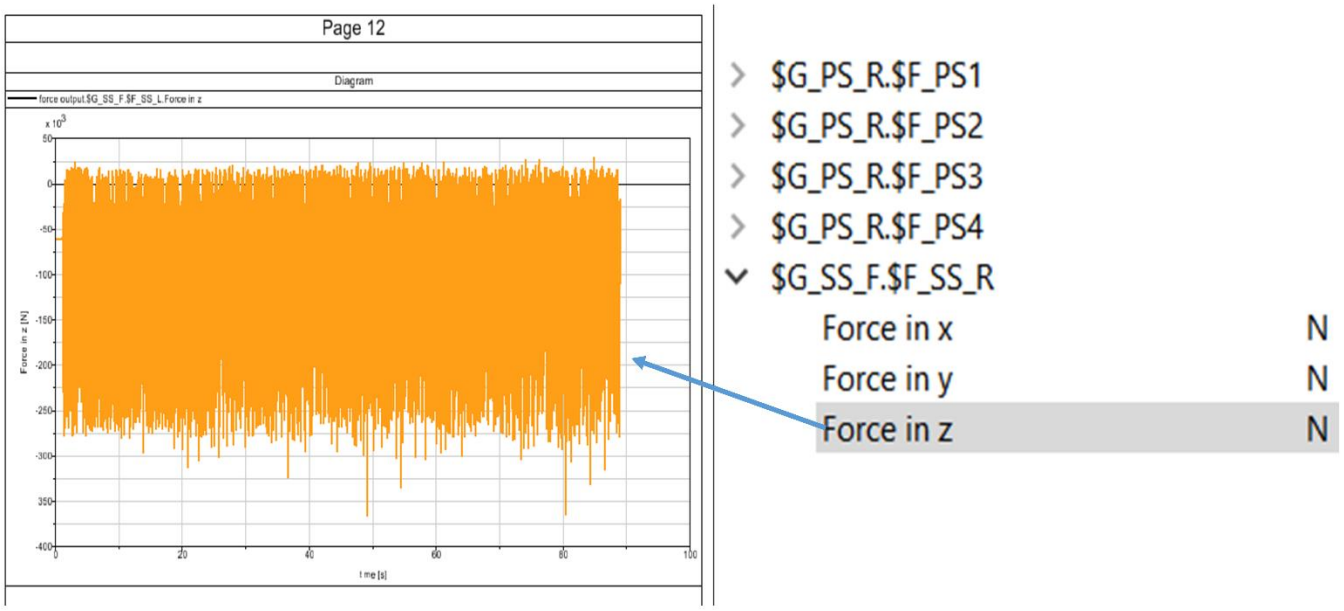

Figure 3. 14.Extraction of dynamic force time history

3.4.3. CAD and FEM modelling

Three dimensional model of front bogie frame based on technical specification from EDR was modelled by using SOLIDWORKS as CAD tool. The 3D model from this CAD tool is shown on figure 3.18. The CAD model has been saved as IGS format and exported to the finite element tool with ANSYS Workbench. The FEM model is shown on figure 3.19. This FE method has been used to analysis stress and strain distribution on the highly affected front bogie frame structure due to wheel OOR. The analysis has been done through the main 3 processes which are pre-processing, processing and post-processing.

I. Pre-processing

This step is characterized by generating the model first, but in this study the model was created by using other software (SOLIDWORKS 2019). So the IGS file from SOLIDWORKS has been imported into ANSYS Workbench 2020R as the initial step. Assignment of material properties for

bogie frame has also took place in this stage. The material properties for bogie frame used in the study made by Q450NQR1 steel has been shown in tables 3.1 and 3.2. Also generation of element mesh has been performed under this stage. The triangular element type has been used. Element size was 15 mm, the number of elements are 164751 and 287277 as number of nodes.

II. Processing

This is the analysis stage that composed by assigning the boundary conditions (loads and constraints) and solving the system to get required solution. The boundary conditions used in the study is shown on figure 4.10 that consider both vertical, lateral and longitudinal effect on a bogie frame.

III. Post-processing

This last stage is based on visualizing the results and listing the required results either by tabular or printing. In this study the stress and strain distribution were the main required results from FEM that have been used for fatigue life prediction with nCode software.

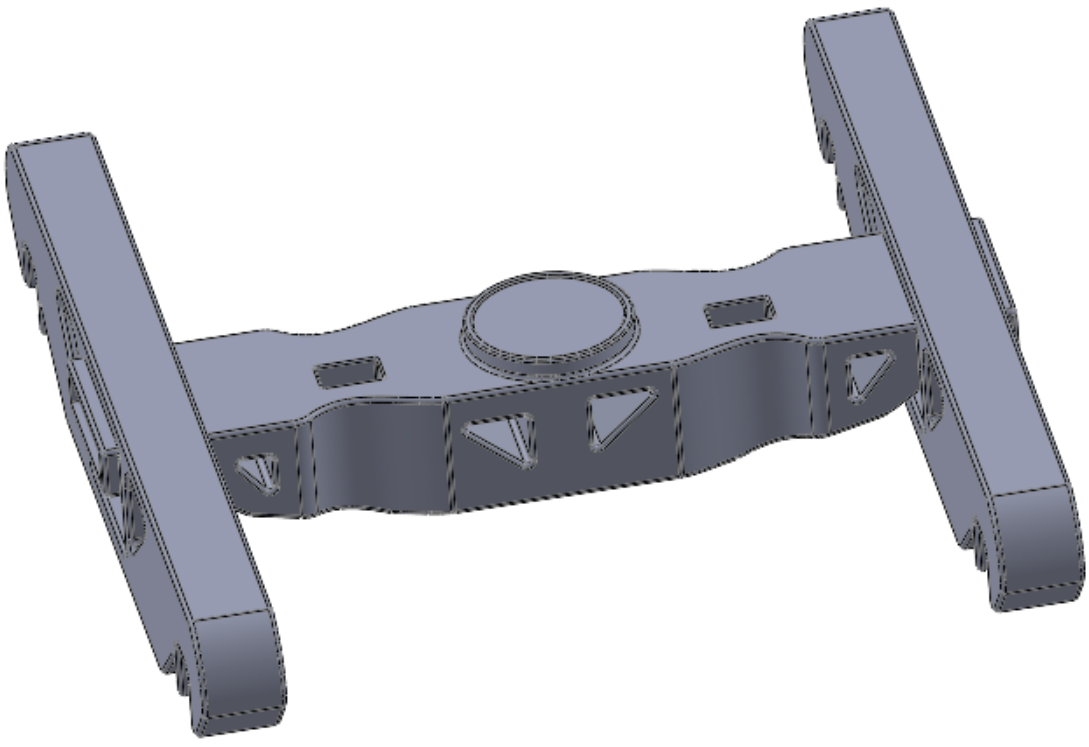

Figure 3. 15. 3D CAD model of front bogie frame in SOLIDWORKS

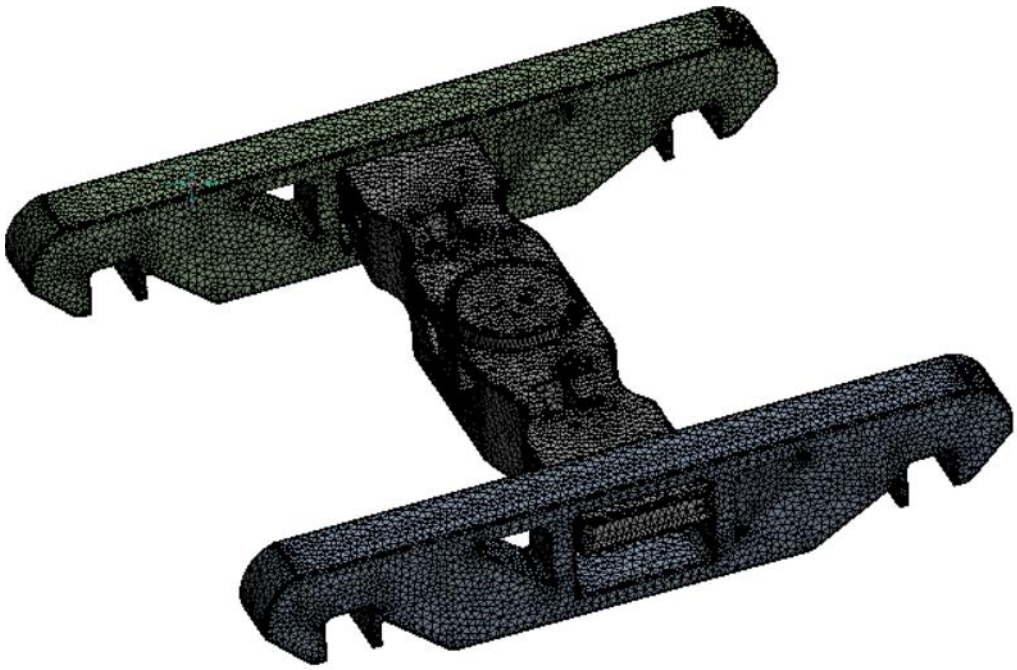

Figure 3. 16. FEM model in ANYS Workbench

Note: The mesh independence analysis has shown in the results section of finite element after dynamic forces analysis because it has been performed based on dynamic forces results from SIMPACK

Table 3. 1. Chemical properties for Q450NQR1 Weathering steel used for bogie frame at EDR [54]

Element	C	Si	Mn	P	S	Al	Cr	Ni	Cu	Balance
wt %	0.062	0.261	1.01	0.013	0.001	0.03	0.17	0.186	0.296	Fe

Table 3. 2. Mechanical properties for Q450NQR1 Weathering steel used for bogie frame at EDR [54]

Yield strength (MPa)	Tensile strength (MPa)	Poisson ratio	Modulus of Elasticity (GPa)	Density (Kg/m^3)
450	585.6	0.3	200	7850

Chapter 4. Results and discussion

This section details all simulation and calculation results under various scenarios considered to achieve the objective of the study. The scenarios have been based on consideration of 3 various wheel out-of-roundness cases as shown in appendix B used to evaluate the fatigue life of a bogie frame.

4.2. Impact load due to wheel out-of-roundness variation.

The effect of out-of-roundness variation on dynamic loads have been demonstrated by using three simulation scenarios with 3 various cases of OOR, where case 1 is for OOR with maximum radius deviation of 1 mm, case 2 is for 2 mm and case 3 is for 5 mm.

(A) Dynamic load for case 1 with OOR of maximum radius deviation of 1 mm

The dynamic load history for the case of wheel OOR with maximum radius deviation of 1 mm have been shown on figures 4.1 and 4.2 and 4.3 for the vertical, lateral and longitudinal forces, respectively. Figures 4.1 (a), (b), (c), and (d) represent vertical forces on the right side of the bogie frame and its enlargement, and the left side and its enlargement, respectively; Figures 4.2 (a), (b), (c), and (d) represent lateral forces on the right side of the bogie frame and its enlargement, and the left side and its enlargement, respectively and Figures 4.3 (a), (b), (c), and (d) represent longitudinal forces on the right side of the bogie frame and its enlargement, and the left side and its enlargement, respectively . The results from this case simulation has shown that the maximum vertical loads are 155.02 KN and 132.26 KN for the right and left sides, respectively; The lateral forces are 19.014 KN and 18.999 KN for the right and left sides, respectively while the longitudinal forces are 33.302 KN and 21.574 KN for the right and left sides, respectively.

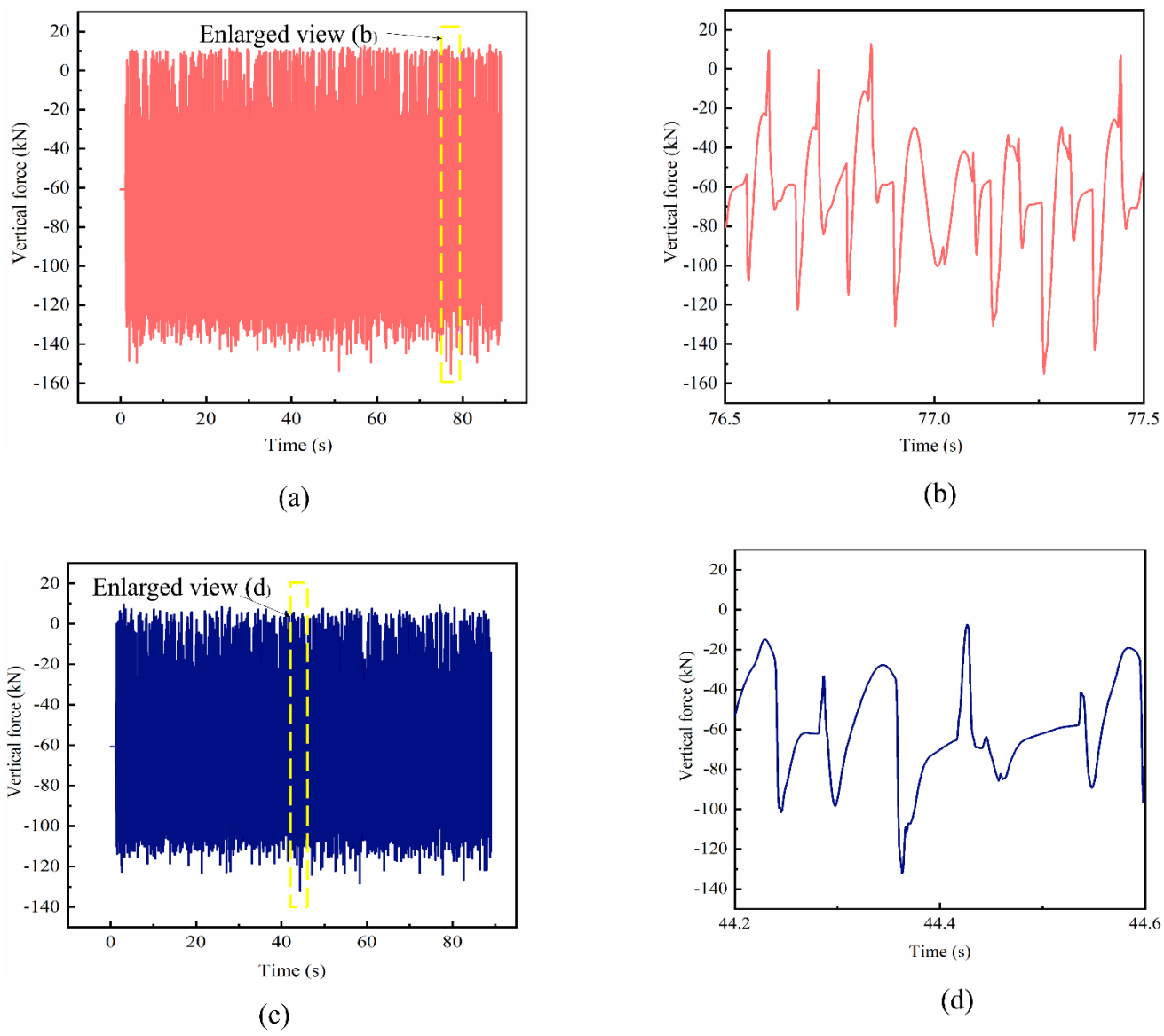

Figure 4. 1. Vertical force at 1 mm: (a) right side, (b) enlargement of (a), (c) left side and (d) enlargement of (c).

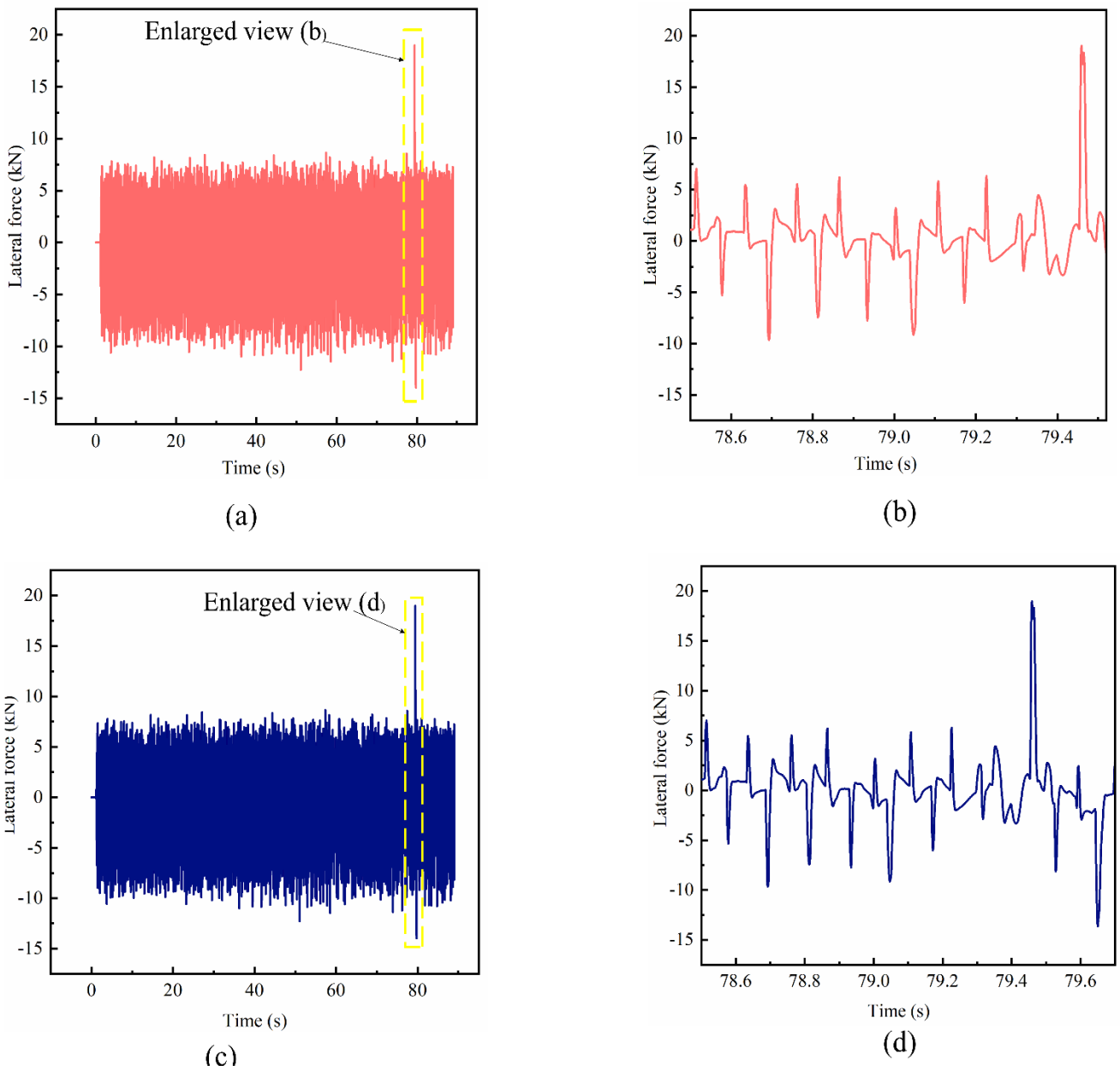

Figure 4. 2. Lateral force at 1 mm: (a) right side, (b) enlargement of (a), (c) left side and (d) enlargement of (c).

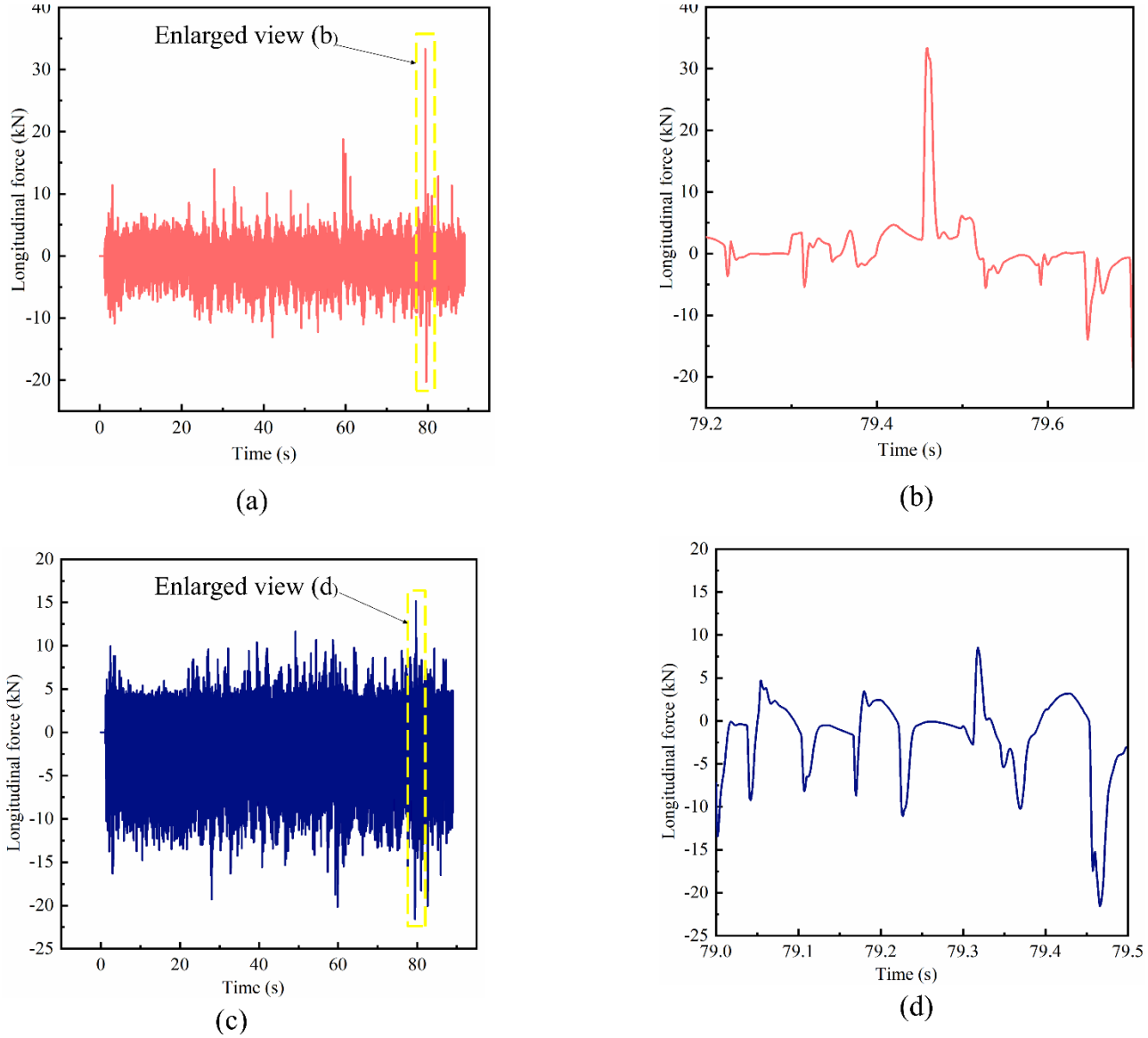

Figure 4. 3. Longitudinal force at 1 mm: (a) right side, (b) enlargement of (a), (c) left side and (d) enlargement of (c).

(B) Dynamic load for the case 2 with OOR of maximum radius deviation of 2 mm

The dynamic load history for the case of wheel OOR with maximum radius deviation of 2 mm have been shown on figures 4.4 and 4.5 and 4.6 for the vertical, lateral and longitudinal forces, respectively. Figures 4.4 (a), (b), (c), and (d) represent vertical forces on the right side of the bogie frame and its enlargement, and the left side and its enlargement, respectively; Figures 4.5 (a), (b), (c), and (d) represent lateral forces on the right side of the bogie frame and its enlargement, and the left side and its enlargement, respectively and Figures 4.6 (a), (b), (c), and (d) represent

longitudinal forces on the right side of the bogie frame and its enlargement, and the left side and its enlargement, respectively . The results from this case simulation has shown that the maximum vertical loads are 198.279 KN and 187.578 KN for the right and left sides, respectively; The lateral forces are 35.009 KN and 34.996 KN for the right and left sides, respectively while the longitudinal forces are 73.392 KN and 49.997 KN for the right and left sides, respectively. From these results it is clear that the dynamic loads for the case of 2 mm are higher than that on the case of 1 mm for both sides of the frame. This indicates that the impact loads are influenced by OOR and forces are increases as OOR increases too.

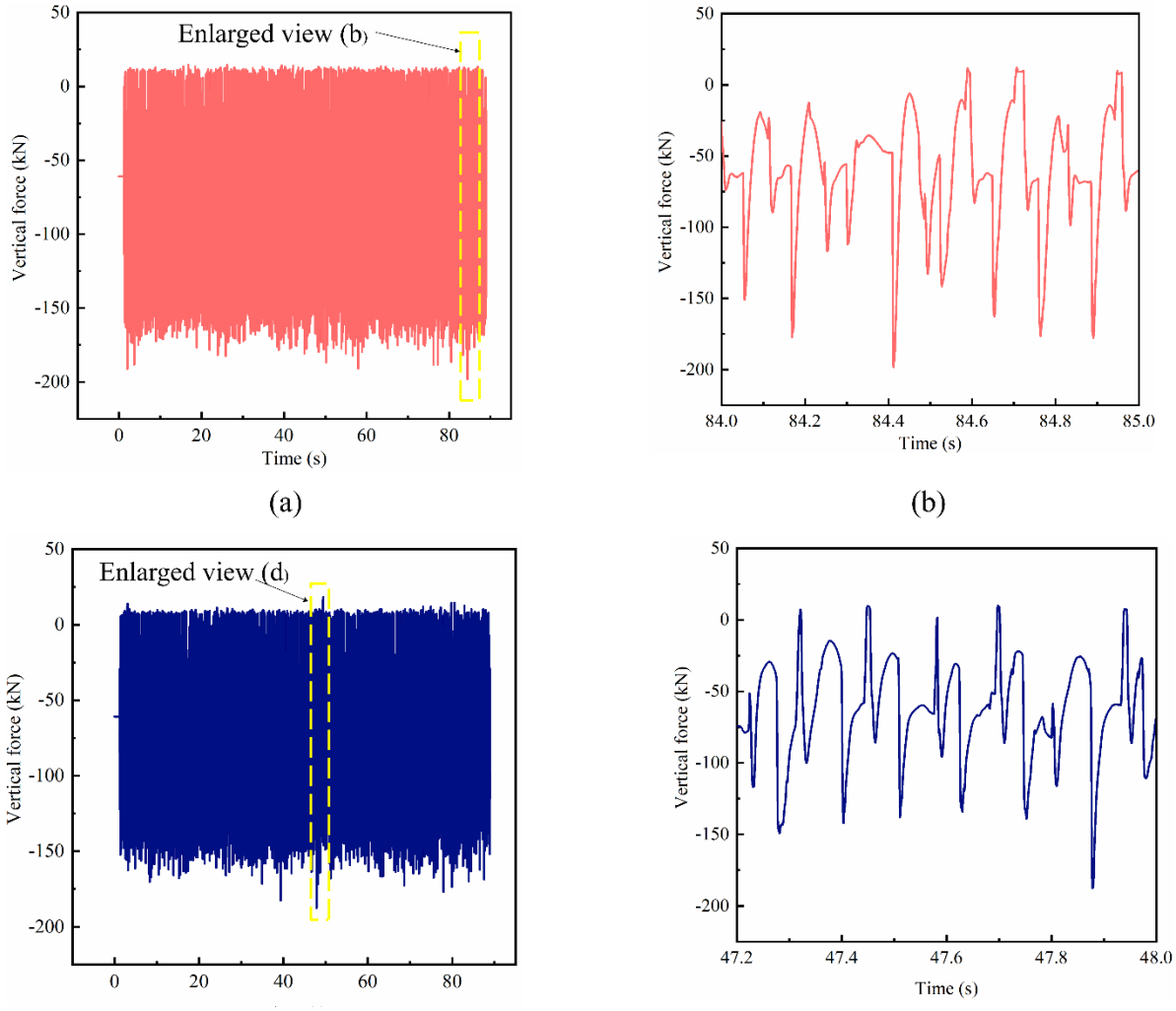

Figure 4. 4. Vertical force at 2 mm: (a) right side, (b) enlargement of (a), (c) left side and (d) enlargement of (c).

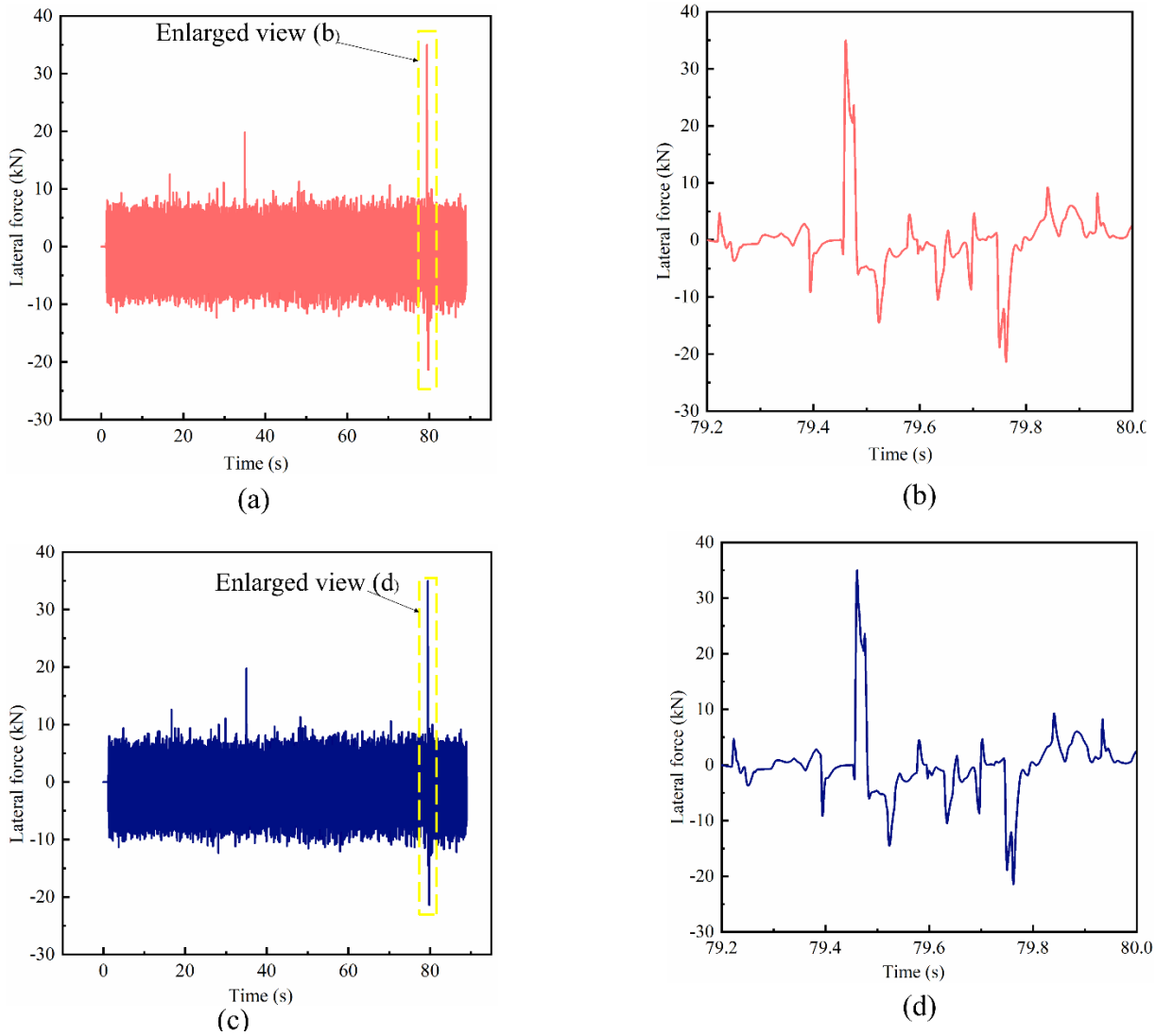

Figure 4. 5. Lateral force at 2 mm: (a) right side, (b) enlargement of (a), (c) left side and (d) enlargement of (c).

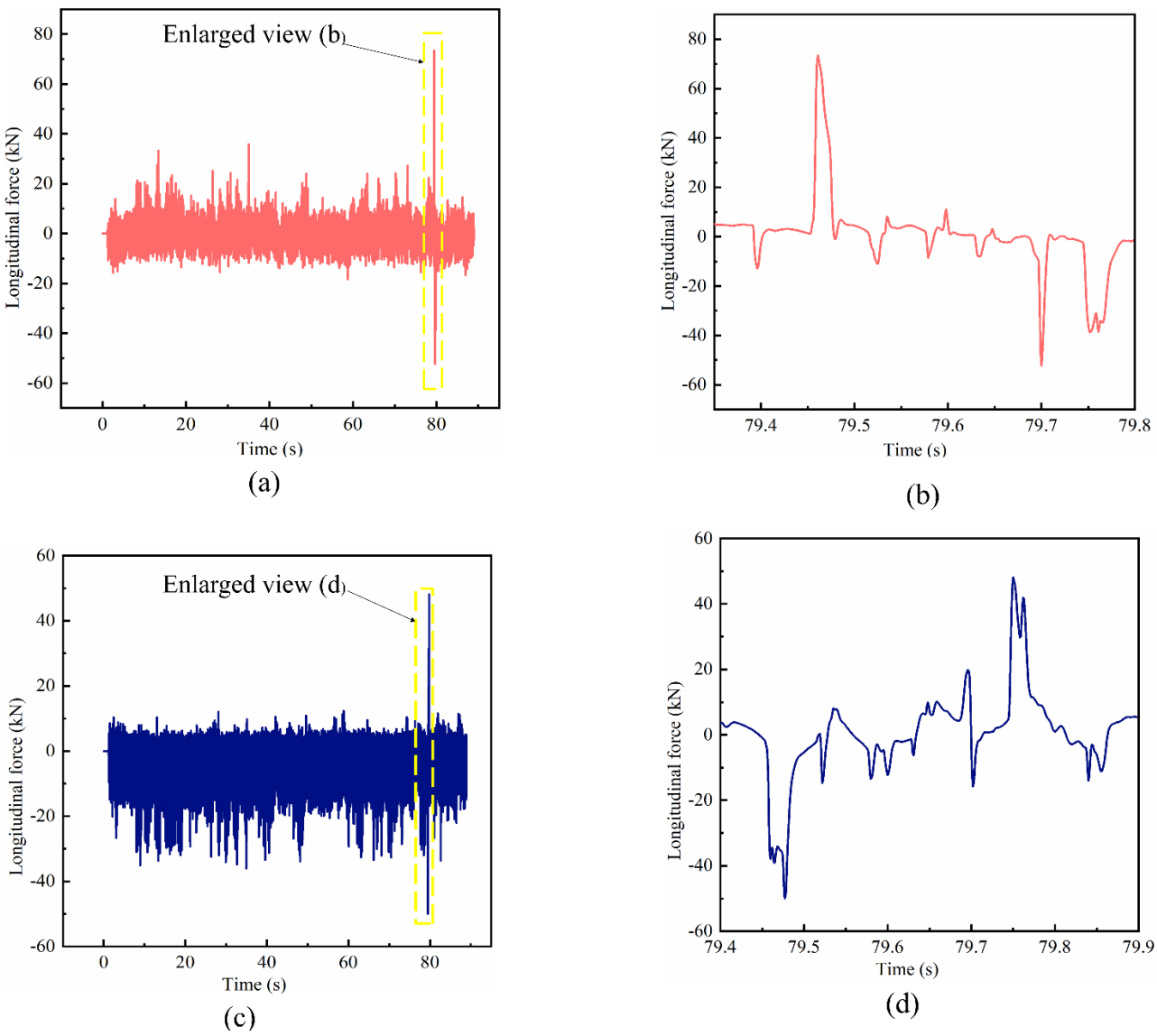

Figure 4. 6. Longitudinal force at 2 mm: (a) right side, (b) enlargement of (a), (c) left side and (d) enlargement of (c).

(C) Dynamic load at maximum radius deviation of 5 mm

The dynamic load history for the case of wheel OOR with maximum radius deviation of 5 mm have been shown on figures 4.7 and 4.8 and 4.9 for the vertical, lateral and longitudinal forces, respectively. Figures 4.7 (a), (b), (c), and (d) represent vertical forces on the right side of the bogie frame and its enlargement, and the left side and its enlargement, respectively; Figures 4.8 (a), (b), (c), and (d) represent lateral forces on the right side of the bogie frame and its enlargement, and the left side and its enlargement, respectively and Figures 4.9 (a), (b), (c), and (d) represent longitudinal forces on the right side of the bogie frame and its enlargement, and the left side and

its enlargement, respectively . The results from this case simulation has shown that the maximum vertical loads are 366.361 KN and 351.585 KN for the right and left sides, respectively; The lateral forces are 45.185 KN and 45.155 KN for the right and left sides, respectively while the longitudinal forces are 86.324 KN and 63.126 KN for the right and left sides, respectively. From these results it is clear that the dynamic loads for the case of 5 mm are higher than that on both case of 2 mm and 1 mm for both sides of the frame. These results from both three cases of multibody simulation in SIMPACK can confirm with the general trend that the increase in radius deviation of wheel out-of-roundness induce high impact loads that increase stresses distribution in the component as well as affect the life as demonstrated in next section.

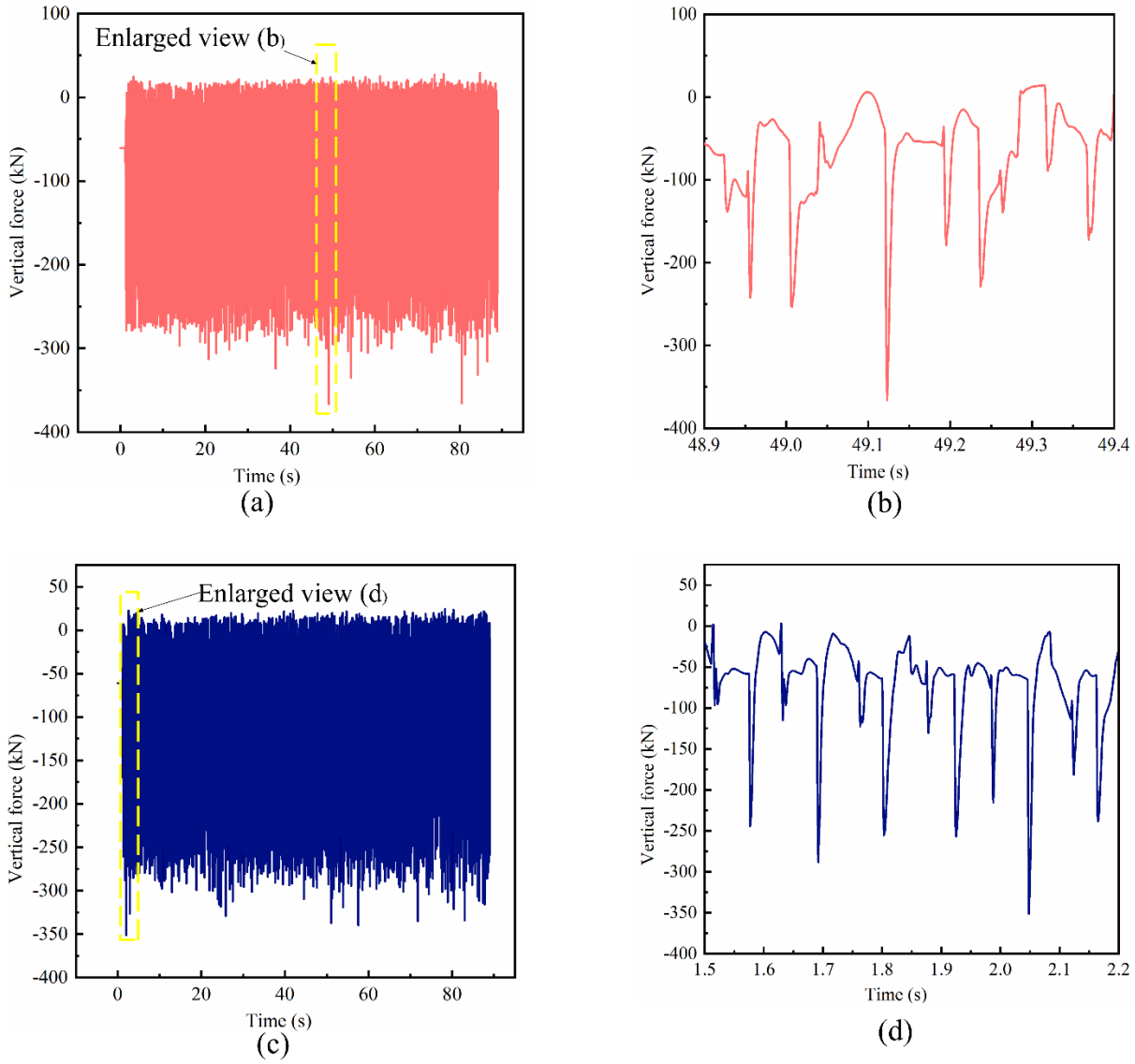

Figure 4. 7. Vertical force at 5 mm: (a) right side, (b) enlargement of (a), (c) left side and (d) enlargement of (c).

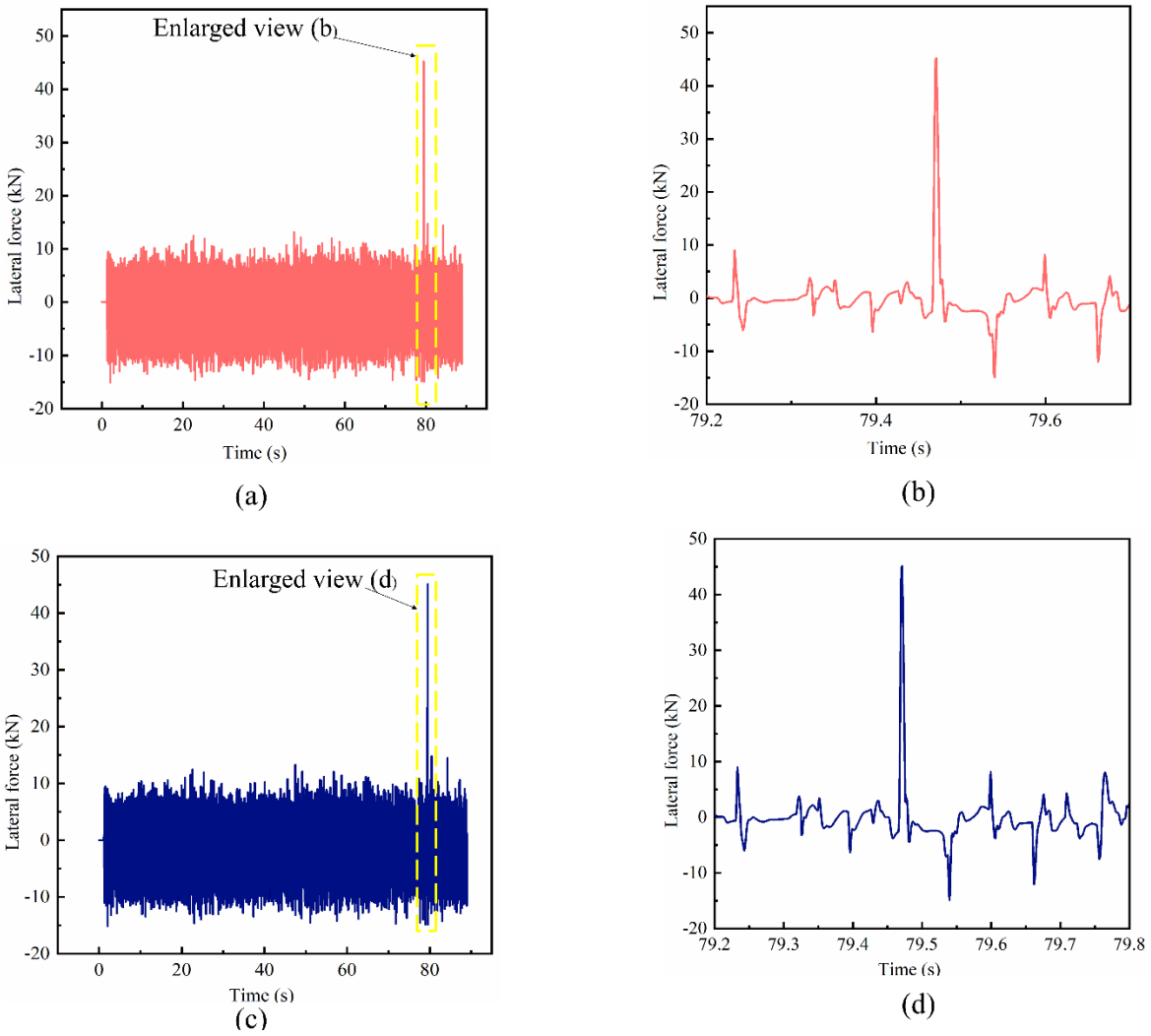

Figure 4. 8. Lateral l force at 5 mm: (a) right side, (b) enlargement of (a), (c) left side and (d) enlargement of (c).

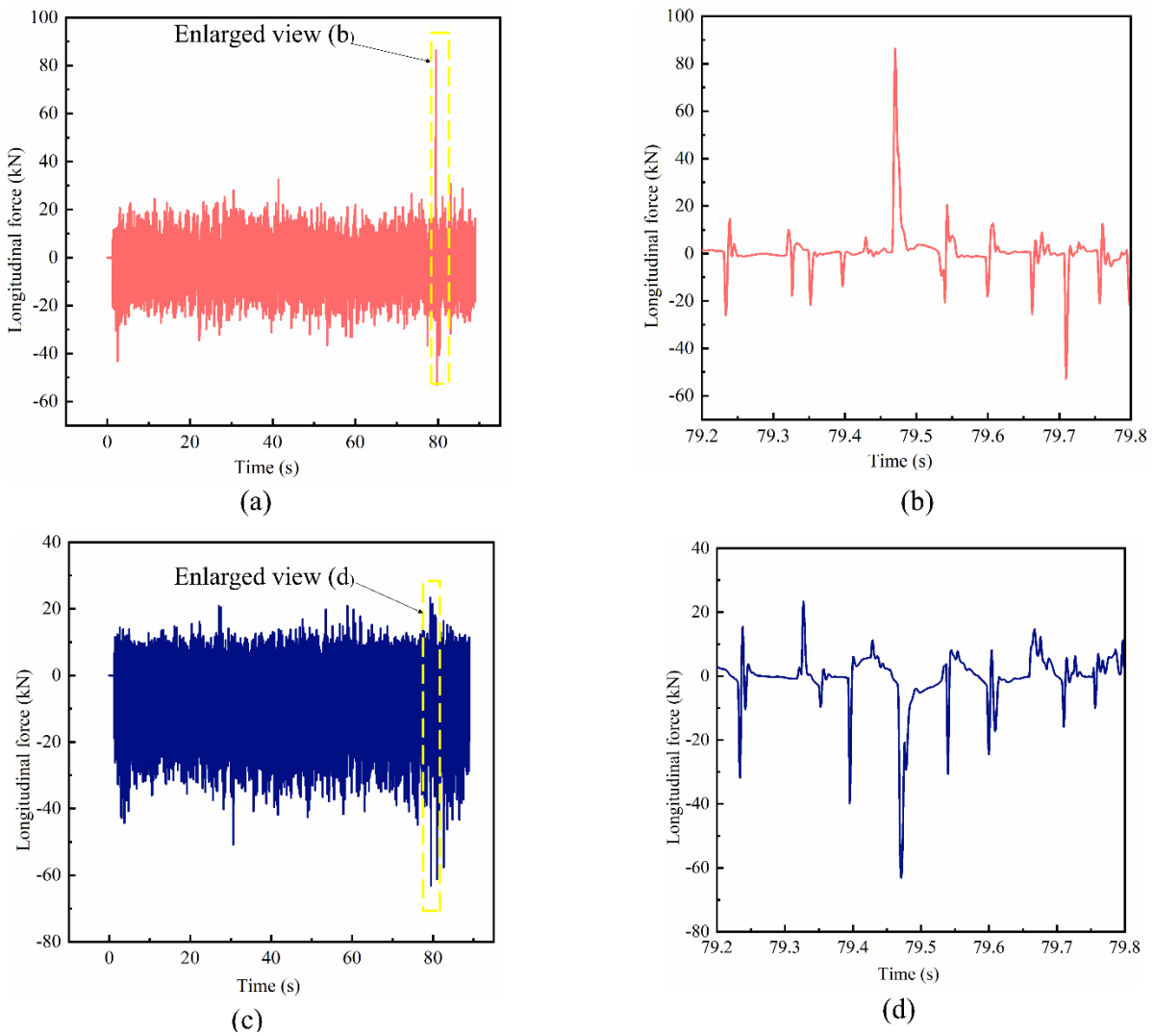

Figure 4. 9. Longitudinal force at 5 mm: (a) right side, (b) enlargement of (a), (c) left side and (d) enlargement of (c).

Table 4. 1. Summary of maximum dynamic forces induced on a bogie frame

Case of OOR	Max vertical force (KN)		Max lateral forces (KN)		Max longitudinal forces (KN)	
	Right side	Left side	Right side	Left side	Right side	Left side
with 1 mm	155.020	132.259	19.014	18.999	33.302	21.574
With 2 mm	198.279	187.578	35.009	34.996	73.392	49.997
With 5 mm	366.361	351.585	45.185	45.155	86.324	63.126

Table 4.1 summarize the extracted maximum dynamic forces components induced on a highly affected bogie frame with integration of wheel OOR.

4.3. Finite element analysis

Based on the dynamic forces extracted from multibody system SIMPACK on the highly affected bogie frame due to integration of wheel OOR the FEM analysis has been performed to provide stress and strain distributions used in lifecycles prediction. The maximum dynamic forces induced on a bogie frame for vertical, lateral and longitudinal directions as summarized in table 4.1 have been used for FEM analysis by using boundary conditions and load conditions shown on figure 4.10 (a) and (b).

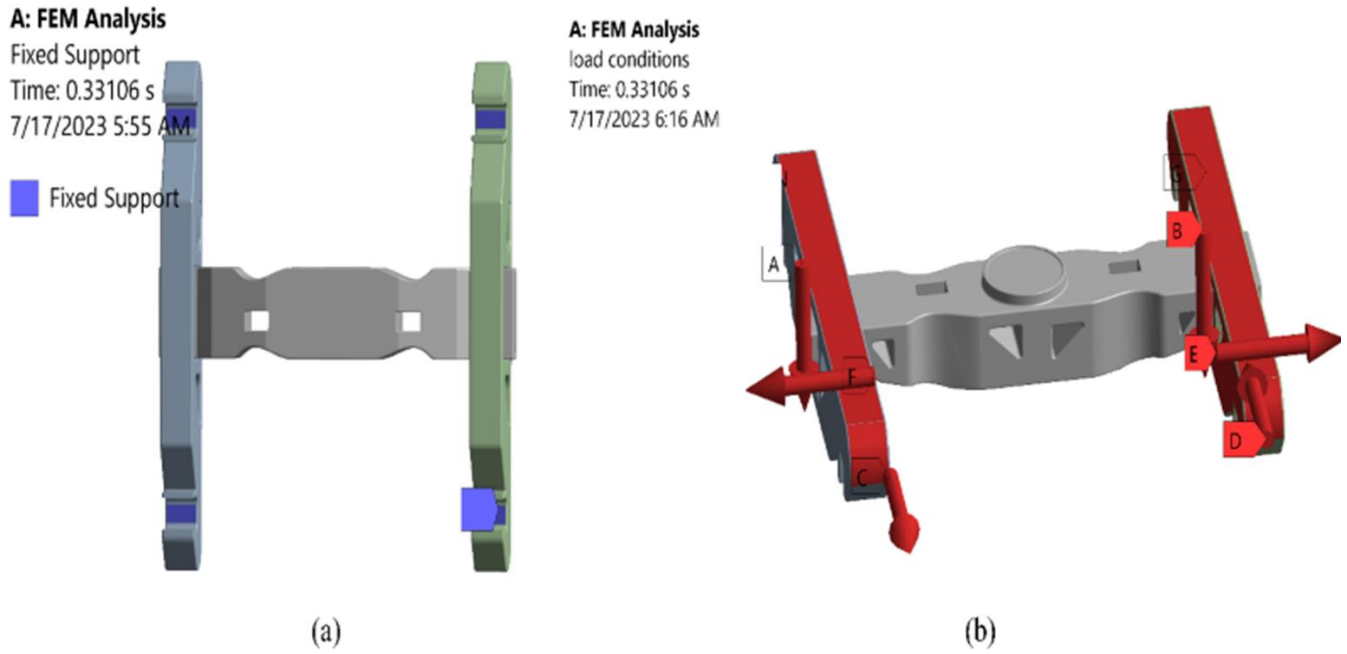

Figure 4. 10. Fixed support and load conditions

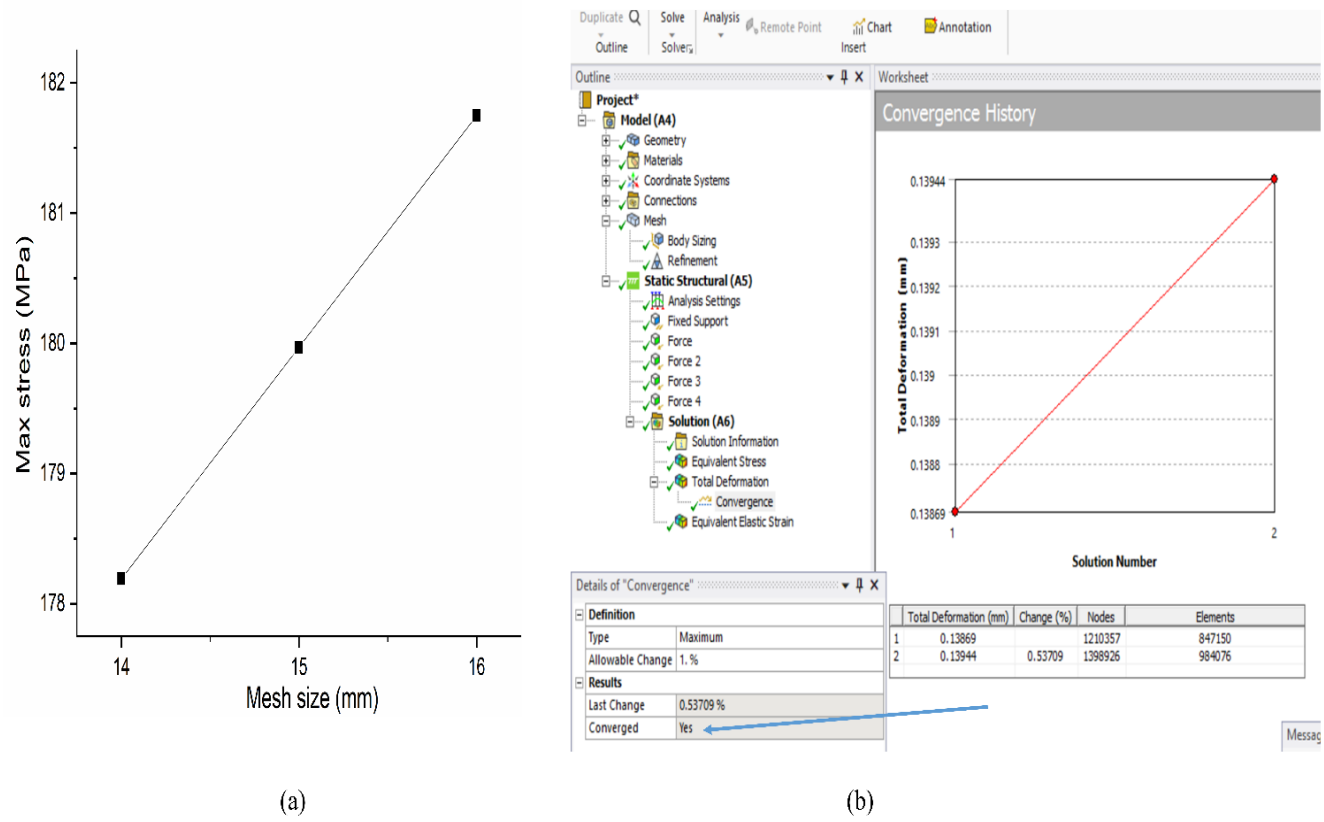

(a) (b)

Figure 4. 11. Mesh independence analysis

In the FEM analysis the mesh size of 15 mm has been used to get the necessary results. Figure 4.11 shows mesh independence analysis with comparing maximum stress obtained by using mesh size of 14 mm, 15 mm and 16 mm where the results shown to be equal as shown on figure 4.11 (a) and enhanced by (b) which shows the status of convergence in 2 iteration processes under allowable change of 1% for total deformation.

(A) Stress distribution

The stress distribution on bogie frame is shown on figure 4.12 (a), (b) and (c) for OOR cases with maximum radius deviation of 1 mm, 2 mm and 5 mm, respectively. The results shows that the maximum stresses are 179.79 MPa, 237.71 MPa and 342.22MPa for case (a), (b) and (c), respectively. These results clearly indicate that the wheel OOR variation have great impact on stress distribution and the trend is that the stresses increase as radius deviation of wheel OOR increases.

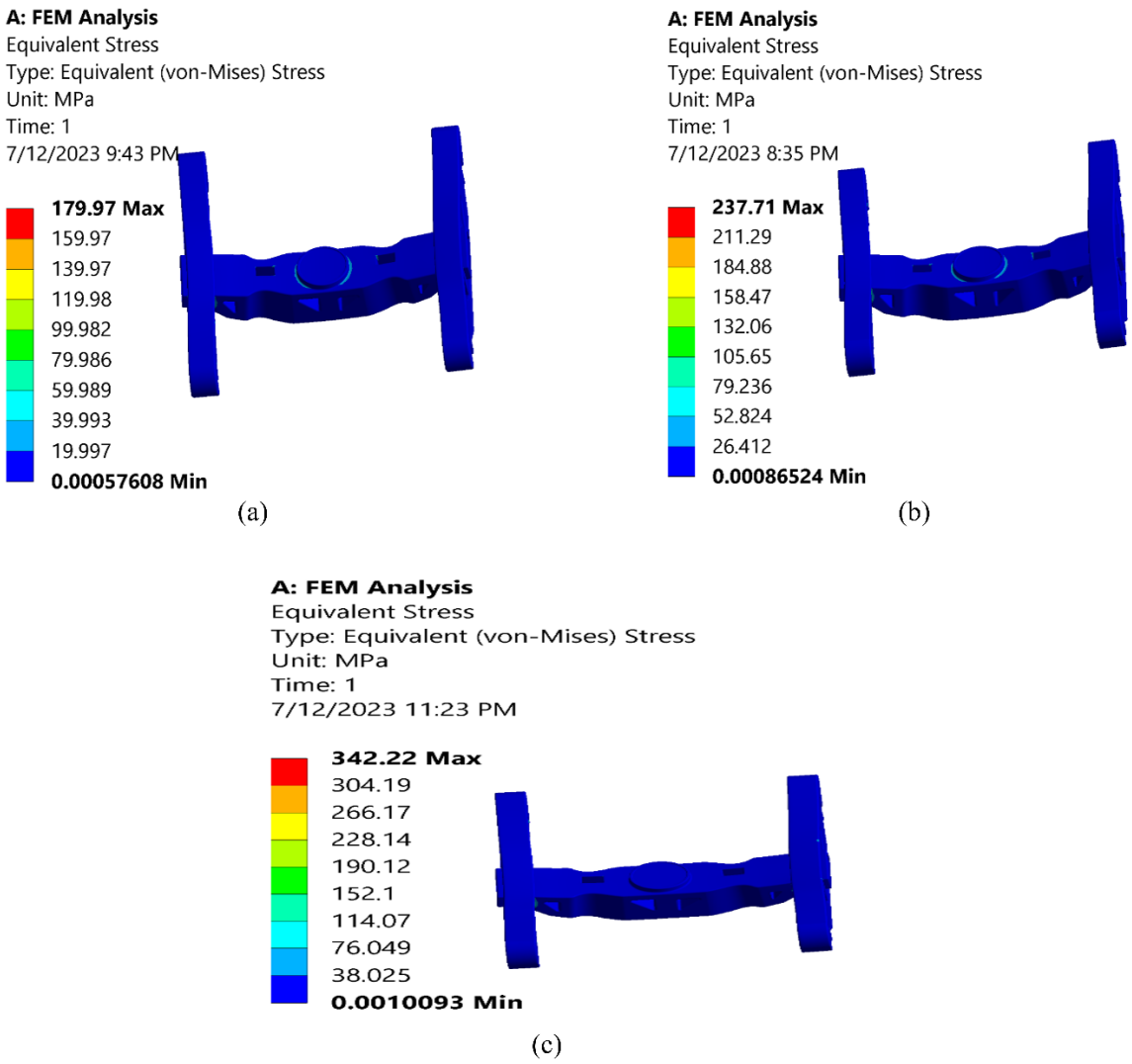

Figure 4. 12. Stress distribution under OOR with: (a) 1 mm, (b) 2 mm and (c) 5 mm

(B) Strain distribution

The strain distribution on bogie frame is shown on figure 4.13 (a), (b) and (c) for OOR cases with maximum radius deviation of 1 mm, 2 mm and 5 mm, respectively. The results shows that the maximum strain are 1.0007e-3, 1.3217e-3, and 1.9089e-3 for case (a), (b) and (c), respectively. These results clearly indicate that the wheel OOR variation have great impact on strain distribution and it has the same trend as for stress distribution where strain increase as OOR radius deviation increases.

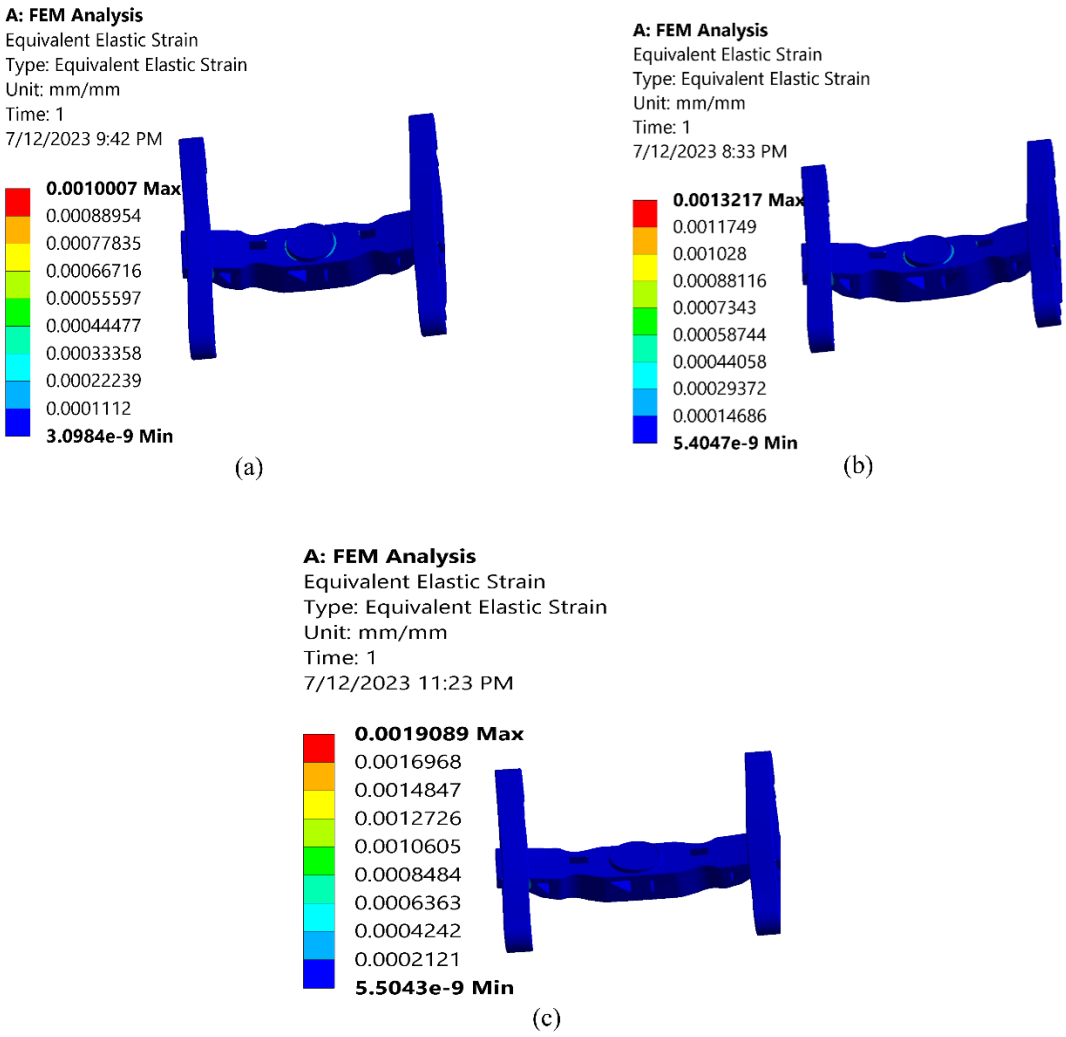

Figure 4. 13. Strain distribution under OOR with: (a) 1 mm, (b) 2 mm and (c) 5 mm

(C) Total deformation distribution

The total deformation distribution on bogie frame is shown on figure 4.14 (a), (b) and (c) for OOR cases with maximum radius deviation of 1 mm, 2 mm and 5 mm, respectively. The results shows that the maximum deformation are 0.30444 mm, 0.40563 mm and 0.5148 mm for case (a), (b) and (c), respectively. These results also clearly indicate that the wheel OOR variation have great impact on total deformation distribution and it has the same trend as for stress and strain distribution where deformation increase as OOR radius deviation increases**.**

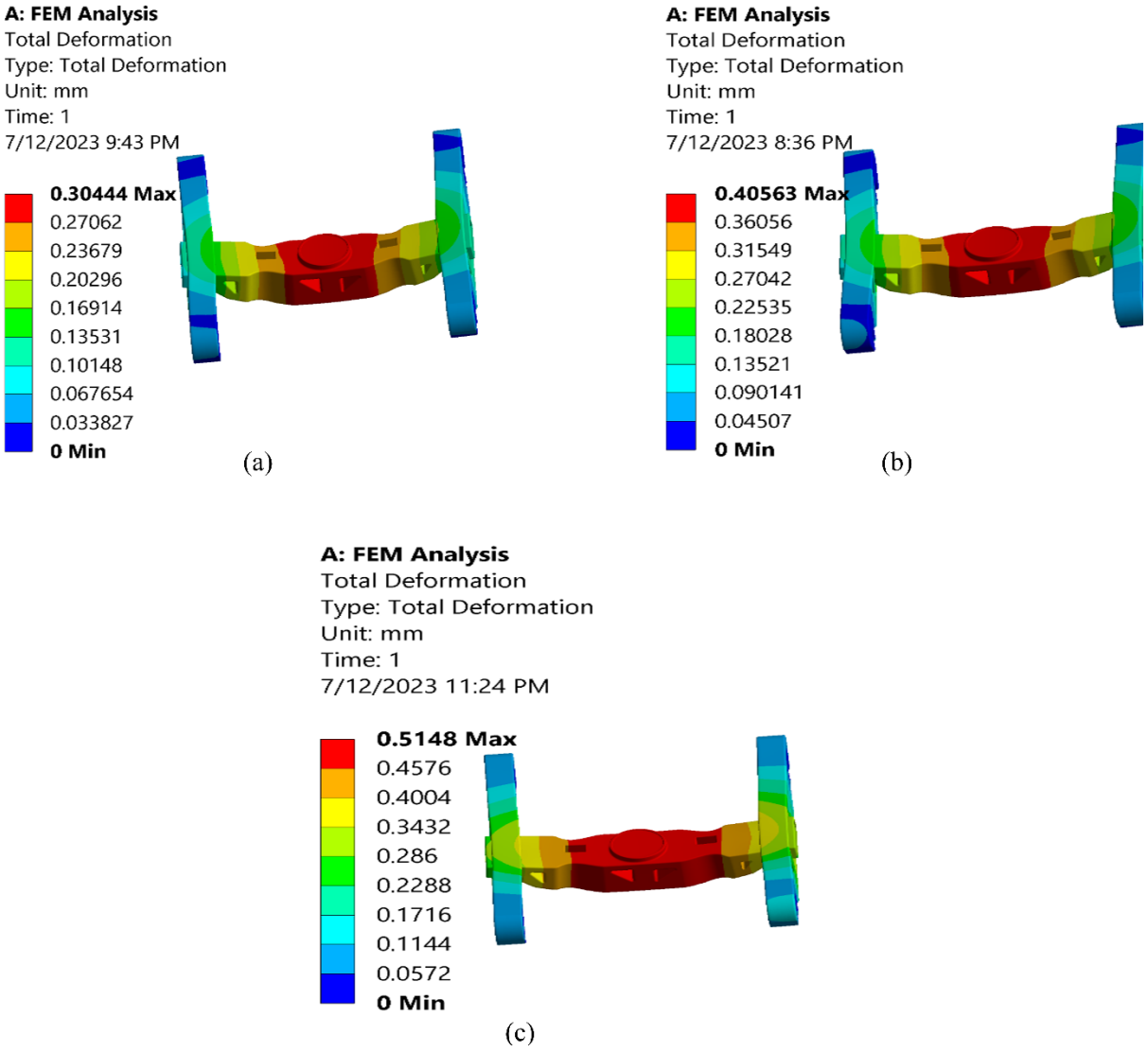

Figure 4. 14. Total deformation distribution

4.4. Fatigue life estimation

(A) Simulated fatigue life from nCode software

The simulated fatigue lifecycles has been shown on figure 4.15 (a), (b) and (c) for OOR cases with maximum radius deviation of 1 mm, 2 mm and 5 mm, respectively. The results show that the life cycles are $8.2e^7$, $7.2e^6$ and $4.44e^5$ cycles for the case (a), (b) and (c), respectively. These results clearly indicate that the wheel OOR variation have significant effect on the lifecycles of the bogie frame and the trend is that the lifecycles decrease as OOR radius deviation increases. With reference to the literature from [27] the life of bogie frame must be expected to be greater than $2e^6$

cycles, so this indicates that the studied bogie frame will operate below the recommended standard limit for fatigue life in the case of wheel OOR with maximum radius deviation of 5 mm. Therefore, it is a crucial to analyse the effect of OOR variation on a bogie frame with aim of providing the maximum level of OOR the bogie wheel can operate on without affect the lifecycles of a bogie frame. For this case of Ethio-Djibouti the good optimized OOR level is not to exceed the radius deviation of 2 mm. So the re-profiling action should be taken before exceeding radius deviation of 2 mm.

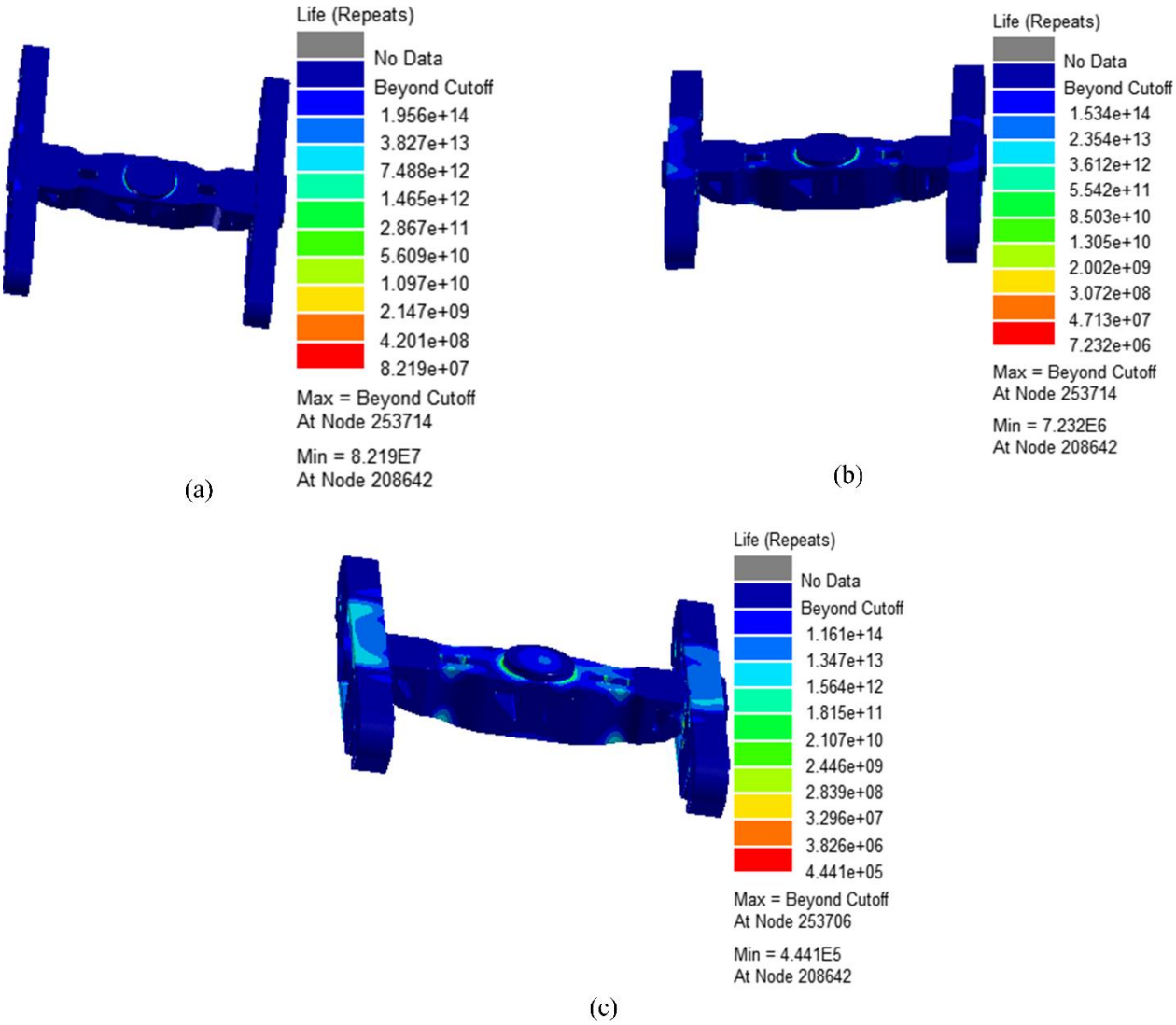

Figure 4. 15. Simulation lifecycles under OOR with: (a) 1 mm, (b) 2 mm and (c) 5 mm

(B) Calculation of fatigue life

In this study, the analytical calculations of bogie frame's fatigue life cycles have been performed based on the best approach of Smith Watson Topper (SWT) to provide analytical results that have been compared with simulation results for the validation of the work. The SWT approach take into consideration both stresses and strains induced in the structure. The mathematical expression of SWT fatigue life estimation approach is shown in the equation 4.1 [29].

$$\sigma_{max}\frac{\Delta\varepsilon}{2} = \frac{(\sigma_f')^2}{E}(2N_f)^{2b} + \sigma_f'\varepsilon_f'(2N_f)^{b+c} \quad (4.1)$$

Where the symbols ε_f', σ_f', c and b are fatigue constants characteristics; stand for, respectively, the fatigue coefficient of ductility, fatigue coefficient of strength, fatigue exponent of ductility and fatigue strength exponent. While σ_{max}, $\frac{\Delta\varepsilon}{2}$, N_f and E stand for maximum stress, strain amplitude, fatigue life cycles and young modulus of the material, respectively.

The fatigue properties constants for bogie frame structural steel used in the study have been referenced from [55] as the following:

$\sigma_f' = 903.3$ MPa, $\varepsilon_f' = 0.288, b = -0.102$ and $c = -0.499$ And E=200 MPa.

From figures 4.12 and 4.13, $\sigma_{max} = 179.79$ MPa, $\frac{\Delta\varepsilon}{2} = 5.004 * 10^{-4}$ for the case 1 with out-of-roundness of 1 mm;$\sigma_{max} = 237.71$ MPa, $\frac{\Delta\varepsilon}{2} = 6.609 * 10^{-4}$ for the case 2 with OOR of 2 mm and $\sigma_{max} = 342.22$ MPa, $\frac{\Delta\varepsilon}{2} = 9.545 * 10^{-4}$ for the case 3 with OOR of 5 mm. By replacing the appropriate values into equation (4.1), the estimated fatigue life cycles for a bogie frame are $7.8*10^7$ cycles, $6.7*10^6$ cycles and $4.1*10^5$ cycles for the case 1, case 2 and case 3, respectively.

(C) Validation of the results

The validation of the results for the lifecycles of the bogie frame has been performed by comparing the numerical results simulated from nCode software with analytical results calculated based on Smith Watson Topper approach. The results from both approaches are shown in the table 4.2 and it is clear from the table that the simulation and analytical results are in good relation which validate the work for the life prediction of a railway bogie frame.

Table 4. 2. Comparison between simulated and calculated life

Case	Simulated life	Calculated life	Deviation
1 with OOR of 1 mm	$8.2e^7$	$7.8e^7$	4.9%
2 with OOR of 2 mm	$7.2e^6$	$6.7e^6$	6.9%
3 with OOR of 5 mm	$4.4e^5$	$4.1e^5$	6.8%

Chapter 5. Conclusion, Recommendation and Future work

5.1. Conclusion

In this study, the influence of wheel out-of-roundness on the fatigue life of a bogie frame has been analyzed. The dynamic response load histories and stress distributions for various out-of-roundness cases have been analyzed. Finally, the fatigue life prediction and its analysis for bogie frame under the influence of wheel out-of-roundness condition variation have been conducted. From the study, the following conclusions can be drawn:

1. The variation of wheel out-of-roundness affect the dynamic load on a bogie frame where forces increases as OOR increases, which in turn increase the stress distribution on a bogie frame.

2. The increase in stresses and strains distribution decrease the fatigue life of the component as demonstrated based on the well-known fatigue life calculation approach of Smith Watson Topper.

3. The wheel OOR variation have significant impact on the life of a bogie frame as an example shown from the study where the fatigue lifecycles are 8.2e7, 7.2e6 and 4.44e5 cycles for the case of OOR with maximum radius deviation of 1 mm, 2 mm and 5 mm, respectively.

4. It is a crucial to analyse the effect of OOR variation on a bogie frame with aim of providing the maximum level of OOR the bogie wheel can operate on without affect the lifecycles of a bogie frame

5.2. Recommendation

- This study has shown that the studied bogie frame will operate below the recommended standard limit for fatigue life in the case of wheel OOR with maximum radius deviation of 5 mm and for this case of Ethio-Djibouti the good optimized OOR level is not to exceed the radius deviation of 2 mm. So the re-profiling action should be taken before exceeding radius deviation of 2 mm that providing a good range of fatigue life.

- Based on the results from the study that show the effect of wheel out-of-roundness variation, it is highly recommended to take into account the influence of wheel OOR in the fatigue life prediction of a bogie frame.

5.3. Future work

- This study was based on integration of out-of-roundness into multibody system for analyzing its effect through simulation scenarios, but the future work that will be based on practical fatigue test in laboratory by using fatigue test rig to analyse the fatigue life of the bogie running with various cases of wheel out-of-roundness will help to understand well the real effect of the wheel out-of-roundness.
- The further study that will take into account the variation of other parameters such as curvature, suspension, coefficient of friction, speed, material properties and so on in combination with wheel OOR will be important.
- The bogie frame used in this study was considered as rigid body, therefore, the future work that will consider flexible body to compare the results with rigid case will be better.

References

[1] Y. Zhang, P. Wu, and Y. Song, "Strength test and modal analysis for a standardized high-speed EMU motor bogie frame," in *2015 4th International Conference on Sensors, Measurement and Intelligent Materials*, 2016: Atlantis Press, pp. 1128-1132.

[2] X.-Z. Liu, "Railway Wheel out-of-roundness and its effects on vehicle–track dynamics: a review," *Data Mining in Structural Dynamic Analysis*, pp. 41-64, 2019.

[3] X. Wu *et al.*, "A study of polygonal wheel wear through a field test programme," *Vehicle System Dynamics*, vol. 57, no. 6, pp. 914-934, 2019.

[4] X. Wu, S. Rakheja, W. Cai, M. Chi, A. Ahmed, and S. Qu, "A study of formation of high order wheel polygonalization," *Wear*, vol. 424, pp. 1-14, 2019.

[5] W. Cai *et al.*, "A long-term tracking test of high-speed train with wheel polygonal wear," *Vehicle System Dynamics*, vol. 59, no. 11, pp. 1735-1758, 2021.

[6] Y. Wu, X. Du, H.-j. Zhang, Z.-f. Wen, and X.-s. Jin, "Experimental analysis of the mechanism of high-order polygonal wear of wheels of a high-speed train," *Journal of Zhejiang University-SCIENCE A*, vol. 18, no. 8, pp. 579-592, 2017.

[7] R. Fröhling, U. Spangenberg, and E. Reitmann, "Root cause analysis of locomotive wheel tread polygonisation," *Wear*, vol. 432, p. 102911, 2019.

[8] G. Tao, L. Wang, Z. Wen, Q. Guan, and X. Jin, "Measurement and assessment of out-of-round electric locomotive wheels," *Proceedings of the Institution of Mechanical Engineers, Part F: Journal of Rail and Rapid Transit*, vol. 232, no. 1, pp. 275-287, 2018.

[9] G. Tao, L. Wang, Z. Wen, Q. Guan, and X. Jin, "Experimental investigation into the mechanism of the polygonal wear of electric locomotive wheels," *Vehicle System Dynamics*, vol. 56, no. 6, pp. 883-899, 2018.

[10] G. Tao, Z. Wen, G. Chen, Y. Luo, and X. Jin, "Locomotive wheel polygonisation due to discrete irregularities: simulation and mechanism," *Vehicle System Dynamics*, vol. 59, no. 6, pp. 872-889, 2021.

[11] G.-q. Tao, X.-l. Liu, Z.-f. Wen, and X.-s. Jin, "Formation process, key influencing factors, and countermeasures of high-order polygonal wear of locomotive wheels," *Journal of Zhejiang University-SCIENCE A*, vol. 22, no. 1, pp. 70-84, 2021.

[12] J. C. Nielsen, R. Lundén, A. Johansson, and T. Vernersson, "Train-track interaction and mechanisms of irregular wear on wheel and rail surfaces," *Vehicle System Dynamics,* vol. 40, no. 1-3, pp. 3-54, 2003.

[13] X. Jin, L. Wu, J. Fang, S. Zhong, and L. Ling, "An investigation into the mechanism of the polygonal wear of metro train wheels and its effect on the dynamic behaviour of a wheel/rail system," *Vehicle System Dynamics,* vol. 50, no. 12, pp. 1817-1834, 2012.

[14] G. Tao, Z. Wen, X. Liang, D. Ren, and X. Jin, "An investigation into the mechanism of the out-of-round wheels of metro train and its mitigation measures," *Vehicle System Dynamics,* vol. 57, no. 1, pp. 1-16, 2019.

[15] G. Tao, C. Xie, H. Wang, X. Yang, C. Ding, and Z. Wen, "An investigation into the mechanism of high-order polygonal wear of metro train wheels and its mitigation measures," *Vehicle System Dynamics,* vol. 59, no. 10, pp. 1557-1572, 2021.

[16] W. Cai, M. Chi, G. Tao, X. Wu, and Z. Wen, "Experimental and numerical investigation into formation of metro wheel polygonalization," *Shock and Vibration,* vol. 2019, 2019.

[17] K. Lv, K. Wang, Z. Chen, C. Cai, and L. Guo, "Influence of wheel eccentricity on vertical vibration of suspended monorail vehicle: experiment and simulation," *Shock and Vibration,* vol. 2017, 2017.

[18] Y. Jiang *et al.*, "Detection and alleviation of the abnormal vibration of the monorail based on experiment and simulation," *Journal of Low Frequency Noise, Vibration and Active Control,* vol. 38, no. 2, pp. 282-295, 2019.

[19] J. Mu, J. Zeng, C. Huang, Y. Sun, and H. Sang, "Experimental and numerical investigation into development mechanism of wheel polygonalization," *Engineering Failure Analysis,* vol. 136, p. 106152, 2022.

[20] *Exploring Roundness*, 3 ed. (A fundamental guide to the measurement of cylindrical form). Leicester LE4 9JQ, England: Taylor Hobson Limited.

[21] *International Standard, ISO 12181-1*, 2011. [Online]. Available: https://standards.iteh.ai/catalog/standards

[22] Y. Song and Z. Wang, "Research on The Control of Out-of-Round Wheel Profiles of High-Speed Railway Derived From Numerical Simulations," *International Journal of Online and Biomedical Engineering (iJOE),* vol. 9, no. S6, 2013, doi: 10.3991/ijoe.v9iS6.2924.

[23] M. Zehsaz, F. V. Tahami, A. Z. Asl, and F. Ahmadian, "Effect of increasing speed on stress of biaxial bogie frames," *Engineering,* vol. 3, no. 3, p. 276, 2011.

[24] J.-W. Seo, H.-M. Hur, H.-K. Jun, S.-J. Kwon, and D.-H. Lee, "Fatigue design evaluation of railway bogie with full-scale fatigue test," *Advances in Materials Science and Engineering,* vol. 2017, 2017.

[25] L. Fan-Song, W. Ping-Bo, N. Yi-Zhao, and S. Ye, "Fatigue Evaluation of Railway Vehicle Bogie Frame by Different Methods," in *2014 International Conference on Mechanics and Civil Engineering (icmce-14)*, 2014: Atlantis Press, pp. 844-852.

[26] R. Xiu, M. Spiryagin, Q. Wu, S. Yang, and Y. Liu, "Fatigue life assessment methods for railway vehicle bogie frames," *Engineering Failure Analysis,* vol. 116, p. 104725, 2020.

[27] B. Wang, S. Xie, Q. Li, and Z. Ren, "Fatigue damage prediction of metro bogie frame based on measured loads," *International Journal of Fatigue,* vol. 154, p. 106532, 2022.

[28] F. Guo, S. Wu, J. Liu, W. Zhang, Q. Qin, and Y. Yao, "Fatigue life assessment of bogie frames in high-speed railway vehicles considering gear meshing," *International Journal of Fatigue,* vol. 132, p. 105353, 2020.

[29] T. Łagoda, S. Vantadori, K. Głowacka, M. Kurek, and K. Kluger, "Using the Smith-Watson-Topper Parameter and Its Modifications to Calculate the Fatigue Life of Metals: The State-of-the-Art," *Materials,* vol. 15, no. 10, p. 3481, 2022.

[30] O. A. Nour, "Develoing a material for improving fatigue strenght of welded bogie frame of Addis Abeba Light Rail Transit.," Masters, Addis Ababa University 2017.

[31] K. Daher, "Strength and fatigue analysis of composite bogie frame," Masters, Addis Ababa University, 2017.

[32] A. Johansson and J. C. Nielsen, "Out-of-round railway wheels—wheel-rail contact forces and track response derived from field tests and numerical simulations," *Proceedings of the Institution of Mechanical Engineers, Part F: Journal of Rail and Rapid Transit,* vol. 217, no. 2, pp. 135-146, 2003.

[33] A. Pieringer, W. Kropp, and J. C. Nielsen, "The influence of contact modelling on simulated wheel/rail interaction due to wheel flats," *Wear,* vol. 314, no. 1-2, pp. 273-281, 2014.

[34] L. Jing and L. Han, "Further study on the wheel–rail impact response induced by a single wheel flat: the coupling effect of strain rate and thermal stress," *Vehicle System Dynamics,* vol. 55, no. 12, pp. 1946-1972, 2017.

[35] J. Bian, Y. Gu, and M. H. Murray, "A dynamic wheel–rail impact analysis of railway track under wheel flat by finite element analysis," *Vehicle System Dynamics,* vol. 51, no. 6, pp. 784-797, 2013.

[36] R. Uzzal, A. Ahmed, and S. Rakheja, "Analysis of pitch plane railway vehicle—track interactions due to single and multiple wheel flats," *Proceedings of the Institution of Mechanical Engineers, Part F: Journal of Rail and Rapid Transit,* vol. 223, no. 4, pp. 375-390, 2009.

[37] R. U. A. Uzzal, W. Ahmed, and R. B. Bhat, "Impact analysis due to multiple wheel flats in three-dimensional railway vehicle-track system model and development of a smart wheelset," *Proceedings of the Institution of Mechanical Engineers, Part F: Journal of Rail and Rapid Transit,* vol. 230, no. 2, pp. 450-471, 2016.

[38] X. Liu and W. Zhai, "Analysis of vertical dynamic wheel/rail interaction caused by polygonal wheels on high-speed trains," *Wear,* vol. 314, no. 1-2, pp. 282-290, 2014.

[39] J. Zhang, X. Xiao, G. Han, Y. Deng, and X. Jin, "Study on abnormal interior noise of high-speed trains," in *Noise and Vibration Mitigation for Rail Transportation Systems*: Springer, 2015, pp. 691-698.

[40] T. Wu and D. Thompson, "A hybrid model for the noise generation due to railway wheel flats," *Journal of Sound and Vibration,* vol. 251, no. 1, pp. 115-139, 2002.

[41] X. Wu and M. Chi, "Study on stress states of a wheelset axle due to a defective wheel," *Journal of Mechanical Science and Technology,* vol. 30, no. 11, pp. 4845-4857, 2016.

[42] X. Wu, M. Chi, and P. Wu, "Influence of polygonal wear of railway wheels on the wheel set axle stress," *Vehicle System Dynamics,* vol. 53, no. 11, pp. 1535-1554, 2015.

[43] D. W. Barke and W. K. Chiu, "A review of the effects of out-of-round wheels on track and vehicle components," *Proceedings of the Institution of Mechanical Engineers, Part F: Journal of Rail and Rapid Transit,* vol. 219, no. 3, pp. 151-175, 2005.

[44] X.-s. Jin, "Key problems faced in high-speed train operation," in *China's High-Speed Rail Technology*: Springer, 2018, pp. 27-45.

[45] Y. Sun, L. Wei, C. Liu, H. Dai, S. Qu, and W. Zhao, "Dynamic stress analysis of a metro bogie due to wheel out-of-roundness based on multibody dynamics algorithm," *Engineering Failure Analysis,* vol. 134, p. 106051, 2022.

[46] G. Tao, Z. Wen, X. Jin, and X. Yang, "Polygonisation of railway wheels: a critical review," *Railway Engineering Science,* vol. 28, no. 4, pp. 317-345, 2020, doi: 10.1007/s40534-020-00222-x.

[47] G. Tao, M. Liu, Q. Xie, and Z. Wen, "Wheel–rail dynamic interaction caused by wheel out-of-roundness and its transmission between wheelsets," *Proceedings of the Institution of Mechanical Engineers, Part F: Journal of Rail and Rapid Transit,* vol. 236, no. 3, pp. 247-261, 2021, doi: 10.1177/09544097211016582.

[48] S. Qu, J. Wang, D. Zhang, D. Li, and L. Wei, "Failure analysis on bogie frame with fatigue cracks caused by hunting instability," *Engineering Failure Analysis,* vol. 128, 2021, doi: 10.1016/j.engfailanal.2021.105584.

[49] A. Momhur, Y. Zhao, L. Quan, S. Yazhou, and X. Zou, "Flexible-Rigid Wheelset Introduced Dynamic Effects due to Wheel Tread Flat," *Shock and Vibration,* vol. 2021, 2021.

[50] S. Iwnicki, *Handbook of railway vehicle dynamics*. CRC press, 2006.

[51] F. Li, S. Yang, Z. Yang, H. Shi, J. Zeng, and Y. Ye, "A novel vertical elastic vibration reduction for railway vehicle carbody based on minimum generalized force principle," *Mechanical Systems and Signal Processing,* vol. 189, p. 110035, 2023.

[52] A. Johansson, "Out-of-round railway wheels—assessment of wheel tread irregularities in train traffic," *Journal of Sound and Vibration,* vol. 293, no. 3-5, pp. 795-806, 2006.

[53] J. Dižo, M. Blatnický, and A. Pavlík, "Process of modelling the freight wagon multibody system and analysing its dynamic properties by means of simulation computations," in *MATEC Web of Conferences*, 2018, vol. 235: EDP Sciences, p. 00027.

[54] T. Cong *et al.*, "Microstructure evolution and mechanical properties of two kinds of weathering steel welded joints," *Fatigue & Fracture of Engineering Materials & Structures,* vol. 45, no. 12, pp. 3622-3639, 2022.

[55] Z. Xia, D. Kujawski, and F. Ellyin, "Effect of mean stress and ratcheting strain on fatigue life of steel," *International Journal of Fatigue,* vol. 18, no. 5, pp. 335-341, 1996.

Appendix

Appendix A. Technical parameters used

The technical parameters for bogie and freight wagon used at Ethio-Djibouti have been detailed in Tables A.1, A.2, A.3 and Figure A.1.

Table A. 1 . Technical parameter for freight wagon used (Source: Ethio-Djibouti railway line project office)

No	Parameter	Description
1	Bogie configuration	BO-BO
2	Material	Q450NQR1 high strength weathering steel
3	Length of a single wagon	13976 mm
4	Length between bogie centers	9210 mm
5	Maximum car height	3617 mm
6	Maximum car width	3300 mm
7	Length inside carbody	13000 mm
8	Width inside carbody	2890 mm
9	Height inside carbody	2075 mm
10	Coupler centerline height	880 mm
11	Wheel diameter	840 mm
12	Height from floor surface to rail surface(empty)	1083 mm
13	Load capacity	70 ton

14	Dead weight	≤ 24.8 ton

Table A. 2. Technical parameter for WZ35 bogie used (Source: Ethio-Djibouti railway line project office)

No	Parameter	Description
1	Gauge	1435 mm
2	Axle load	25 ton
3	Axle type	Type E
4	Fixed wheel base	1830 mm
5	Distance between journal centers	1981 mm
6	Distance between side bearing centers	1520 mm
7	Distance from center plate surface to rail surface (center plate load 63.46 KN)	680 mm
8	Diameter of lower center plate	375 mm
9	Distance from lower center plate surface to lower side bearing surface (free state)	93 mm
10	Distance from lower center plate surface to lower side bearing surface (working state)	83 mm
11	Wheel diameter	840 mm
12	Dead weight	≤ 4.7 ton
13	Designed speed	100 km/h
14	Operation speed	80 km/h
15	Wheel flange thickness (new profile)	32 mm
16	Wheel flange thickness limit for worn profile	≥ 26 mm

Table A. 3. Main parameters used in multibody modelling with SIMPACK (Source: Ethio-Djibouti railway line project office)

Parameter	Symbol	Value	Unit
Carbody mass	Mc	24800	Kg
Carbody roll moment of inertia	Ixx	96000	$Kg.m^2$
Carbody pitch moment of inertia	Iyy	1700000	$Kg.m^2$
Carbody yaw moment of inertia	Izz	1650000	$Kg.m^2$
Bogie frame mass	Mb	4700	Kg
Bogie frame roll moment of inertia	Ixx	2100	$Kg.m^2$
Bogie frame pitch moment of inertia	Iyy	2600	$Kg.m^2$
Bogie frame yaw moment of inertia	Izz	4000	$Kg.m^2$
Wheelset mass	Mw	1800	Kg
Wheelset roll moment of inertia	Ixx	800	$Kg.m^2$
Wheelset pitch moment of inertia	Iyy	140	$Kg.m^2$
Wheelset yaw moment of inertia	Izz	800	$Kg.m^2$
Longitudinal stiffness of primary suspension	Kx	5450000	N/m
Lateral stiffness of primary suspension	Ky	5450000	N/m
Vertical stiffness of primary suspension	Kz	9000000	N/m
Longitudinal damping of primary suspension	Cx	5000	Ns/m
Lateral damping of primary suspension	Cy	5000	Ns/m
Vertical damping of primary suspension	Cz	10500	Ns/m

Longitudinal stiffness of secondary suspension	Kxx	130000	N/m
Lateral stiffness of secondary suspension	Kyy	130000	N/m
vertical stiffness of secondary suspension	Kzz	240000	N/m
Longitudinal damping of secondary suspension	Cx	15000	Ns/m
Lateral damping of secondary suspension	Cy	15000	Ns/m
vertical damping of secondary suspension	Cz	25000	Ns/m

中国中车 CRRC

中车山东机车车辆有限公司
CRRC SHANDONG CO., LTD.

编号：YJWB-PX-05

轮对旋修

Wheelset reprofilling

1. 车轮尺寸外观检查：轮辋厚≥26mm，轮辋宽≥134mm，轮缘厚≥28mm，轮缘高 27±1mm，倒角 5×5mm，车轮直径 min=786mm，轮对内距 1350-1356mm，踏面圆周磨耗超过 3mm 需镟修。轮对外观踏面擦伤，局部凹陷＞0.2mm 需镟修。同一轮对，两轮直径差小于 1mm，粗糙度为 Ra25um.

Wheel size visual inspection: rim thickness **≥ 26mm**, rim width **≥ 134**mm, rim thickness **≥ 28mm**, rim height **27±1mm**, chamfer **5×5mm**, wheel diameter **min=786mm**, wheelset inner distance **1350-1356mm**, tread circumference If the wear exceeds **3mm**, it needs to be repaired. The wheelset has scratches on the appearance of the tread surface, and local depressions **> 0.2mm** need to be repaired. The same wheel

Figure A. 1.Wheelset re-profilling operation limits at EDR (Source : Ethio-Djibouti Railway maintenance department)

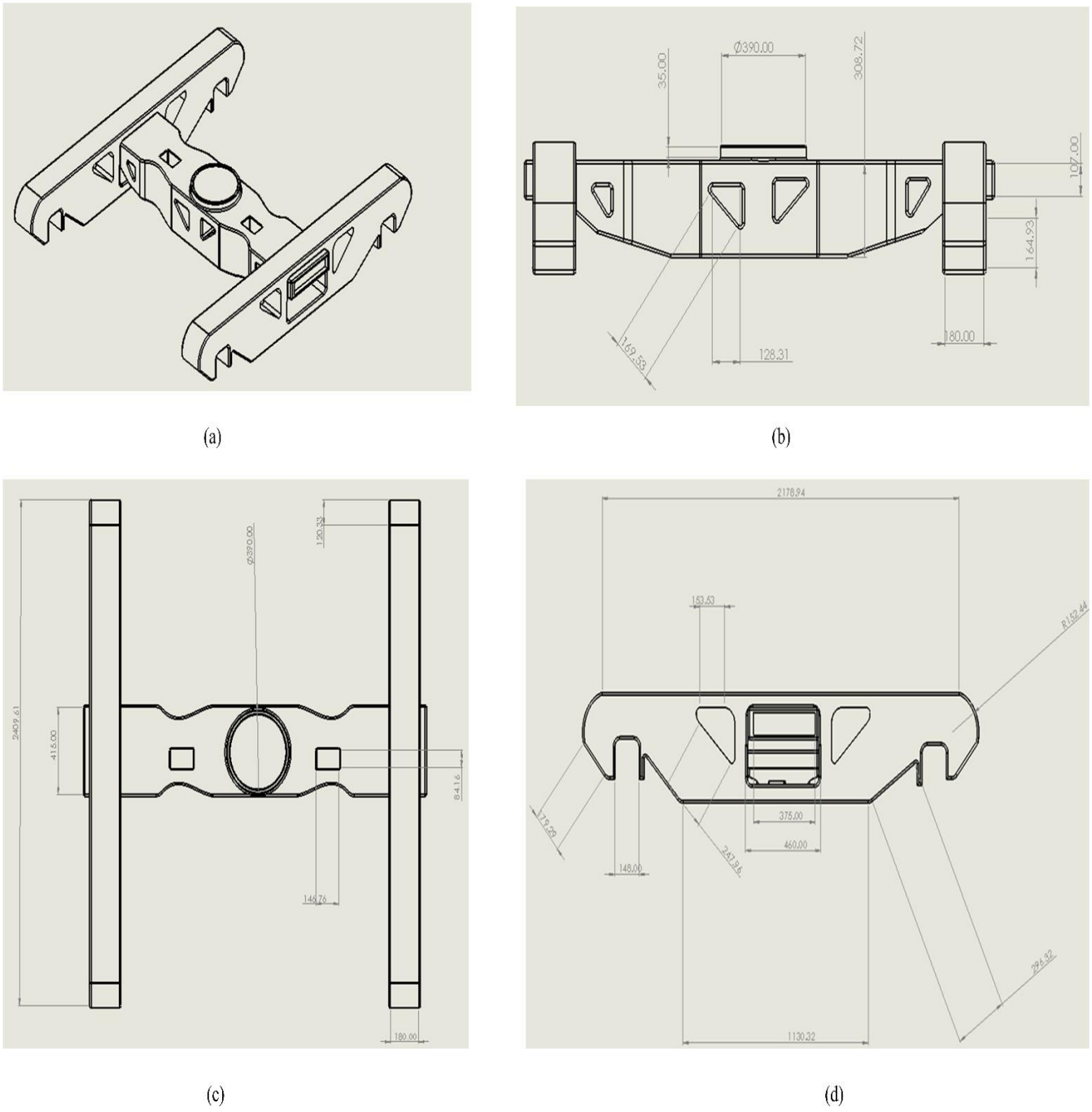

Figure A. 2. Dimensions used to design bogie frame in CAD

Appendix B. Out-of-roundness data used (from maintenance department at EDR)

Table B. 1. OOR with maximum radius deviation of 1 mm

Theta(Rad)	Δr(m)	Theta(Rad)	Δr(m)	Theta(Rad)	Δr(m)	Theta(Rad)	Δr(m)	Theta(Rad)	Δr(m)
0	0.001	1.48396839	0.000925	2.96793678	0.000786	4.4519052	0.000834	5.935873557	0.000875
0.031573796	0.000995	1.51554219	0.00093	2.99951057	0.000783	4.483479	0.000826	5.967447352	0.000885
0.063147591	0.000987	1.54711598	0.000874	3.03108437	0.000778	4.5150528	0.00082	5.999021148	0.000895
0.094721387	0.000978	1.57868978	0.000869	3.06265817	0.000775	4.5466266	0.000818	6.030594943	0.000904
0.126295182	0.000969	1.61026357	0.000865	3.09423196	0.000771	4.5782003	0.000819	6.062168739	0.000914
0.157868978	0.000959	1.64183737	0.000861	3.12580576	0.000766	4.6097741	0.00082	6.093742534	0.000924
0.189442773	0.000949	1.67341116	0.000858	3.15737955	0.000889	4.6413479	0.00082	6.12531633	0.000934
0.221016569	0.000939	1.70498496	0.000856	3.18895335	0.000891	4.6729217	0.000818	6.156890125	0.000944
0.252590364	0.000929	1.73655875	0.000853	3.22052714	0.000884	4.7044955	0.000812	6.188463921	0.000954
0.28416416	0.00092	1.76813255	0.00085	3.25210094	0.000876	4.7360693	0.000804	6.220037716	0.000964
0.315737955	0.000911	1.79970634	0.000847	3.28367473	0.000867	4.7676431	0.000796	6.251611512	0.000973
0.347311751	0.000904	1.83128014	0.000845	3.31524853	0.000858	4.7992169	0.000792	6.283185307	0.001
0.378885546	0.000899	1.86285394	0.000844	3.34682232	0.00085	4.8307907	0.000794		
0.410459342	0.000895	1.89442773	0.000841	3.37839612	0.000842	4.8623645	0.000798		
0.442033137	0.000894	1.92600153	0.000836	3.40996992	0.000833	4.8939383	0.000806		
0.473606933	0.000897	1.95757532	0.000835	3.44154371	0.000823	4.9255121	0.000815		
0.505180728	0.000902	1.98914912	0.000839	3.47311751	0.000812	4.9570859	0.000824		
0.536754524	0.000906	2.02072291	0.00084	3.5046913	0.000803	4.9886597	0.000835		
0.568328319	0.000912	2.05229671	0.000838	3.5362651	0.000794	5.0202335	0.000845		
0.599902115	0.000921	2.0838705	0.00084	3.56783889	0.000785	5.0518073	0.000855		
0.63147591	0.00093	2.1154443	0.000846	3.59941269	0.000777	5.0833811	0.000865		
0.663049706	0.000939	2.1470181	0.00085	3.63098648	0.000771	5.1149549	0.000875		
0.694623501	0.000948	2.17859189	0.000845	3.66256028	0.000773	5.1465287	0.000886		
0.726197297	0.000958	2.21016569	0.000839	3.69413408	0.000779	5.1781025	0.000896		
0.757771092	0.000967	2.24173948	0.000839	3.72570787	0.000787	5.2096763	0.000906		
0.789344888	0.000977	2.27331328	0.000845	3.75728167	0.000796	5.2412501	0.000916		
0.820918683	0.000987	2.30488707	0.000851	3.78885546	0.000805	5.2728239	0.000926		
0.852492479	0.000997	2.33646087	0.000853	3.82042926	0.000815	5.3043976	0.000936		
0.884066274	0.001006	2.36803466	0.000848	3.85200305	0.000824	5.3359714	0.000946		
0.91564007	0.001012	2.39960846	0.000843	3.88357685	0.000833	5.3675452	0.000954		
0.947213865	0.001009	2.43118226	0.000838	3.91515064	0.000841	5.399119	0.000956		
0.978787661	0.001002	2.46275605	0.000833	3.94672444	0.000841	5.4306928	0.000951		
1.010361456	0.000993	2.49432985	0.000829	3.97829824	0.000831	5.4622666	0.000944		
1.041935252	0.000984	2.52590364	0.000824	4.00987203	0.000821	5.4938404	0.000935		
1.073509047	0.000974	2.55747744	0.000819	4.04144583	0.000826	5.5254142	0.000926		
1.105082843	0.000964	2.58905123	0.000815	4.07301962	0.000836	5.556988	0.000916		
1.136656638	0.000955	2.62062503	0.00081	4.10459342	0.000843	5.5885618	0.000906		
1.168230434	0.000945	2.65219882	0.000806	4.13616721	0.000848	5.6201356	0.000896		
1.19980423	0.000936	2.68377262	0.000801	4.16774101	0.000853	5.6517094	0.000886		
1.231378025	0.000927	2.71534641	0.000796	4.1993148	0.000851	5.6832832	0.000876		
1.262951821	0.000919	2.74692021	0.000792	4.2308886	0.000843	5.714857	0.000868		
1.294525616	0.000914	2.77849401	0.000787	4.26246239	0.000844	5.7464308	0.00086		

1.326099412	0.000912	2.8100678	0.000783	4.29403619	0.000851	5.7780046	0.000855		
1.357673207	0.000913	2.8416416	0.00078	4.32560999	0.000856	5.8095784	0.000852		
1.389247003	0.000916	2.87321539	0.000779	4.35718378	0.000855	5.8411522	0.000852		
1.420820798	0.000918	2.90478919	0.00078	4.38875758	0.00085	5.872726	0.000858		
1.452394594	0.000921	2.93636298	0.000783	4.42033137	0.000843	5.9042998	0.000866		

Table B. 2. OOR with maximum radius deviation of 2 mm

Theta(Rad)	Δr(m)	Theta(Rad)	Δr(m)	Theta(Rad)	Δr(m)	Theta(Rad)	Δr(m)
0	0.0019894	1.657624265	0.001853	3.315248529	0.001689	4.972872793	0.001743
0.033152486	0.001974	1.69077675	0.001838	3.348401014	0.001699	5.006025279	0.001754
0.066304971	0.0019566	1.723929235	0.001825	3.381553499	0.001713	5.039177764	0.001752
0.099457456	0.0019376	1.75708172	0.00182	3.414705985	0.001729	5.07233025	0.001733
0.132609941	0.0019175	1.790234206	0.001821	3.44785847	0.001747	5.105482734	0.001718
0.165762427	0.0018971	1.823386691	0.001828	3.481010955	0.001766	5.13863522	0.00172
0.198914912	0.0018775	1.856539176	0.001838	3.51416344	0.001785	5.171787705	0.001716
0.232067397	0.0018582	1.889691661	0.00185	3.547315926	0.001805	5.204940191	0.001701
0.265219882	0.0018392	1.922844147	0.001865	3.580468411	0.001825	5.238092676	0.001685
0.298372368	0.0018221	1.955996632	0.001881	3.613620897	0.001844	5.271245161	0.001669
0.331524853	0.0018075	1.989149118	0.001897	3.646773381	0.001859	5.304397646	0.001654
0.364677339	0.0017971	2.022301602	0.001557	3.679925867	0.001869	5.337550132	0.00164
0.397829823	0.0017906	2.055454088	0.001549	3.713078353	0.001871	5.370702617	0.00163
0.430982309	0.0017886	2.088606573	0.001642	3.746230838	0.001864	5.403855102	0.001623
0.464134794	0.001794	2.121759059	0.001732	3.779383323	0.001847	5.437007587	0.001616
0.49728728	0.0018033	2.154911543	0.001823	3.812535808	0.001829	5.470160073	0.001608
0.530439764	0.0018122	2.188064029	0.001825	3.845688294	0.001811	5.503312558	0.001604
0.56359225	0.0018239	2.221216514	0.001832	3.878840779	0.001796	5.536465044	0.001605
0.596744735	0.001841	2.254369	0.001837	3.911993265	0.001783	5.569617528	0.001609
0.629897221	0.0018594	2.287521485	0.001842	3.945145749	0.00177	5.602770014	0.001613
0.663049706	0.0018776	2.32067397	0.00185	3.978298235	0.001759	5.635922499	0.001617
0.696202191	0.0018961	2.353826455	0.001859	4.01145072	0.001749	5.669074985	0.001622
0.729354676	0.0019153	2.386978941	0.001863	4.044603206	0.001738	5.702227469	0.001633
0.762507162	0.0019344	2.420131426	0.001853	4.07775569	0.00173	5.735379955	0.001648
0.795659647	0.0019542	2.453283911	0.001838	4.110908176	0.001638	5.76853244	0.001665
0.828812132	0.0019739	2.486436397	0.0019	4.144060661	0.001635	5.801684926	0.001681
0.861964617	0.0019931	2.519588882	0.00182	4.177213147	0.001625	5.834837411	0.001674
0.895117103	0.0020111	2.552741368	0.001821	4.210365632	0.001614	5.867989896	0.001656
0.928269588	0.0020234	2.585893853	0.001828	4.243518117	0.0016	5.901142381	0.001716
0.961422074	0.0020183	2.619046338	0.001838	4.276670602	0.001588	5.934294867	0.001732
0.994574558	0.0020045	2.652198823	0.00185	4.309823088	0.001579	5.967447352	0.001751
1.027727044	0.0019867	2.685351309	0.001865	4.342975573	0.001571	6.000599837	0.00177

1.060879529	0.0019678	2.718503794	0.001881	4.376128058	0.001564	6.033752322	0.00179
1.094032015	0.0016995	2.751656279	0.001897	4.409280543	0.001561	6.066904808	0.001809
1.127184499	0.0016903	2.784808764	0.00191	4.442433029	0.001561	6.100057293	0.001829
1.160336985	0.0016787	2.81796125	0.001915	4.475585514	0.001564	6.133209779	0.001849
1.19348947	0.0016772	2.851113735	0.001898	4.508738	0.001566	6.166362264	0.001868
1.226641956	0.0016894	2.884266221	0.001879	4.541890484	0.001566	6.199514749	0.001887
1.259794442	0.0017025	2.917418705	0.001861	4.57504297	0.001568	6.232667235	0.001908
1.292946926	0.0017051	2.950571191	0.001841	4.608195455	0.001573	6.26581972	0.001927
1.326099412	0.0016962	2.983723676	0.001821	4.641347941	0.001583	6.283185307	0.001989
1.359251897	0.001685	3.016876162	0.0018	4.674500425	0.001598		
1.392404383	0.0016755	3.050028646	0.00178	4.707652911	0.001614		
1.425556867	0.0016664	3.083181132	0.001759	4.740805396	0.001632		
1.458709353	0.0016578	3.116333617	0.00174	4.773957882	0.001648		
1.491861838	0.0016485	3.149486103	0.001721	4.807110366	0.001665		
1.525014324	0.0018418	3.182638587	0.001703	4.840262852	0.001681		
1.558166808	0.0018502	3.215791073	0.00169	4.873415337	0.001697		
1.591319294	0.0018591	3.248943558	0.001681	4.906567823	0.001713		
1.624471779	0.0018629	3.282096044	0.001682	4.939720309	0.001729		

Table B. 3. OOR with maximum radius deviation of 5 mm

Theta(Rad)	Δr(m)	Theta(Rad)	Δr(m)	Theta(Rad)	Δr(m)	Theta(Rad)	Δr(m)
0	0.005102	0.61822506	0.004752	1.23645012	0.004461	1.85467518	0.003933
0.012616838	0.005075	0.6308419	0.004727	1.24906696	0.004435	1.86729202	0.003909
0.025233676	0.005036	0.64345874	0.00469	1.2616838	0.004414	1.87990886	0.003878
0.037850514	0.004991	0.65607557	0.004656	1.27430064	0.004394	1.8925257	0.003855
0.050467352	0.004943	0.66869241	0.004643	1.28691747	0.004378	1.90514253	0.003844
0.06308419	0.004892	0.68130925	0.004646	1.29953431	0.004365	1.91775937	0.003842
0.075701028	0.004839	0.69392609	0.004664	1.31215115	0.004353	1.93037621	0.003844
0.088317866	0.00479	0.70654293	0.004688	1.32476799	0.004336	1.94299305	0.003852
0.100934704	0.00474	0.71915976	0.004719	1.33738482	0.00432	1.95560989	0.003863
0.113551542	0.004692	0.7317766	0.004759	1.35000166	0.004312	1.96822672	0.003873
0.12616838	0.004648	0.74439344	0.004798	1.3626185	0.004307	1.98084356	0.003887
0.138785218	0.004611	0.75701028	0.004838	1.37523534	0.004292	1.9934604	0.003895
0.151402056	0.004584	0.76962712	0.004874	1.38785218	0.004265	2.00607724	0.003893
0.164018894	0.004568	0.78224395	0.004885	1.40046901	0.004262	2.01869408	0.003873
0.176635732	0.004563	0.79486079	0.004842	1.41308585	0.004279	2.03131091	0.003841
0.189252569	0.004577	0.80747763	0.004793	1.42570269	0.004284	2.04392775	0.0038
0.201869407	0.0046	0.82009447	0.004746	1.43831953	0.004274	2.05654459	0.003758
0.214486245	0.004623	0.83271131	0.004697	1.45093637	0.004284	2.06916143	0.003716
0.227103083	0.004653	0.84532814	0.004646	1.4635532	0.004318	2.08177826	0.003676
0.239719921	0.004696	0.85794498	0.004593	1.47617004	0.004336	2.0943951	0.003642
0.252336759	0.004743	0.87056182	0.004542	1.48878688	0.004312	2.10701194	0.003605
0.264953597	0.00479	0.88317866	0.004487	1.50140372	0.004282	2.11962878	0.003567
0.277570435	0.004837	0.8957955	0.004438	1.51402056	0.004279	2.13224562	0.003527
0.290187273	0.004886	0.90841233	0.004389	1.52663739	0.00431	2.14486245	0.003495
0.302804111	0.004935	0.92102917	0.004345	1.53925423	0.004343	2.15747929	0.00347
0.315420949	0.004985	0.93364601	0.00431	1.55187107	0.00435	2.17009613	0.003454
0.328037787	0.005035	0.94626285	0.004289	1.56448791	0.004327	2.18271297	0.003454
0.340654625	0.005084	0.95887969	0.00429	1.57710475	0.004299	2.19532981	0.003461
0.353271463	0.00513	0.97149652	0.004309	1.58972158	0.004274	2.20794664	0.003473
0.365888301	0.005162	0.98411336	0.004335	1.60233842	0.004251	2.22056348	0.003484
0.378505139	0.005149	0.9967302	0.00437	1.61495526	0.004229	2.23318032	0.003501
0.391121977	0.005113	1.00934704	0.004411	1.6275721	0.004205	2.24579716	0.003518
0.403738815	0.005068	1.02196388	0.004457	1.64018894	0.004181	2.258414	0.003543
0.416355653	0.00502	1.03458071	0.004505	1.65280577	0.004157	2.27103083	0.003574
0.428972491	0.004969	1.04719755	0.004554	1.66542261	0.004133	2.28364767	0.003607
0.441589329	0.004921	1.05981439	0.004605	1.67803945	0.00411	2.29626451	0.003637
0.454206167	0.004871	1.07243123	0.004657	1.69065629	0.004085	2.30888135	0.003657
0.466823005	0.004822	1.08504807	0.004703	1.70327313	0.004061	2.32149819	0.003663
0.479439843	0.004775	1.0976649	0.004743	1.71588996	0.004038	2.33411502	0.003656
0.492056681	0.004728	1.11028174	0.004768	1.7285068	0.004015	2.34673186	0.003635
0.504673519	0.004689	1.12289858	0.004773	1.74112364	0.003996	2.3593487	0.003608
0.517290357	0.004663	1.13551542	0.004754	1.75374048	0.003981	2.37196554	0.00358
0.529907195	0.004651	1.14813226	0.004713	1.76635732	0.003975	2.38458238	0.003555
0.542524033	0.004657	1.16074909	0.004666	1.77897415	0.003979	2.39719921	0.003528
0.555140871	0.004674	1.17336593	0.00462	1.79159099	0.003993	2.40981605	0.003494
0.567757708	0.004685	1.18598277	0.004582	1.80420783	0.004008	2.42243289	0.00346
0.580374546	0.004698	1.19859961	0.004547	1.81682467	0.003996	2.43504973	0.003426
0.592991384	0.00472	1.21121645	0.004515	1.82944151	0.003972	2.44766657	0.003403
0.605608222	0.004742	1.22383328	0.004488	1.84205834	0.003952	2.4602834	0.003399

Theta(Rad)	Δr(m)	Theta(Rad)	Δr(m)	Theta(Rad)	Δr(m)	Theta(Rad)	Δr(m)
2.472900241	0.003399	3.091125302	0.00343	3.70935036	0.004081	4.32757542	0.004104
2.485517079	0.003397	3.10374214	0.003469	3.7219672	0.004127	4.34019226	0.004114
2.498133917	0.003387	3.116358978	0.003507	3.73458404	0.004155	4.3528091	0.004124
2.510750755	0.003377	3.128975816	0.003545	3.74720088	0.004167	4.36542594	0.004138
2.523367593	0.003367	3.141592654	0.00358	3.75981771	0.004175	4.37804277	0.004166
2.535984431	0.003355	3.154209492	0.003619	3.77243455	0.004178	4.39065961	0.004203
2.548601269	0.00334	3.16682633	0.00366	3.78505139	0.00417	4.40327645	0.004248
2.561218107	0.003326	3.179443167	0.003701	3.79766823	0.004145	4.41589329	0.004288
2.573834945	0.00331	3.192060005	0.003732	3.81028507	0.004117	4.42851013	0.004271
2.586451783	0.003296	3.204676843	0.003747	3.8229019	0.004081	4.44112696	0.004224
2.599068621	0.003285	3.217293681	0.003752	3.83551874	0.004051	4.4537438	0.004181
2.611685459	0.003279	3.229910519	0.003747	3.84813558	0.004027	4.46636064	0.004223
2.624302297	0.003282	3.242527357	0.003725	3.86075242	0.004007	4.47897748	0.004274
2.636919135	0.003294	3.255144195	0.003694	3.87336926	0.00399	4.49159432	0.004324
2.649535973	0.00331	3.267761033	0.003666	3.88598609	0.003982	4.50421115	0.004375
2.662152811	0.003328	3.280377871	0.003631	3.89860293	0.003983	4.51682799	0.004421
2.674769649	0.003345	3.292994709	0.003596	3.91121977	0.003989	4.52944483	0.004465
2.687386487	0.003353	3.305611547	0.003565	3.92383661	0.003995	4.54206167	0.004505
2.700003325	0.00336	3.318228385	0.003541	3.93645345	0.003996	4.55467851	0.004543
2.712620163	0.003372	3.330845223	0.00351	3.94907028	0.004	4.56729534	0.004566
2.725237001	0.003385	3.343462061	0.003472	3.96168712	0.004012	4.57991218	0.004546
2.737853839	0.003394	3.356078899	0.00344	3.97430396	0.004037	4.59252902	0.004506
2.750470677	0.003398	3.368695737	0.003465	3.9869208	0.004076	4.60514586	0.004463
2.763087515	0.003397	3.381312575	0.003505	3.99953764	0.004118	4.6177627	0.004416
2.775704353	0.003399	3.393929413	0.003528	4.01215447	0.004163	4.63037953	0.00437
2.788321191	0.00341	3.406546251	0.003546	4.02477131	0.004205	4.64299637	0.004324
2.800938029	0.003431	3.419163089	0.003562	4.03738815	0.004249	4.65561321	0.004277
2.813554866	0.003462	3.431779927	0.003574	4.05000499	0.004289	4.66823005	0.004228
2.826171704	0.003493	3.444396765	0.003582	4.06262183	0.004329	4.68084689	0.004181
2.838788542	0.003522	3.457013603	0.003586	4.07523866	0.004369	4.69346372	0.004136
2.85140538	0.003544	3.469630441	0.003588	4.0878555	0.004411	4.70608056	0.004099
2.864022218	0.00356	3.482247279	0.003591	4.10047234	0.004447	4.7186974	0.00407
2.876639056	0.003569	3.494864117	0.003592	4.11308918	0.004475	4.73131424	0.004055
2.889255894	0.003564	3.507480955	0.003589	4.12570602	0.004468	4.74393108	0.004049
2.901872732	0.003545	3.520097793	0.00358	4.13832285	0.004422	4.75654791	0.004051
2.91448957	0.003521	3.532714631	0.003569	4.15093969	0.004382	4.76916475	0.004061
2.927106408	0.003497	3.545331469	0.003569	4.16355653	0.004388	4.78178159	0.004077
2.939723246	0.003477	3.557948306	0.003587	4.17617337	0.004379	4.79439843	0.004099
2.952340084	0.00346	3.570565144	0.00362	4.18879021	0.004338	4.80701527	0.004129
2.964956922	0.003446	3.583181982	0.00366	4.20140704	0.004297	4.8196321	0.00416
2.97757376	0.003424	3.59579882	0.003702	4.21402388	0.004258	4.83224894	0.004197
2.990190598	0.00339	3.608415658	0.003739	4.22664072	0.00422	4.84486578	0.004237
3.002807436	0.00336	3.621032496	0.00378	4.23925756	0.004185	4.85748262	0.004277
3.015424274	0.003337	3.633649334	0.003823	4.2518744	0.004158	4.87009946	0.004321
3.028041112	0.003321	3.646266172	0.003865	4.26449123	0.004141	4.88271629	0.004364
3.04065795	0.003309	3.65888301	0.003905	4.27710807	0.004123	4.89533313	0.00441
3.05327478	0.003321	3.67149984	0.003944	4.28972491	0.004102	4.90794997	0.004454
3.06589162	0.003358	3.68411668	0.003986	4.30234175	0.004092	4.92056681	0.004501
3.07850846	0.003394	3.69673352	0.00403	4.31495858	0.004095	4.93318365	0.004545

Theta(Rad)	Δr(m)	Theta(Rad)	Δr(m)	Theta(Rad)	Δr(m)
4.94580048	0.004578	5.52617503	0.004299	6.106549576	0.004377
4.95841732	0.004595	5.53879187	0.004256	6.119166414	0.004419
4.97103416	0.004588	5.55140871	0.004215	6.131783252	0.004466
4.983651	0.004558	5.564025543	0.004183	6.14440009	0.004516
4.99626784	0.004518	5.576642381	0.004173	6.157016928	0.004565
5.00888467	0.004506	5.589259219	0.004177	6.169633765	0.004614
5.02150151	0.004534	5.601876057	0.004184	6.1822506	0.004665
5.03411835	0.004545	5.614492895	0.004185	6.19486744	0.004716
5.04673519	0.004512	5.627109733	0.004174	6.20748428	0.004765
5.05935202	0.004469	5.639726571	0.004145	6.22010112	0.004815
5.07196886	0.004423	5.652343409	0.004102	6.23271796	0.004867
5.0845857	0.004379	5.664960247	0.004063	6.24533479	0.004917
5.09720254	0.004337	5.677577085	0.004043	6.25795163	0.004967
5.10981938	0.004295	5.690193923	0.004049	6.27056847	0.005017
5.12243621	0.004248	5.702810761	0.004072	6.28318531	0.005102
5.13505305	0.004197	5.715427599	0.004111		
5.14766989	0.004144	5.728044437	0.004158		
5.16028673	0.004096	5.740661275	0.004206		
5.17290357	0.004051	5.753278113	0.004258		
5.1855204	0.004008	5.765894951	0.004311		
5.19813724	0.003966	5.778511789	0.004363		
5.21075408	0.003935	5.791128626	0.004415		
5.22337092	0.003942	5.803745464	0.004467		
5.23598776	0.003973	5.816362302	0.004518		
5.24860459	0.004014	5.82897914	0.004569		
5.26122143	0.004062	5.841595978	0.004621		
5.27383827	0.004108	5.854212816	0.004673		
5.28645511	0.004157	5.866829654	0.004726		
5.29907195	0.004204	5.879446492	0.004776		
5.31168878	0.00425	5.89206333	0.004826		
5.32430562	0.004292	5.904680168	0.004866		
5.33692246	0.004293	5.917297006	0.004879		
5.3495393	0.004242	5.929913844	0.004854		
5.36215614	0.004191	5.942530682	0.004817		
5.37477297	0.004216	5.95514752	0.004771		
5.38738981	0.004265	5.967764358	0.004723		
5.40000665	0.004299	5.980381196	0.004672		
5.41262349	0.004327	5.992998034	0.004621		
5.42524033	0.004353	6.005614872	0.00457		
5.43785716	0.00434	6.01823171	0.00452		
5.450474	0.004303	6.030848548	0.004471		
5.46309084	0.004306	6.043465386	0.004426		
5.47570768	0.004341	6.056082224	0.004388		
5.48832452	0.004366	6.068699062	0.00436		
5.50094135	0.004364	6.0813159	0.004346		
5.51355819	0.004338	6.093932738	0.004348		

Appendix C: Typical example of time dynamic load history picked from SIMPACK at OOR of 5 mm

Table C. 1. Example of dynamic time varying loads picked from SIMPACK on case of OOR with 5 mm

Time(s)	Force(N)	Time(s)	Force(N)	Time(s)	Force(N)	Time(s)	Force(N)
0.005	-60822	2.577	-185573	3.551	-93881.3	88.956	-87526
0.006	-60822	2.578	-278751	3.552	-93024.1	88.957	-87373
0.007	-60822	2.579	-263910	3.553	-89224	88.958	-97081.9
0.008	-60822	2.58	-248115	3.554	-85425.4	88.959	-103527
0.009	-60822	2.581	-241735	3.555	-82605.4	88.96	-99957.6
0.01	-60822	2.582	-216591	3.556	-80177.7	88.961	-88188.5
0.011	-60822	2.583	-182014	3.557	-77247.2	88.962	-73467.9
0.012	-60822	2.584	-157214	3.558	-73771	88.963	-60336.4
0.013	-60822	2.585	-147396	3.559	-70010.7	88.964	-50598.5
0.014	-60822	2.586	-142275	3.56	-66384.1	88.965	-44375.2
0.015	-60822	2.587	-136617	3.561	-63363.8	88.966	-40751.4
0.016	-60822	2.588	-132590	3.562	-61233.5	88.967	-38403.8
0.017	-60822	2.589	-133769	3.563	-60002.1	88.968	-36581.5
0.018	-60822	2.59	-137357	3.564	-59608.6	88.969	-34847.8
0.019	-60822	2.591	-138704	3.565	-59298.1	88.97	-33007.8
0.236	-60822	2.592	-137492	3.566	-57296.6	88.971	-31035.9
0.237	-60822	2.593	-135823	3.567	-56299.2	88.972	-29032.9
0.238	-60822	2.594	-134935	3.568	-57271	88.973	-27187
0.239	-60822	2.595	-132841	3.569	-57068.8	88.974	-25817.5
0.24	-60822	2.596	-129092	3.57	-55387.8	88.975	-25008.6
0.241	-60822	2.597	-124974	3.571	-53363	88.976	-24727
0.242	-60822	2.598	-121467	3.572	-51773.6	88.977	-24737.8
0.243	-60822	2.599	-118519	49.11	-6313.46	88.978	-24856
0.244	-60822	2.6	-115818	49.111	-8960.5	88.979	-24945.2
0.245	-60822	2.601	-113758	49.112	-11877.6	88.98	-25010.1
0.246	-60822	2.602	-112801	49.113	-15045.3	88.981	-25097.9
0.247	-60822	2.603	-112986	49.114	-18314	88.982	-25259.3
0.48	-60822	2.604	-113812	49.115	-21886.8	88.983	-25523.3
0.481	-60822	2.605	-114926	49.116	-25551.5	88.984	-25953.3
1.551	-72008.9	2.606	-116274	49.117	-29087.2	88.985	-26534.1
1.552	-71655.6	2.607	-117725	49.118	-32441.8	88.986	-27217
1.553	-71259.8	2.608	-119096	49.119	-35667.5	88.987	-27942.1
1.554	-70840.9	2.609	-120227	49.12	-38555.8	88.988	-28655.8
1.555	-70413.1	2.61	-120985	49.121	-63921.7	88.989	-29324.2
1.556	-69985.1	2.611	-121407	49.122	-293583	88.99	-29926.9